DESIGN-BASED OPTIMIZATION OF A CUSTOM PERMANENT MAGNET FOCUSED ON A REDUCED RAW-MATERIAL CONSUMPTION

Anubhav Vishwakarma

Doctoral Dissertation
Jožef Stefan International Postgraduate School
Ljubljana, Slovenia

Supervisor: Asst. Prof. Dr. Matej Andrej Komelj, Jožef Stefan International Postgraduate School and K7 Department Jožef Stefan Institute, Ljubljana, Slovenia.

Evaluation Board:
Prof. Dr. Kristina Žužek, Jožef Stefan International Postgraduate School and K-7 Department Nanostructured Materials, Jožef Stefan Institute, Ljubljana, Slovenia.
Prof. Dr. Aleš Belič, Lek d.d. and Faculty for Electrical Engineering, University of Ljubljana, Slovenia.
Dr. Paul John McGuiness, Institute of Metals and Technology, Ljubljana, Slovenia.

MEDNARODNA PODIPLOMSKA ŠOLA JOŽEFA STEFANA
JOŽEF STEFAN INTERNATIONAL POSTGRADUATE SCHOOL

Anubhav Vishwakarma

DESIGN-BASED OPTIMIZATION OF A CUSTOM PERMANENT MAGNET FOCUSED ON A REDUCED RAW-MATERIAL CONSUMPTION

Doctoral Dissertation

OPTIMIZACIJA NAMENSKEGA TRAJNEGA MAGNETA NA OSNOVI NAČRTOVANJA S CILJEM ZMANJŠANJA PORABE SUROVIN

Doktorska Disertacija

Supervisor: Asst. Prof. Dr. Matej Andrej Komelj

Ljubljana, Slovenia, April 2024

Dedicated to my family, especially my father …
मेरे परिवार, विशेषकर मेरे पिता जी के चरणों में समर्पित …

Acknowledgments

First and foremost, I would like to thank Lord Shiva for fulfilling the dreams of my father and uncle (" My Guru" for my Ph.D. course). After my Master and during my internship I was confused regarding the best option for the future- further studies or a job. My uncle became the charioteer of my career, telling me that I would soon get a Ph.D. position because he had a confidence in me. My uncle taught me a lot through his experiences, and he promised me plenty of new knowledge about research and life if I went for further studies. He advised me to take this opportunity and to become one among less than 10 percent of the highly-educated Indians. On the basis of his motivation, I applied, and I was accepted for this Ph.D. position on the 26th of June 2019, almost a month after the pivotal conversation. My uncle and my father always believed that I could succeed. They would like to see the title Dr. in front of my name.

I would like to express my sincere thanks to Asst. Prof. Matej Komelj (honorary whom I call "Guru Ji"). Thank you for making it possible for me to complete my Ph.D. I have learned a lot not only about science but also about life during these precious four years at the Jožef Stefan Institute, especially at the K7 department. I would like to extend special thanks to Matej for his encouragement, guidance, advice, ideas, and beneficial discussions. He has been an excellent supervisor throughout this PhD process. He provided unwavering support and believed in my ability to complete the research on time. I will always be grateful to him for his constant availability, lending support, and assistance. He has not only taught me about science but also shared his life experiences, teaching me how to deal with real life. He is not just my "Supervisor" to me; he cared for me like his own child and stood with me in every problem raised here. I have run out of words to say about my "Guru Ji." He assisted me to look deeper into my results and analyze every detail from a critical point of view, and I have learned a lot from him. Thanks a lot, Matej!

Prof. Matej, who made me who I am today. I have collected every piece of advice, guidance, support, and vision of the future that has shown me the way to success, and I will always remember his advice. I feel fortunate to be his student because I must have done some excellent work in my previous life, and then I have a supervisor ('Guru') like you. I would especially like to thank him for the daily meetings, especially Thursday meetings, the opportunity to travel to many places for conferences and workshops, and everything that happened during my Ph.D. and coming future achievements.

I express my sincere gratitude to the members of the Ph.D. Committee, Prof. dr. Kristina Žužek, Prof. dr. Aleš Belič, and Dr. Paul John McGuiness, for their comprehensive review and proofreading of my dissertation within a tight timeframe. Their corrections and advice significantly improved the quality and clarity of my work. Their prompt and effective communication also facilitated the timely amendment of the thesis. There are many people who have helped me during my PhD.

First of all, I would like to express my gratitude to the senior and junior members of the magnetic group for their valuable suggestions and advice every Thursday. Their helpful information encouraged me to think outside the box during my PhD work. I am also grateful to Prof. dr. Sašo Šturm for providing me with the working facilities of the department.

I am grateful for the immense support, good energy, and beautiful moments provided by my colleagues at the Department of Nanostructured Materials during the past four years. Although I only see my real family once a year, I am thankful for having a family away from home in my colleagues.

I would like to thank Marija Šebjan (Mojca) and Sabina Cintauer (secretary, K7) for their assistance regarding my business-trip travel plans and Upravna Enota official documents; their smiles and help were greatly appreciated. I would like to thank Sanja Fider for her work on the project and for providing financial information.

I would like to express my gratitude to all the individuals in the K7 department whom I had the pleasure of meeting during my PhD at the Department of Nanostructured Materials.

Outside the workspace, I would like to thank Asst. Prof. dr. Manoj Kumar Singh and Dr. Monalisa for being my first friends in Ljubljana. They taught me about the city and where to buy groceries and took me on my first walking tour of the city center. I am incredibly grateful to Dr. Manoj Kumar Singh, who invited me every Saturday for lunch and a tour around the city center.

I would like to thank Matej Komelj's family, especially Saša and the children. During the pandemic, everyone was scared, and I didn't know anyone here except Matej. I didn't have much contact with my real family (India) at that time, and they played a significant role in my life; they invited me to their house for lunch and to meet his family. After meeting his family and all the family members who gave me so much love and care, I feel like I am with my family. Thank you for your faith and support. It was a pleasant experience to spend time with your family while hiking and having lunch at your home. I will always remember your hospitality and support during that time. Thank you again!

I would like to express my gratitude to Bani's family for welcoming me as a part of their family. Bani especially considers me her best friend. There are significant differences between Bani and me. I first met her when she was only 16 months old, and we became best friends. I hope you are not unaware that we are friends and that we spent our childhood together. I have no words to express my feelings about your unforgettable moments. After meeting your family, all the members gave me a lot of love, care, and support from all the members. I always feel like I am with my own family. It has always been a fantastic memory for me to be with you and your family for the city tour, lunch, and dinner at your home. I always remember your hospitality, love, support, and care. Your family has been great company during my stay in Ljubljana, and I feel fortunate to have you around. It is hard to return what you gave me in thanks for your appreciation.

Again, I would like to express my gratitude to my uncle and his family for their help and support. Their inspiration and kindness have been invaluable in helping me reach the pinnacle of my education. You are the first guide of my Ph.D. journey and have always helped me. I can never forget the moments spent with you in Indore and at your home. You are always a source of inspiration to me.

I would like to thank my friends from India, and it would be unfair not to give them credit. They have called every day to ask how I am, and they have always stood firm through the ups and downs of the weather; our daily conversation together reassures us that our wonderful friendship is forever.

More than anything else in the world, reaching the pinnacle of my life would never have been possible without the unwavering support of my family, especially my father. When I was at school, there were many ups and downs in my family, and everyone was broken, but he always taught me to be honest and hardworking, and his guidance developed the uncompromising and integrity qualities of my personality. His optimism and anticipatory vision for me to become an engineer and then a scientist was impressive. He always advised me to be moderate in my career to achieve higher goals. Although my words will never be enough to define your infinite contributions to my life, my gratitude to him cannot be limited. I am grateful for having a father like you who always believed in my abilities. Your faith has been the driving force that pushed me forward and made my life meaningful.

Lastly, in my life, I have been blessed with eternal happiness by my dearest siblings. They are also my best friend. The process of writing my thesis was easy and enjoyable with your support and guidance. You have brought me this far with your trust and immense support throughout my educational and professional career. The time that I have spent with you has got to be the best part of my life, and I miss it every day.

I sincerely pray for the family's well-being, contentment, devotion, blessings, and eternal inseparability. I sincerely wish everyone a happy and contented life. I do not have enough words to describe the contribution you have made through your immense support and trust in my life.

Abstract

Permanent magnets are vital parts of various devices, above all, those which are essential for the transition to a green society. However, they are made of materials, including rare-earth elements, for which unlimited availability cannot be taken for granted. Therefore, it is desirable to reduce the content of these materials but without affecting the technologically relevant properties. Whereas the conventional solution to this problem is an appropriate material modification, the subject of this thesis is an alternative approach, i.e., a custom design for a particular application to use less material without losing performance. The focus is on the permanent magnet as a source of magnetic field in an induction-based self-charger for portable devices. It is supposed that the required magnetic-flux time dependence is achieved either with an oscillating magnet and a static coil or with a static magnet and an oscillating coil.

The performance indicator is the average induced voltage normalized to the magnet volume, theoretically predicted by applying the finite-element method. The innovation is notches in the considered magnets, which make the resulting field sufficiently inhomogeneous even in the case of a uniform, uniaxial magnetization, and which simultaneously contribute to a smaller volume, and hence to reduced material consumption.

To determine the most appropriate geometrical parameters of the magnets, an optimization analysis is conducted. Basically, the considered magnet geometries are characterized by three parameters, of which two are optimized simultaneously while the third is kept fixed. The obtained sets of optimum parameters yield better results than arrangements of standard magnets with non-trivial magnetization patterns, proving the advantages and applicability of the proposed problem solution.

Povzetek

Trajni magneti so bistveni sestavni deli različnih naprav, tudi tistih, ki so ključne za prehod v zeleno družbo. Narejeni so iz materialov, ki vsebuje elemente redkih zemelj, katerih dostopnost ni nujno zagotovljena. Zato je zaželjeno zmanjšati njihovo vsebnost, brez vpliva na tehnološko pomembne lastnosti. Običajna rešitev tega problema je ustrezna sprememba materiala, vsebina te disertacije pa je alternativni pristop s posebnim oblikovanjem magnetov za določeno uporabo z namenom porabiti manj materiala za isti učinek. Težišče je na trajnem magnetu kot izviru magnetnega polja za samo-polnilec prenosnih naprav na osnovi indukcije. Privzeto je, da potrebno časovno odvisnost magnetnega pretoka dosežemo s tresočim-se magnetom in mirujočo tuljavo ali z mirujočim magnetom in tresočo-se tuljavo.

Merilo za zmogljivost je povprečna inducirana napetost, normirana na prostornino magneta, izračunana s pomočjo metode končnih elementov. Novost predstavljajo utori v obravnavanih magnetih, ki povzročijo dodatno nehomogenost nastalega polja tudi v primeru enakomerne namagnetenosti, hkrati pa zmanjšujejo prostornino in s tem porabo materiala.

Najustreznejši geometrijski parametri so določeni s pomočjo optimizacijske analize. V osnovi je geometrija magneta določena s tremi parametri, od katerih v tem postopku hkrati spreminjamo dva, medtem ko ima tretji konstantno vrednost. Dobljeni nabor optimalnih parametrov vodi do boljših rezultatov kot običajne postavitve z netrivialnimi vzorci namagnetenosti, kar dokazuje prednosti in uporabnost predlagane rešitve.

Contents

List of Figures

List of Tables

Abbreviations

NG	… Natural Gas
LNG	… Liquefied Natural Gas
TTF	… Title Transfer Facility
mmBtu	… One million British thermal units
EJ	… Exajoule
GW	… Gigawatt
GT	… Gigatons
BPSRWE	… BP Statistical Review of World Energy
CI	… Carbon Intensity
IEA	… International Energy Agency
WEC	… Conversion of wave energy
FPE	… System of Free Piston Engines
ICT	… Information and Communication Technology
AC	… Alternating current
DC	… Direct Current
SEMH	… Self-Generator Electromagnet Harvester (SEMH)
LG	… Linear Generator
PMs	… Permanent Magnet
PMLG	… Permanent-Magnet Linear Generator
LIC	… Linear Induction Generator
LSRG	… Linear Switched-Reluctance Generator
b/d	… Barrel per day
R-TM	… Rare earth, transition-metal
TM	… Transition metal
FEM	… Finite-element method
PDEs	… Partial differential equations
FDM	… Finite-Difference Methods
FVM	… Finite-Volume Methods
SI	… International System
OM	… Oscillating Magnet
SM	… Static Magnet
OC	… Oscillating Coil
OIC	… Oscillating Iron-core
REPM	… Rare-Earth Permanent Magnet
RE	… Rare Earth
EU	… European Union
EVs	… Electric Vehicles
GWEC	… Global Wind-Energy Council
HEVs	… Hybrid Electric Vehicles
MRI	… Magnetic Resonance Imaging
SRWE	… Statistical Review of World Energy
SGEH	… Self-generation Electromagnetic Harvester
OIC	… Oscillating Iron-core
REEs	… Rare-earth elements
GBE	… Grain-Boundary Engineering
EEC	… Electromechanical Energy Conversion
PDEs	… Partial differential equations
MOP	… Magnet Optimization Parameters
OP	… Optimum Performance

OM	… Optimization Magnet
NV	… Normalized Voltage
SM	… Solid Magnet
AM	… Axial Magnet
NM	… Normal Magnet
HM	… Halbach Magnet
AM	… Additive manufacturing

Symbols

L	… Length	m
m	… Mass	kg
t	… Time	s
ν	… Frequency	Hz
ω	… Angular Frequency	s^{-1}
F	… Force	N
U	… Electrical voltage	V
P	… Power	W
q	… Charge	As
ρ	… Charge Density	Asm^{-3}
I	… Electric Current	A
j	… Electric-Current Density	Am^{-2}
E	… Electric Field	V/m
R	… Resistance	**Ω**
ϕ	… Magnetic Flux (V)	Tm^2
B	… Magnetic-Flux Density	T
H	… Magnetic Field	Am^{-1}
M	… Magnetization	Am^{-1}
μ_r	… Magnetic permeability	
c	… Velocity of light	m/s
χ	… Magnetic susceptibility	
T	… Temperature	K
T_c	… Curie Temperature	K
μ	… Magnetic Moment	NmT^{-1}
B_r	… Remanent Magnetization (Remanence)	T
$(BH)_{max}$	… Maximum Energy Product	KJ/m3
H_c	… Coercivity	Am^{-1}
D_0	… Diameter	
L_1	… Notch height	
L_2	… Notch width	

* All symbols adapted from Classical Electrodynamics by JOHN DAVID JACKSON.

Chapter 1

Introduction

1.1 Motivation

Over the past few decades, billions of people have been affected by energy crises and environmental degradation. These issues have been exacerbated by an increasing population and human activities, which have threatened the availability of energy resources [1]. The world's future well-being is closely intertwined with the energy requirements of our civilization, which have grown exponentially in the last two centuries, as shown in Figure 1.1. Energy is the most valuable commodity, and our global society relies heavily on its extraction, distribution, conversion, and consumption on a daily basis [2]. The recent conflict between Russia and Ukraine, as well as even more recent events in the Near East, have led to a disruption in energy supplies, particularly electricity and gas, in many European countries because they rely heavily on the natural resources from Russia and Arabia. Another issue is the growing concern over the impact of human-generated carbon dioxide emissions on the Earth's climate [3][4] since 83% of the global energy demand is currently met through the use of fossil fuels [5]. The consensus among many is that at some point in the future, the transition to a sustainable energy system will become necessary.

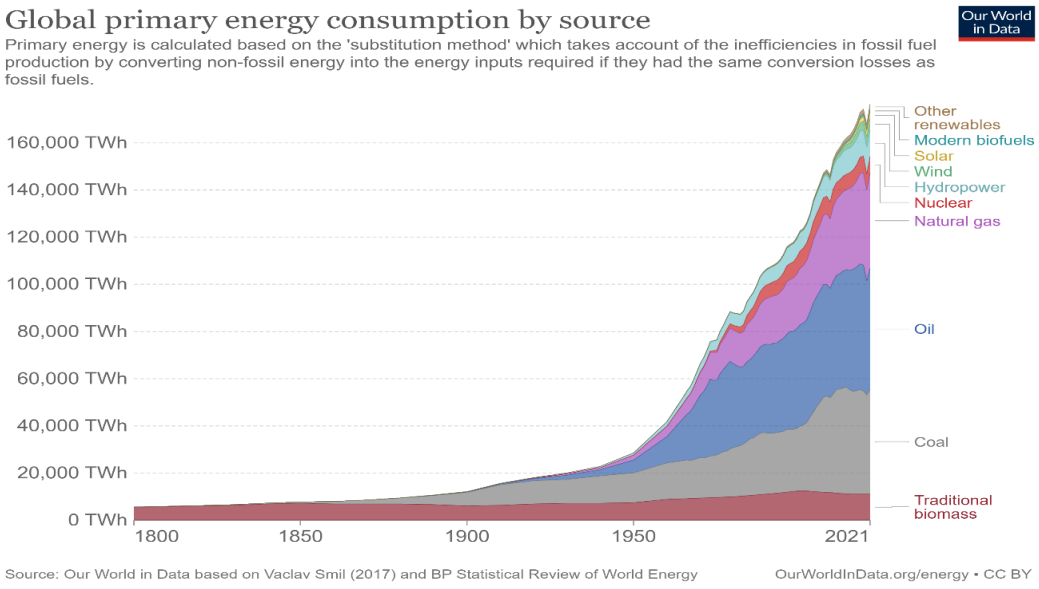

Figure 1.1: Primary energy consumption by source worldwide [6]

Although there is a lot of development in renewable-energy technologies, fossil fuels such as coal, natural gas, and oil remain the world's primary energy sources [7]. **Therefore, new technologies need to be developed to mitigate the effects of CO_2 emissions, increase energy production and increase the efficiencies of the existing energy systems** [8]. In 2021, carbon

dioxide emissions, including those from energy use, industrial processes, flaring, and methane (measured in carbon dioxide equivalent), increased by 5.7% to reach 39.0 GtCO2. On the other hand, the increase in carbon dioxide emissions from flaring and methane, as well as those arising from industrial processes, was more moderate, with respective hikes of 2.9% and 4.6% [6][7].

Another technological problem of the modern society is a limited availability of the natural resources due to various reasons ranging from geological, ecological, economical as well as political. Besides the recycling, as an **approach to save raw materials**, the most logical solution i**s a smart design of novel devices by minimizing their consumption**.

1.2 Energy Consumption in the Portable Electronic Sector

Portable electronics refers to a diverse range of appliances, such as smartphones, tablets, laptops, e-readers, portable gaming devices, and many more. These devices have become indispensable in our daily routines, contributing substantially to our energy consumption [1][9]. The International Energy Agency (IEA) has released a report stating that the information and communication technology (ICT) sector, encompassing portable electronic devices, consumed around 1500 TWh of global energy in 2019 [8][6]. This accounts for approximately 6% of the world's electricity demand and is predicted to grow further in the upcoming years. Energy efficiency of electrical devices in general can be achieved by optimizing the design characterized in terms of various parameters, such as power density, torque, weight, and volume [10].

1.3 Energy Generation by Renewable Energy

Renewable energy has become increasingly popular in recent years due to its potential to provide a cleaner and more sustainable future by utilizing natural sources such as solar, wind, hydro, geothermal, and biomass [6]. The application of these energy sources can help to reduce greenhouse-gas emissions and promote a more eco-friendly approach to energy production [8]. While electricity constitutes just a fraction of our energy consumption, Figure 1.2 presents the proportion of electricity generated from renewable technologies, with Slovenia producing 34% of its energy from renewable sources [11]. Hydroelectric power dominates modern renewable sources globally, excluding traditional biomass, but solar and wind energy are expanding at a fast pace. As of 2019, renewable technologies accounted for approximately 11% of primary energy worldwide, based on their share in the energy mix, which includes electricity, transportation, and heating. Renewable energy sources generate around one-quarter of the world's electricity [6][8].

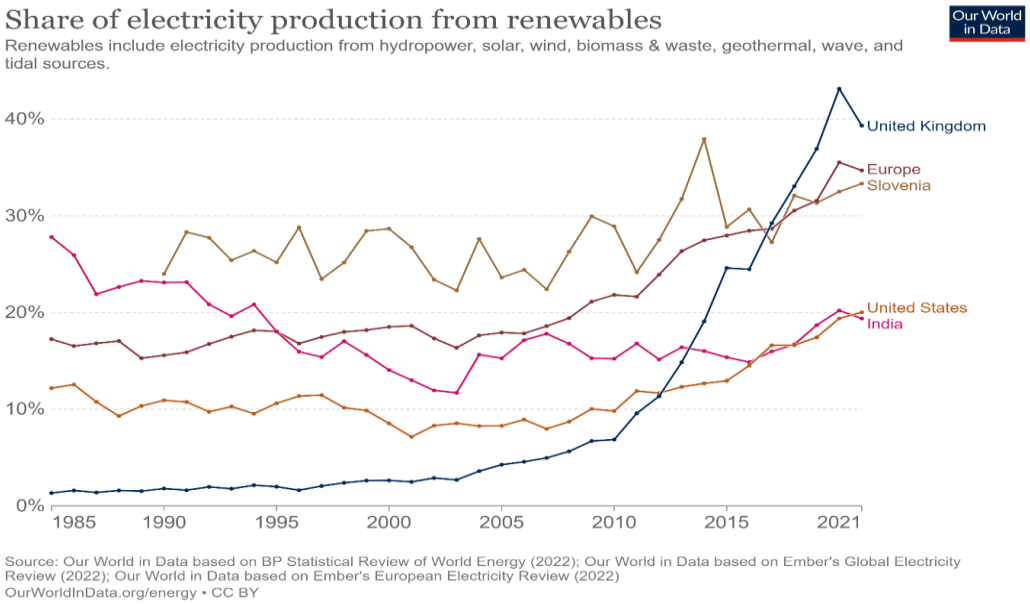

Figure 1.2: Per year energy production from renewable sources [6].

Renewable energy will be essential for the electronics sector, considering that the sector accounts for 10% of the total energy consumption, as indicated by the chart. Recent estimates

suggest that the electricity consumption of a smartphone may exceed current levels, highlighting the need for further research on the issue [8][7]. A promising option is to use the human body as an energy source.

1.3.1 Renewable Energy Generation by Human Body

As home appliances and wearable electronics continue to emerge, people consume more energy to carry out their daily activities [12][13]. However, it is possible to generate energy from the human body itself through walking, making it a considerable energy source worth exploring [14]. Figure 1.3 illustrates the potential of power generation from typical movements performed by an average person of medium build on a daily basis [15][16]. It has been estimated that the energy generated from these sources is sufficient to power computers and other electronics that are essential in modern daily life [17].

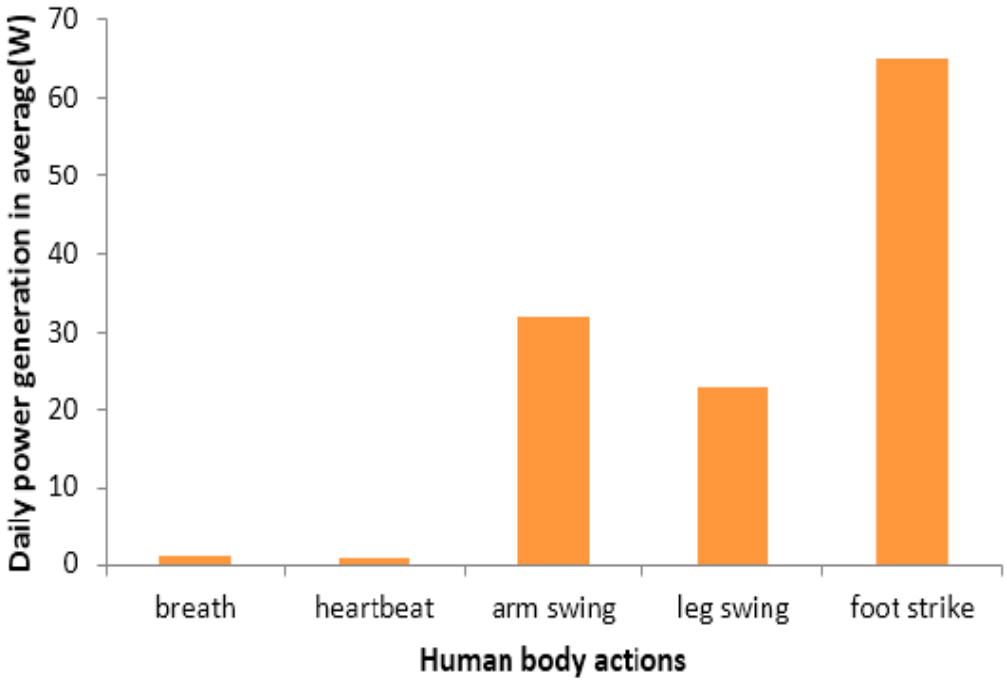

Figure 1.3: Generated energy by different human-body activities [18].

The kinetic energy of a walking human is generated by converting stored chemical energy through the intermediate step of limbs' movement. This conversion process is remarkably efficient in terms of a high ratio between the resulting mechanical energy and the chemical energy of the nutrients [17].

A small part, negligible in comparison with the kinetic energy of a human body, can be potentially harnessed for other purposes [19]. However, it needs to be converted into a regular form that can be effectively distributed and utilized. Electrical energy is the preferred form due to its flexibility in distribution and utilization. There are different methods how to produce electricity by converting other types of energy, for example, photo-electric effect, piezo-electric effect, thermo-electric effect, and electromagnetic inductions. Electric current can be generated by exposing a certain material to electromagnetic radiation, namely to photons, which supply the required energy to excite electrons from the valence to conductive states. A piezo-electric effect occurs when a strain in material implies an electrical polarization, namely a finite voltage. A temperature gradient might cause a diffusion of charges, known as the Seebeck effect, which is reflected by an electrical voltage. However, the most common is the electromagnetic induction, which generates an electrical voltage due to a changing magnetic flux. It does not require any materials with special properties, except for magnets, which are the subject of the present thesis.

1.4 Literature Survey of Self-generating Electromagnetic Harvesters

Self-powered magnetic generators, also referred to as self-charging magnetic harvesters, are devices that generate electrical energy by harnessing mechanical power. The concept of a harvester, based on generating electrical energy from human motion through magnetic induction is not new [20]. The first magnetic harvester prototype was created at the University of California, Berkeley in the 1980s. It utilized a coil and a magnet to produce a low electric current [21]. Since then, numerous research teams worldwide have focused on enhancing the efficiency and effectiveness of magnetic harvesters [22]. In recent decades, portable electronic devices have become ubiquitous in our daily lives. However, the traditional power sources used for these devices, such as batteries, are approaching their limits. As a result, there is a growing need for an ability to recharge portable electronic devices while outdoors, which has re-ignited interest in human energy-harvesting systems [23]. Besides magnetic-induction-based harvesters, there are also other methods, for example, piezoelectric or electrostatic, for the conversion of vibrations into electricity [24]. Piezoelectric and electrostatic transducers are particularly suitable for use on a human body due to their small size and weight, and of these, piezoelectric generators are the simplest type of harvesting device [25].

In [26], a microgenerator utilizing piezoelectric transductions was proposed. However, due to the high impedance of the material causing energy losses, its maximum output power was only 15 mW. Moreover, piezoelectric materials are prone to brittleness [24]. Several electrostatic micropower generators were discussed in [17][27]. The output power of the microgenerator in [28] was 6.5 mW at 10 Hz, while the output power of other generators in [22] was 116 μW or less. Additionally, the electrostatic generator necessitates a pre-charge voltage to operate [28]. The output power of both types of generators falls short of meeting the power needs of current portable devices, which usually require up to 1 W [14]. Finding an outlet while commuting or traveling can be a hassle, and even if one can be found, it is only useful if there is enough time to recharge the device sufficiently [16] [29]. Solar chargers, hand-crank phone chargers, and thermoelectric generators are other options for travelers, commuters, and those who lead an outdoor lifestyle [30]. However, most of these products are expensive and bulky, and they are just another accessory to carry along with the device. An average person requires something smaller, lighter, and more affordable to extend their device's battery life daily [31]. The generation of enough power to charge portable electronic devices by means of electromagnetic induction seems an attractive solution [32]. The so-called linear generators are particularly promising for human energy-harvesting applications due to their low cost, high output power, stable output voltage, and simple structure [33]. They are based on the principles of magnetic induction, and they run on the power of the user’s motion.

1.5 Self-Generator Electromagnet Harvester (SEMH) or Linear Generator

The linear generator is an electromechanical energy converter, powered by the motion of a prime mover along one direction. Similar to the rotary generator, the linear generator utilizes a mechanism that converts mechanical power into electricity, but with one key difference: the presence of an endpoint effect [34]. While a rotary generator's motion is continuous and never reaches an endpoint, the moving part in a linear generator moves linearly until it reaches the endpoint, then reverses direction. This endpoint effect leads to several issues, such as the occurrence of the cogging force [13]. However, the linear engine is a more desirable option when considering energy-efficiency concerns. Since it does not include a crankshaft, rod, or other rotary parts that typically contribute to friction losses, the linear system is both compact and lightweight, with a high efficiency [35]. As a result, a linear generator is a more advantageous choice for applications requiring the conversion of linear thrust force into electricity when compared to rotary electric generators. The working principle of a linear generator is schematically illustrated in Figure 1.4, whereas Figure 1.5 presents an example of a prototype scheme.

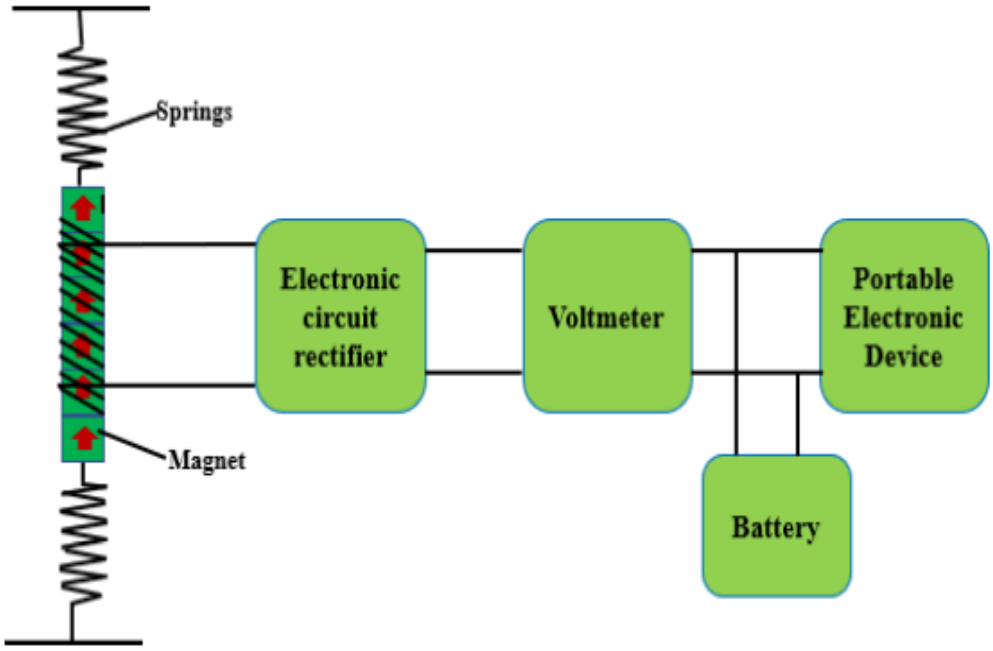

Figure 1.4: Complete line diagram of self-generator electromagnetic harvester.

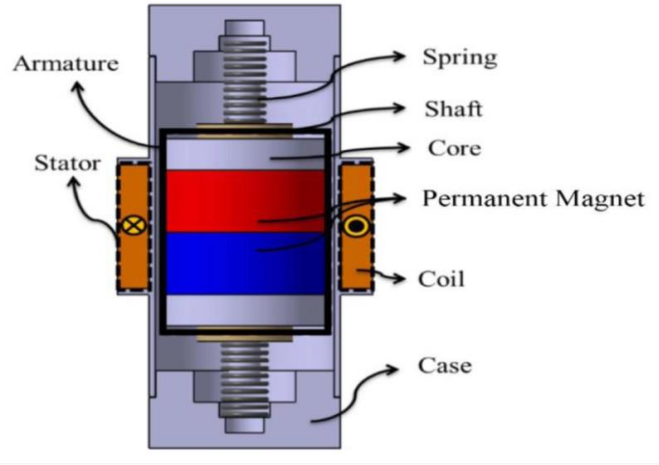

Figure 1.5: Schematic representation of self-generator electromagnetic harvester [36].

1.5.1 Classification of Linear Generators

Linear generators convert linear-motion energy into electricity, characterized by the voltage $U = \sqrt{PR}$, where P and R are the power and the resistance of the load, respectively. There are multiple classification methods used to categorize them. These methods include factors such as the type of motion used, power rating, construction, and application. Additionally, linear generators can be classified on the basis of the primary types [37]. A comprehensive overview of the classification of linear generators is presented in Figure 1.6.

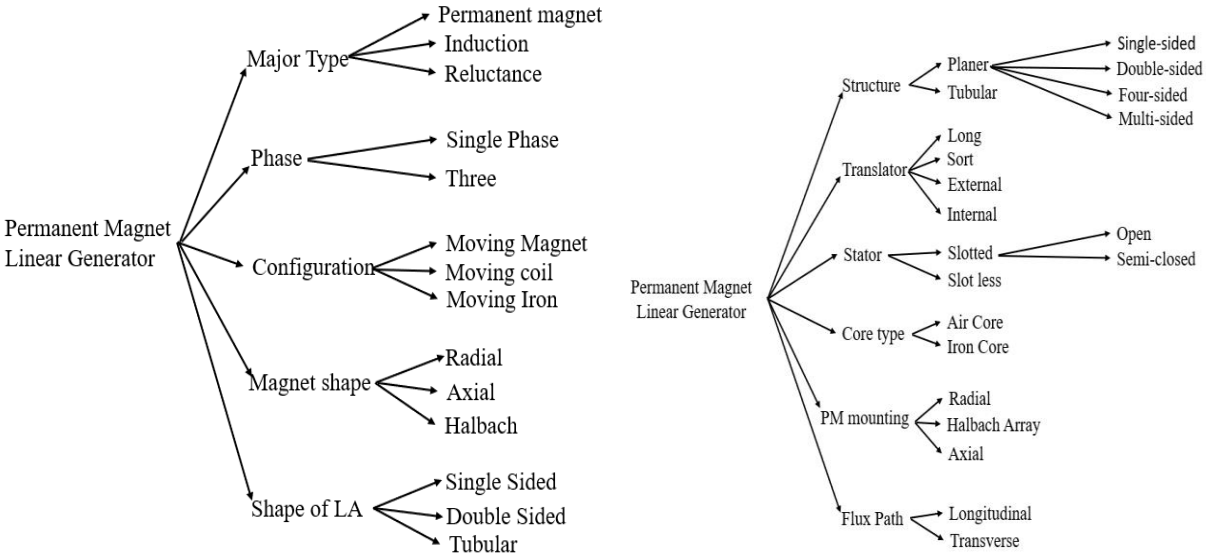

Figure 1.6: Classification of linear generators [38].

Linear generators are classified into three major types.

1. Permanent-Magnet Linear Generator (PMLG)
2. Linear Induction Generator (LIG)
3. Linear Switched-Reluctance Generator (LSRG)

1.5.1.1 Permanent-Magnet Linear Generator (PMLG)

A Permanent-Magnet Linear Generator (PMLG) uses a permanent magnet to produce a magnetic field, converting the reciprocating motion of a system into electrical power. The resulting time dependence of the magnetic flux induces an electrical current in one or more coils. Similar to a permanent-magnet rotary generator, a PMLG typically comprises a coil made of copper windings and laminations to reduce the eddy-current losses. Conventionally, the permanent magnets can be rings, cylinders, or rectangular bars, depending on the system's configuration. High-energy-product rare-earth permanent magnets, known for their large remanent flux densities B_r and large coercivity H_c, defined in Figure 1.7, are normally used in a PMLG. They are widely used in the research and development of various systems that convert the energy stored during linear motion into electricity, including wave-energy conversion, Stirling engines, free-piston engines, micro-energy harvesters, and supercritical CO_2 expanders [39].

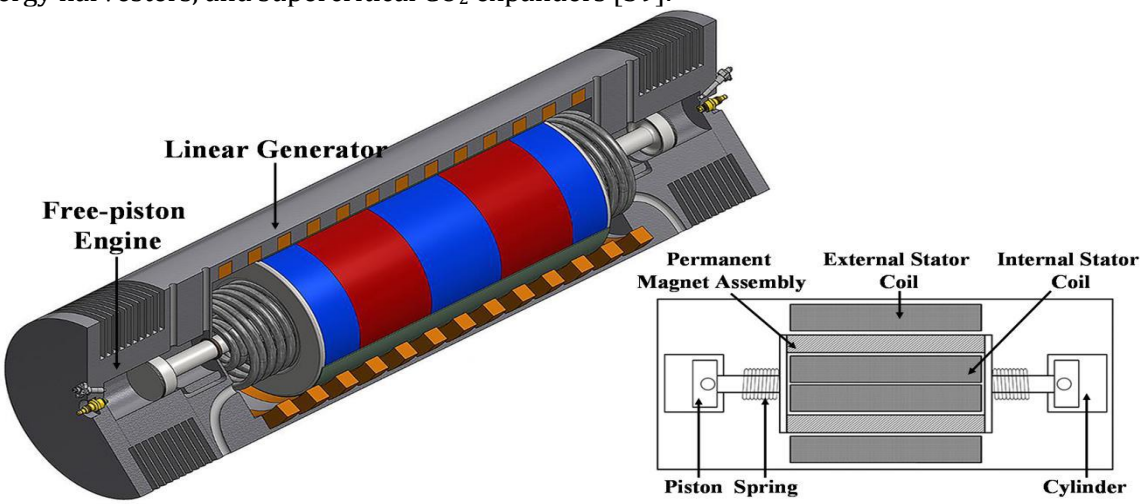

Figure 1.7: Overall model of Permanent-Magnet Linear Generator (PMLG) [40]

A large body of research is being conducted on PMLGs because of the following advantages.

1. High efficiency levels of 90% or more [38]
2. Small air gap in comparison to LIG and LSRG
3. Exhibits high power density
4. Requires low maintenance
5. Operates with low noise levels
6. Does not rely on external magnetization for the translator
7. Possesses a compact size [41][37]

Some of the disadvantages of PMLGs are,

1. Limited power output
2. Higher manufacturing costs in comparison to other generator types
3. Magnet demagnetization due to thermal effects [41]
4. Cogging force present in iron-core machines [41]
5. Limited availability and high cost of high-energy-density (rare-earth) magnets [42]
6. Stray magnetic fields, particularly in single-sided configurations
7. Sensitive to temperature changes, which may negatively impact efficiency and output.

1.6 Phases of Linear Generator

Linear generators can operate in various phase-configuration. modes:

- Single-phase linear generator
- Double-Phase linear generator
- Three-Phase linear generator
- Multi-Phase linear generator

Although the most common are the single and three phases, we briefly discuss all four possibilities.

1.6.1 Single-Phase Linear Generator

It contains one set of windings, resulting in a single-phase output voltage. Single-phase linear generators are easy to construct and maintain, and they produce a sinusoidal waveform output with lower harmonics than their 3-phase counterparts (for short stators) [43]. They are suitable for small power applications in the 1–5 kW range, like a TV set or a refrigerator, whereas for higher power applications, for example, a washing machine, dish washer or professional heavy-duty machinery, the generator size becomes problematic, and three-phase generators are preferred.

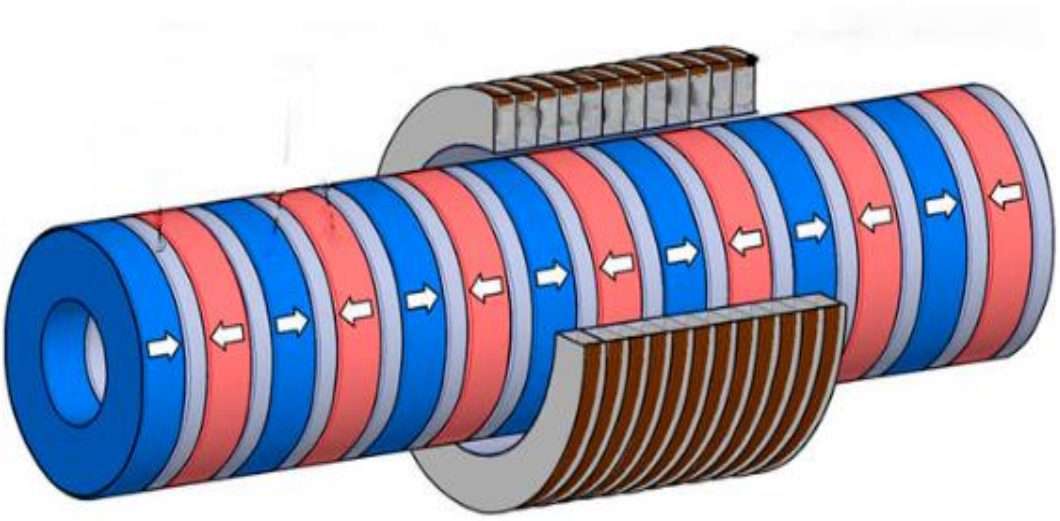

Figure 1.8: Single-phase permanent-magnet linear generator. The magnets in red and blue are magnetized in the opposite directions, surrounded by a single coil in grey.[44]

1.6.2 Three-Phase Linear Generator

This generator is similar to the single-phase linear generators, but it has three sets of coils in the stator instead of one or two. The three-phase windings (A, C, B) in the stator produce a three-phase output voltage, with each phase being 120 degrees out of phase with the other two. The design of the three-phase windings is shown in Figure 1.9. However, constructing three-phase windings can be challenging in smaller, lower-power machines compared to single-phase linear generators. The control of the three-phase linear generator is more complicated too, and in practice, the time dependence of the output voltage is not a perfect harmonic function (sine or cosine), which is, in principle (when the load consists of the so-called active components like capacitors or coils), reflected in a lower efficiency [45].

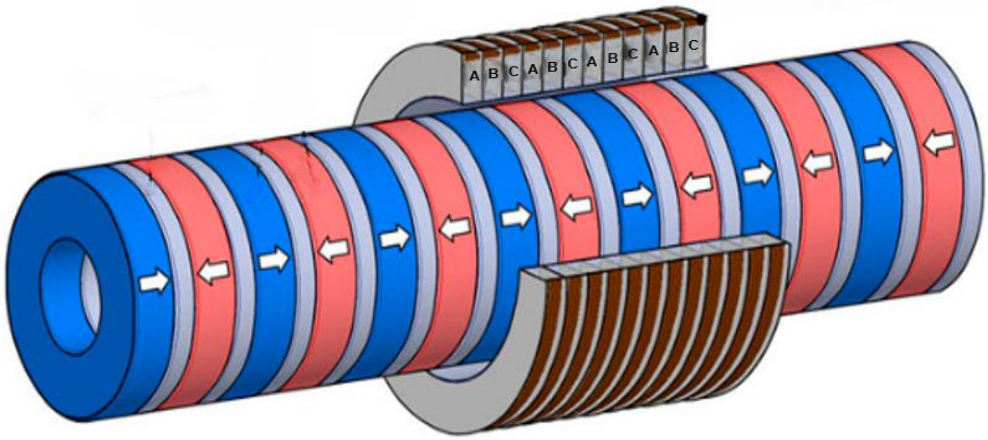

Figure 1.9: Three-phase Permanent-magnet linear generator. The magnets in red and blue are magnetized in the opposite directions, surrounded by an ABC sequence of coils in grey.[44]

1.6.3 Multi-Phase Linear Generator

It operates in a similar way to the three-phase linear generator, but it has more than three sets of coils, resulting in a higher power output and in greater efficiency. The number of phases in a multi-phase linear generator can vary, with the standard options being four, six, eight, and twelve phases [46].

The generator stator consists of multiple sets of coils arranged in a specific pattern, while the translator is equipped with magnets in a non-parallel arrangement (Figure 1.10). As the translator moves back and forth, the magnets pass over the various sets of coils, inducing multiple alternating currents (ACs) at each stage of coils position [29]. The resulting ACs are out of phase with each other, creating a multi-phase power output. These ACs are then rectified and combined to produce a direct current (DC) that can be used for electrical power devices.

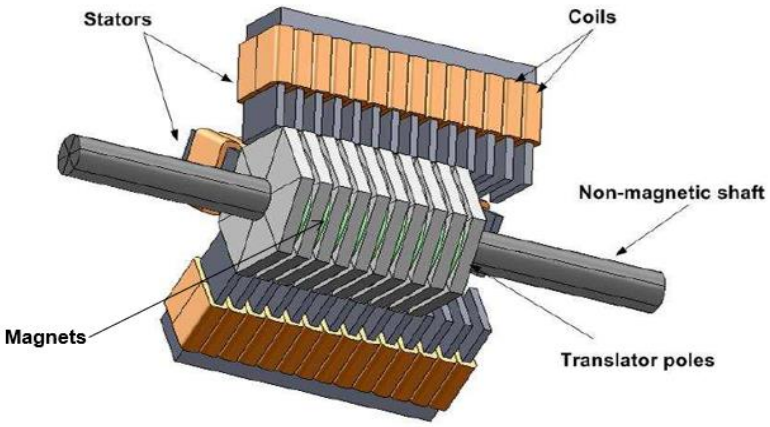

Figure 1.10: Multiphase phase Permanent-magnet linear generator [47]. The magnets, attached to the shaft, are in an anti-parallel arrangement, whereas particular coil stacks are shifted by 1/3 of the inter-magnet distance along the shaft direction relative to each other.

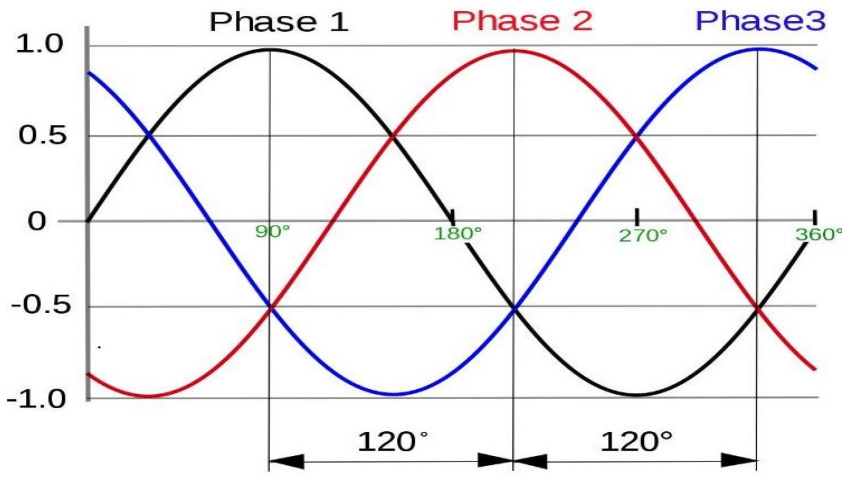

Figure 1.11: The time dependence of the induced voltage in three different coil sets with the phase shifts of 120^0 [48].

However, multi-phase linear generators are more complex, and they require more precise engineering to ensure the proper synchronization of multiple coils. Their primary advantage is the ability to provide a smoother and more constant power output, composed of three sine (cosine) signals shifted by 120o relative to each other, which is desired in applications that require a consistent power supply (Figure 1.11).

1.7 Linear-Generator Configuration

There are three types of linear-generator configurations regarding the distinction between the static and moving parts:
1. Oscillating magnet and static coil,
2. Static magnet and oscillating coil
3. Oscillating Iron-core.

1.7.1 Oscillating-Magnet LG

The stationary part is the copper windings, and the moving element is made of one or more permanent magnets, magnetized non-parallel to each other. The magnets moving along the coils produce a time-dependent magnetic flux, which results in an induced voltage and current [49]. It is the most used linear generator, very similar to a standard rotary permanent-magnet synchronous machine. Its advantages are:
1. The mass that moves is lightweight.
2. The construction is uncomplicated.
3. The air-gap size can be adjusted to match the production and assembly capabilities of the system.

On the other hand, there are certain drawbacks to using a moving-magnet LG,
1. Magnetic fields leak outside the system
2. There is a risk of demagnetization due to thermal and vibrational factors
3. Inadequate control over the magnetic field.

A moving-magnet PMLG is illustrated in Figure 1.12, featuring a static coil surrounding an oscillating magnet attached to a pair of springs.

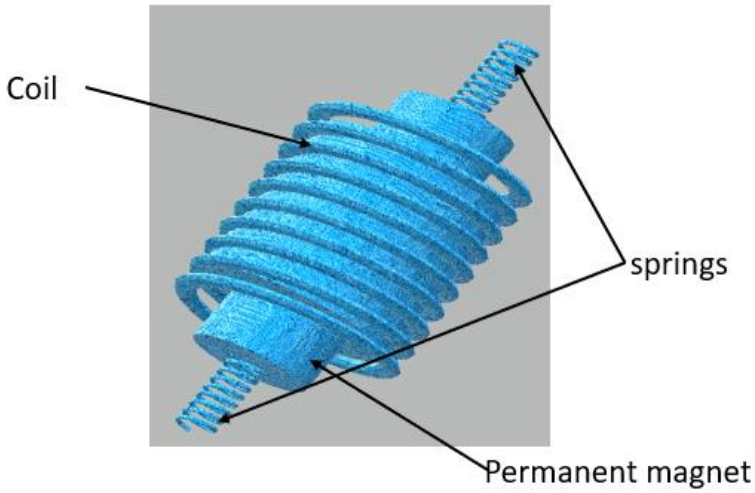

Figure 1.12: Oscillating-magnet linear generator consisting of a static coil surrounding an oscillating magnet attached to a pair of springs.

1.7.2 Static-Magnet LG

The static-magnet linear generator features a stationary component consisting of a single or several magnets and a movable part made up of windings and is presented in Figure 1.13.

The advantages of a moving-coil LG are:

1. Eccentricity-induced radial forces are reduced [50].
2. Demagnetization of the magnets due to the impact force is minimized, since the magnet remains stationary.
3. Field control can be achieved easily.

The disadvantages of the moving-coil linear generator (LG) are:

1. It has a large air gap.
2. Energizing the moving field can be challenging.
3. The construction of large machines can be complicated.

The limited benefits of the moving-coil LG are overshadowed by its drawbacks, making it of relatively little practical importance in the design of linear generators.

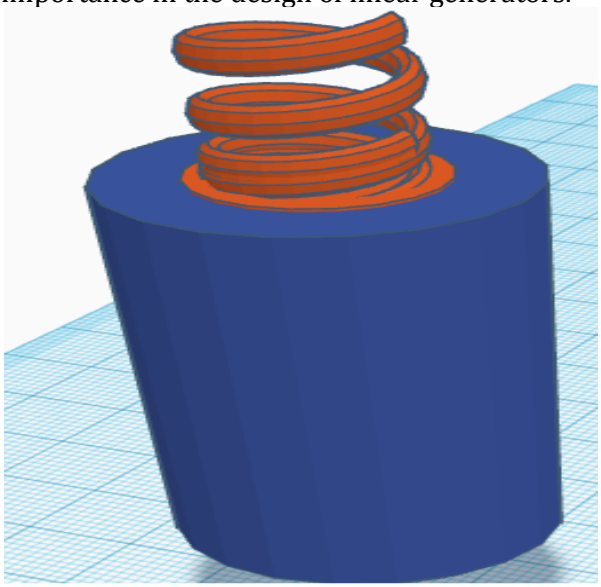

Figure 1.13: Static-magnet linear generator consisting of an oscillating coil surrounded by a single or several static magnets.

1.7.3 Oscillating Iron-Core LG

An alternative to both the oscillating magnet and the moving-coil LG is a setup in which the magnet and the coil are static, whereas the required time dependence of the flux is achieved with an oscillating iron core, presented in Figure 1.14 [51]. Such a system is more robust than the solutions with oscillating magnets or oscillating coils since the core does not have any other roles except for changing the local permeability.

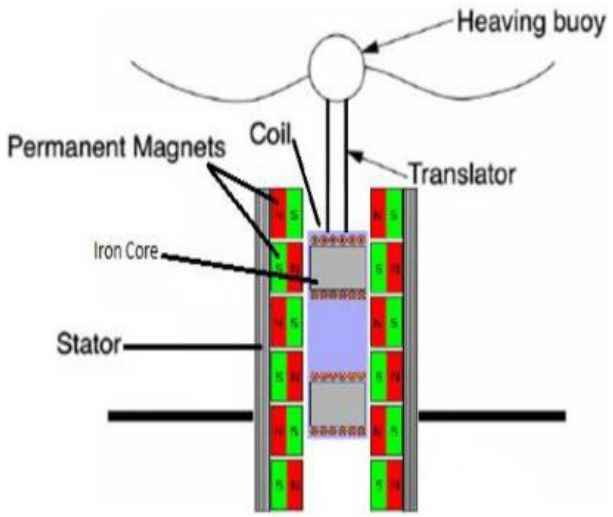

Figure 1.14: Oscillating Iron-Core linear generator [52].

1.8 Magnet Orientation

A certain inhomogeneity of the magnet field inside the generator is required to provide a sufficiently pronounced time dependence of the flux. In this manner, three different magnet arrangements are applied in any of the above-described linear-generator set-ups:

- Normal Magnet
- Radial arrangement,
- Axial arrangement,
- Halbach arrangement,

presented in Figure 1.15. The axial arrangement is the most common since there is evidence for its superiority in terms of a higher power density and efficiency [53][18]. However, for low-speed applications, the cogging forces are higher in axial field machines and this may not be the best option. The advantages of the Halbach magnet arrangement have been studied specifically for wave-energy conversion systems. The common drawback of all three types is that the magnets cannot be magnetized in a single step; therefore, an assembly of differently oriented magnetic parts is required.

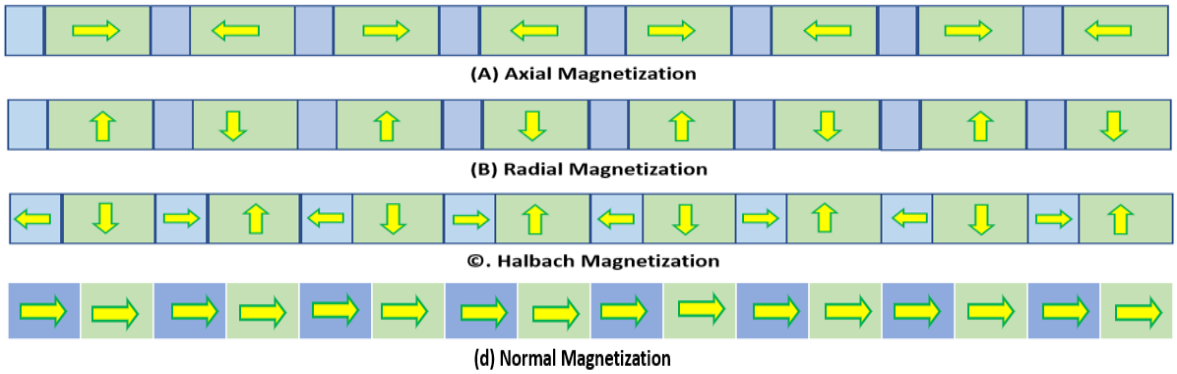

Figure 1.15: There are four type of arrangements for linear generators [54].

1.8.1 Shape of Linear Generators

The permanent-magnet linear generator can have three different shapes: single-sided, double-sided, or tubular. A single-sided linear generator is similar to a rotary generator that has been unrolled onto a flat plane [55]. In contrast, a double-sided linear generator features stator coils on both sides of the translator. The tubular linear generator consists of the static and moving parts surrounding each other. This shape is the most efficient due to its high-power density per unit volume. However, the complex construction [28] processes and high costs associated with the tubular topology are among its disadvantages [56]. Figure 1.16 depicts the single-sided and double-sided linear generators.

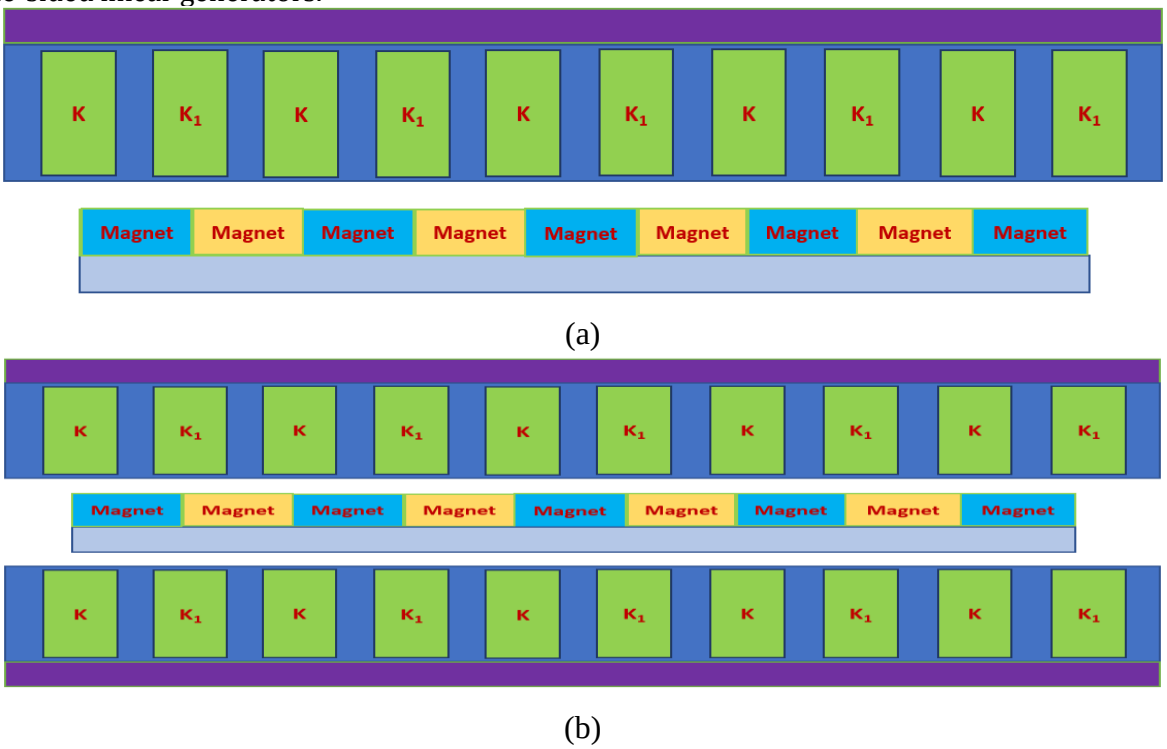

(a)

(b)

Figure 1.16: Single-sided (a) and double-sided (b) linear generators [54].

1.9 End Effect in Linear Generators

The concept of the end effect is specific to linear machines, as opposed to rotary machines which do not have distinct entry and exit points due to their circular motion. The end effect can cause changes in the air gap's magnetic field and is illustrated in Figure 1.17. An analytical model has been developed to examine the effects of the end effect on the magnetic field and force, with differences noted between long-stator and short-stator linear generators [57]. It has been found that the end effects are generally lower in long primary stators compared to short ones and that higher velocities of the mover can lead to smaller end effects in long stators. Various techniques have been applied to reduce the end effects in linear induction motors, including the use of chamfered edges on the end, field-oriented and vector control schemes, and auxiliary poles. In a PMLG system, the end effects can reduce the power contribution from the magnets at the end of the translator due to a high flux leakage, but this can be mitigated by using a longer stator and a shorter translator, modifying the stator-teeth width and shape to reduce the cogging force, or using a skewed PM and reducing the magnet's length, as described in studies [21][58][59].

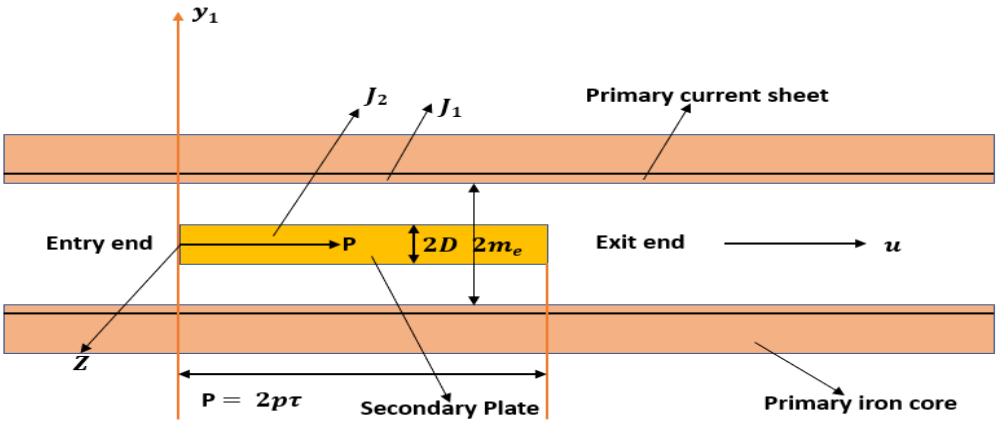

Figure 1.17: End effect of a linear generator [60].

1.10 Cogging Force

The cogging-force results from the attraction between the magnets and the stator laminations in a permanent-magnet machine. This force can lead to unwanted effects such as noise, vibrations, and eccentricity. In linear generators, minimizing the cogging force is important. Various methods have been investigated to achieve this goal. For instance, magnet shapes such as conical and sloped have been examined to decrease the cogging force in PM linear generators, as depicted in Figure 1.18. Another approach involves modifying the stator-teeth width and shape, which has been demonstrated in [41][59][61]. Moreover, a technique that involves reducing the magnet length and utilizing a skewed PM is presented in [62] .

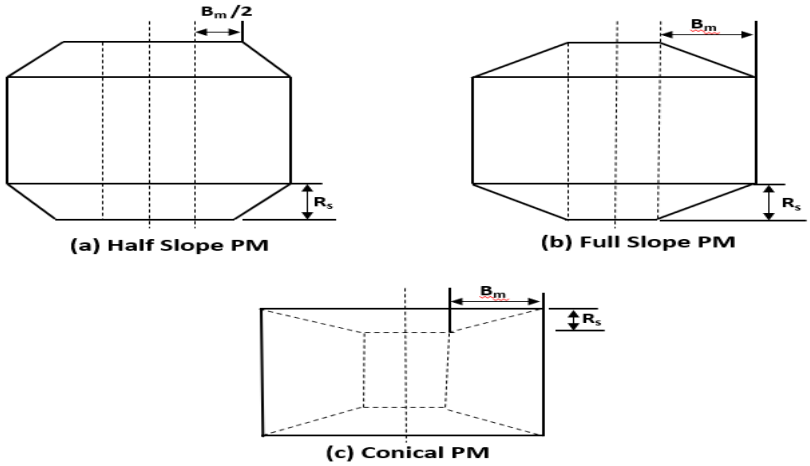

Figure 1.18: Conical Shaped Magnets (a) – Half slope PM (b) – Full slope PM (c) – Conical PM [63].

1.11 Applications of Linear Generators

Research is currently being conducted on a broad range of renewable-energy various applications from the large-scale power stations exploiting the ocean tidal motion by converting the wave energy (WEC) to the systems for harvesting micro energy consumed by implantable electronic medical devices [64]. On the intermediate level there are systems for a regular or an emergency charging of portable electronic devices, which are related to the investigations in the framework of the present thesis.

1.12 Organization of the Dissertation

The thesis is focused on the permanent-magnet design for linear generators as emergency power sources. The oscillating-magnet and the static-magnet linear generators with cylindrical-shaped magnets magnetized along the principle axis are considered. The proposed and tested novelty are notches of different shapes and dimensions engraved in the outer (oscillating magnet) in the inner (static magnet) sides. The following chapters are organized as:

Chapter 2: Theory

This chapter introduces the fundamental concepts and theoretical backgrounds of magnetism. Various rare-earth-based magnetic materials and their properties are introduced.

Chapter 3: Aims and Hypothesis

This chapter describes the problem, presents the project's aims and the research hypotheses of the dissertation.

Chapter 4: Finite-Element Methods and Methodology

This chapter introduces the finite-element-modeling method for solving Poisson's equation, which describes the magnetic field around a permanent magnet.

Chapter 5: Results and Discussion

This chapter presents the results of modeling for two types of the magnet-coil arrangements. The proposed solutions are optimized in terms of geometrical parameters. The calculated normalized voltages are compared with the most common standard solutions.

Chapter 6: Conclusions

This chapter draws the conclusion and presents the future scope of this research. Design improvements to the self-generator system or magnetic harvester are proposed.

Chapter 2

Theory

The process of converting mechanical energy into electricity can range from simple popular-science demonstrations with magnets and coils to highly complex installations, including national electricity grids [65]. Such systems can be modeled either in terms of basic or very complex models. The objective of this chapter is not to present a comprehensive description of electrical devices but rather to review the fundamental principles of magnetism with an emphasis on electromechanical energy conversion [66], [67]. The purpose is to introduce the numerical model utilized in the thesis.

2.1 The Origin of Magnetism

Magnetic field is produced by moving electric charges, in a matter mainly electrons, or it originates from an intrinsic property of elementary particles (electrons) named spin. The spin is quantized in a similar way as the positive and negative elementary charge, namely as up and down. Since the electrons in atoms tend to pair, the up and down contributions in fully-occupied atomic shells cancel out and consequently they do not contribute to magnetism. Only partially occupied atomic shells might exhibit a **finite** spin, and consequently **magnetic moment**, which is the source of magnetic behavior in certain materials.

2.2 Magnetic Terminology / Magnetization and Magnetic Intensity

On the basis of the assumption that some atoms carry magnetic moments $\left(\vec{m}\right)$, the magnetization $\left(\vec{M}\right)$ can be defined as a sum:

$$\vec{M} = \sum \frac{\vec{m}}{V} \tag{2.1}$$

where V is the volume of the sample. The magnetization is both: a response to and a source of a magnetic field. In the SI system, magnetization is measured in ampere/meter [A/m] [68]. The magnetic field is usually characterized the magnetic-flux density $\left(\vec{B}\right)$ measured in Tesla T (1 T=1 kg/As^2) This can be alternatively created by an electric current $\left(I\right)$ running through a coil with *n* turns per unit length:

$$B_0 = \mu_0 nI \tag{2.2}$$

assuming a negligible diameter of the coil with respect to its length.

If a substance with a non-zero magnetization $\vec{M}$ is put into the region of $\vec{B}$. The overall magnetic flux density $\vec{B}$ is changed:

$$\begin{aligned} \vec{B} &\to \vec{B} + \vec{B}_m \\ \vec{B}_m &\to \mu_0 \vec{M} \end{aligned} \tag{2.3}$$

$$\vec{B} \to \vec{B} + \mu_0 \vec{M} \tag{2.4}$$

where $\mu_0 = 4pi \times 10^{-7} Vs / Am$ represents the permittivity of the vacuum. For convenience, it is beneficial to introduce another vector field $\vec{H}$, referred to as the magnetic intensity, defined as:

$$\vec{H} = \frac{\vec{B}}{\mu_0} - \vec{M} \tag{2.5}$$

so that $\vec{B}$ reads as:

$$\vec{B} = \mu_0 \left(\vec{H} + \vec{M} \right) \tag{2.6}$$

It means that the magnetic field inside a material arises in two parts. The first part, represented by $\vec{H}$, is caused by external factors such as permanent magnets or a current flowing through a solenoid. The second part, represented by $\vec{M}$, is due to the specific properties of the material itself.

In fact, the magnetization $\vec{M}$ represents the response to the $\vec{H}$:

$$\vec{M} = \chi \vec{H} \tag{2.7}$$

where the dimensionless χ is the magnetic susceptibility. It quantifies the degree to which a magnetic material reacts to an external field. Materials exhibiting para-magnetism have a small positive value of χ, while materials displaying diamagnetism have a small negative value of χ. In the case of diamagnetic materials, the directions of $\vec{M}$ and $\vec{H}$ are opposite. The equation (2.7) can be rewritten as:

$$\begin{aligned} \vec{B} &= \mu_0 \left(1 + \chi \right) \vec{H} \\ &= \mu_0 \mu_r \vec{H} \\ &= \mu \vec{H} \end{aligned} \tag{2.8}$$

The magnetic permeability, denoted as $\mu_r = 1 + \chi$, is a dimensionless quantity that can be interpreted as the magnetic counterpart of the dielectric constant in electrostatics.

$$\mu = \mu_0 \mu_r = \mu_0 \left(1 + \chi \right) \tag{2.9}$$

As shown in Eq. (2.8), magnetic permeability $\left(\mu = \left| \frac{\vec{B}}{\vec{H}} \right| \right)$ determines the degree of magnetic flux density induced by an external magnetic field.

2.3 Classification of Magnetic Materials/Magnetic Properties of Materials

Different materials can be categorized according to their response to external magnetic fields.

2.3.1 Diamagnetism

Magnetic moments in diamagnetic substances tend to align opposite to the direction of the external field. As a result, the field force lines are expelled from a diamagnetic sample, as shown in Figure 2.1. Although diamagnetism is present in all materials, its effect is usually too weak to be observed due to other effects like para-magnetism or ferromagnetism [69].

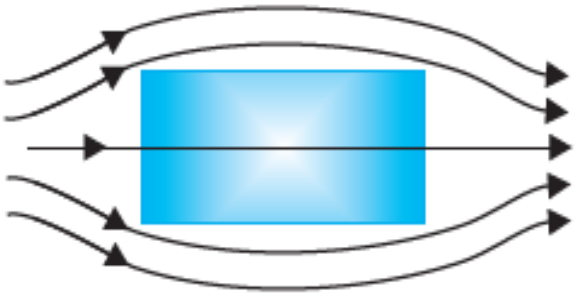

Figure 2.1: Behavior of magnetic field lines for a diamagnetic sample [69].

Perfect diamagnetic materials are superconductors. Below their transition temperature (which is usually very low), they exhibit zero electrical resistance and discrete values of magnetic susceptibility $(\chi = -1)$ and permeability $(\mu_r = 0)$ [70]. As a result, a magnet repels a superconductor, and vice versa, in a phenomenon called the Meissner effect, named after its discoverer.

2.3.2 Paramagnetism

Paramagnetic substances respond to an external magnetic field by aligning the magnetic moments in its direction. This is quantitatively described by a positive susceptibility and the permeability ($\mu_r > 1$). Therefore, the density of the magnetic field force lines is higher within a paramagnetic sample [70][69], as demonstrated in Figure 2.2.

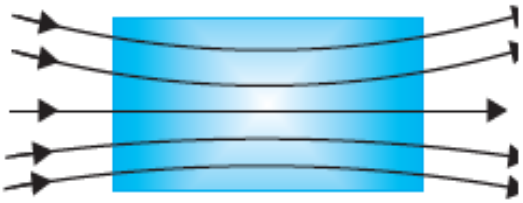

Figure 2.2: Behavior of magnetic field lines in a paramagnetic sample [69].

The magnetic susceptibility χ and permeability μ_r of a paramagnetic material depend on the temperature as well as on the strength of the field, making the magnetic response nonlinear.

According to the Curie–Weiss Law, the susceptibility of materials that are paramagnetic varies inversely with temperature:

$$\chi = \frac{C}{T - \theta} \tag{2.10}$$

Here, (θ) is a temperature constant, and (C) is the Curie constant.

2.3.3 Ferromagnetism

Ferromagnetic materials exhibit non-zero magnetization even in the absence of an external magnetic field, which is due to a spontaneous parallel ordering of magnetic moments. The ordering is a result of the exchange interaction between magnetic moments as an effect of Coulomb repulsion and the Pauli exclusion principle for electrons described in the frame of quantum mechanics. The spontaneous ordering is present only below the Curie temperature. Upon heating a ferromagnetic phase undergoes a transition to the paramagnetic state. In a real sample, not exposed to a strong-enough field, the regions of magnetic moments pointing in the same direction are localized in so-called magnetic domains [70].

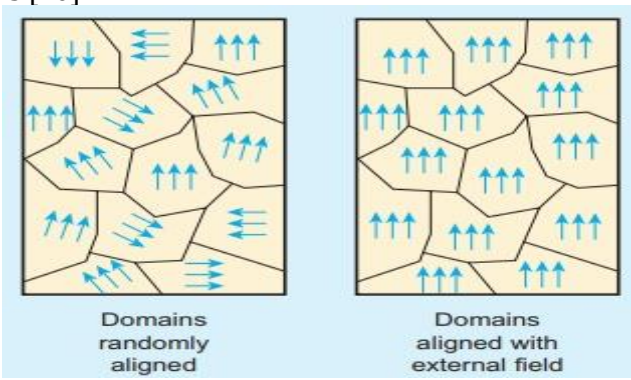

Figure 2.3: Behavior of magnetic field lines for a ferromagnet [71].

The dynamics of domains in an applied field influences the ferromagnetic behavior reflected in the hysteresis loop.

2.3.4 Hysteresis Loop

Magnetization curves, $\vec{M}$ vs $\vec{H}$, are different for different types of magnetic materials. Whereas the response of diamagnetic and paramagnetic materials is linear for a wide range of $\vec{H}$, non-linear patterns are observed for ferromagnetic materials where $\vec{M}$ and χ vary with $\vec{H}$, as illustrated in Figure 2.4.

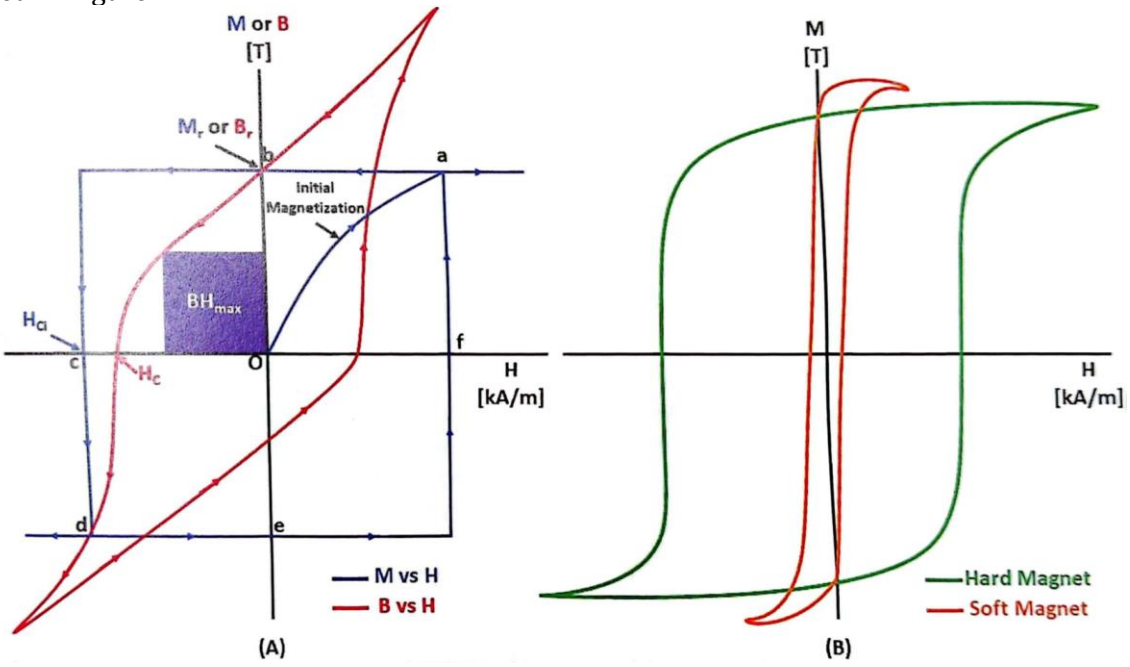

Figure 2.4: Ferromagnetic hysteresis loops have the following characteristics (a) (M vs. H) and (B vs. H). (b) The width of the hysteresis loop determines the so-called magnetic hardness of the material [70].

The origin point "o" represents the demagnetized condition of the material, which does not exhibit any net magnetization $\vec{M}$. At this point, the orientation of the material's domains is random. The magnetic moments start to align parallel to the applied external, which is reflected by a growing magnetization [72][70]. The saturation is achieved at the point "a", characterized by the highest value of $\vec{M}$ when the domains are maximally aligned. For materials with uniaxial magneto-crystalline anisotropy, the $\vec{H}$ required to obtain the saturation $\vec{M}_s$ is lower along the so-called easy axis than in the perpendicular directions. During the magnetization process the magnetic domains tend to rotate in the direction of the external field. In a uniaxial magnet, the majority of the domains are oriented along the easy direction even in the absence of the applied field at point "b" in the second quadrant. The remanence $\vec{M}_r(T)$ is the magnetization at zero external magnetic field. The alignment of domains inside the grains of the complex phase and the compact packing or densification of these grains significantly impact on the remanence $\vec{M}_r$ [73][74]. Switching the external field to the opposite direction makes particular magnetic moments and domains rotate. At a certain value, denoted as the coercivity of the demagnetizing field, the magnetic-flux density $\vec{B}$ or the magnetization $\vec{M}$ vanish.

There are different types of coercivity.

- Normal coercivity, $\vec{H}_c$, is the magnetic field required to reduce the magnetic flux density to zero.
- Intrinsic coercivity, $\vec{H}_{ci}$, is the magnetic field required to reduce the magnetization to zero.

2.4 Intrinsic and Extrinsic Properties of Magnetic Materials

The intrinsic magnetic properties are independent of the microstructure and processing approaches. These properties are related to the chemical composition and crystal structure, or even more precisely to the particular magnetic moments (spin and orbital) and other quantum-mechanical parameters like the crystal-field interactions, exchange and spin-orbit coupling [75][68][69]. They include the saturation magnetization $(\vec{M}_s)$, which corresponds to the state with all magnetic moments maximally-oriented along the direction of the external magnetic field, the Curie temperature T_C, which determines the transition between the ferromagnetic (for the temperatures below T_C) and the paramagnetic state (for the temperatures above T_C), the and magneto-crystalline anisotropy. The latter is associated with the magneto-crystalline-anisotropy energy, which is minimum when the magnetization is along the easy axis (relative to the unit-cell crystallo-graphic directions), and maximum when the magnetization is along the hard direction (or most of-ten within the hard plane, perpendicular to the easy axis).

The **extrinsic properties** depend on the intrinsic properties, on the microstructure, and on the processing details. The most relevant for magnets are remanent magnetization $\vec{M}_r$, and coercivity $\vec{H}_c$, defined in the previous section, of which the former depend on the magnetic moments, whereas the latter directly arises from the magneto crystalline anisotropy.

2.5 Permanent Magnet

Among the materials described in the previous section, the hard-ferromagnetic materials can be applied as magnets. The term "permanent magnet" refers to the fact that it creates a magnetic field due to its inherent properties unlike, for example, an electromagnet, which operates only plugged to a source of electric current running through the coil [76]. The progress of permanent magnets over the past century can be evaluated by examining the increase in the maximum achievable value of $(BH)_{\max}$, which is a measure of the highest amount of energy that can be stored in the magnet. This value is determined by the maximum product of the magnetic field $\vec{B}$ and the magnetic intensity $\vec{H}$. It presents the largest area that can be enclosed within the second quadrant of a $B-H$ hysteresis loop.

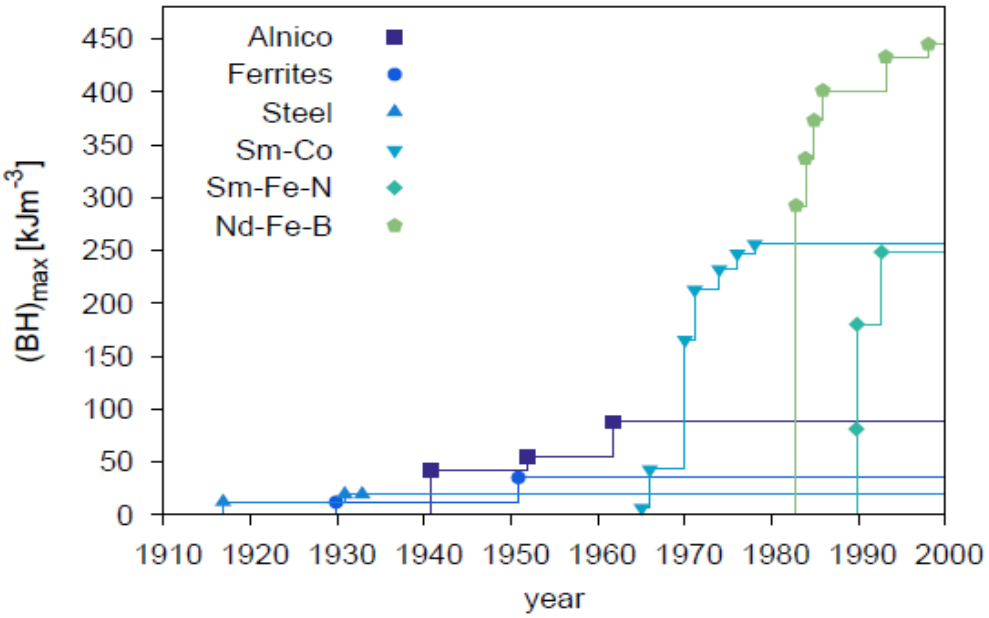

Figure 2.5: Evolution of the maximum achievable $\left(\vec{B}\vec{H}\right)_{\max}$ over the course of the 20th century, with each curve showing a different family of materials [77].

In the early 1900s, cobalt steel was commonly used for permanent magnets until it was replaced by the alnico class of materials, which consisted of alloys made from aluminum, nickel, and cobalt. The alnico class of materials exhibited the highest values of $\left(\vec{B}\vec{H}\right)_{\max}$ at that time. In the 1960s the first rare-earth-transition-metal (R-TM), based on the Sm-Co alloy, permanent magnets appeared [78]. In this type of material, the rare-earth elements provide magneto crystalline anisotropy, required to resist demagnetizing fields, which is essential for large $\left(\vec{B}\vec{H}\right)_{\max}$, whereas the TM sublattice contributes to a high magnetization.

The discovery of the Sm-Co material was important for the field of permanent magnets. However, issues arose regarding the availability of the necessary materials. Samarium, in particular, is one of the least abundant rare-earth elements, and the cobalt supplies were impacted by the civil war that occurred in the Democratic Republic of Congo in 1978 [79]. This region contains the majority of the cobalt resources in the world. The scarcity of materials accelerated the search for new permanent-magnet materials, leading to the discovery of a new family of materials, the $R_2Fe_{14}B$ compounds, which was announced in 1983 at the 29th Magnetism and Magnetic Materials Conference in Pittsburgh [80][81]. Nd-Fe-B magnets are extensively utilized in the EU automotive industry, exhibiting uniform consumption in traditional as well as electric vehicles and wind power, owing to their competency in producing a continuous magnetic field without external power [79][80]. However, rare-earth elements are notorious for their scarcity due to economic uncertainties, geopolitical, and environmental risks. These elements are subjective to high-price volatility since mining becomes more expensive due to running out of resources in old mines and difficulties with opening new mines a lower concentration of the ore. The supply of these elements come and associated semi-finished products come from a short list of countries, including China as the main supplier. Finally, the related mining industry is related to the environment, nature, biodi-versity and health risks.

2.6 Maxwell's Equations

Maxwell's equations are widely recognized as the foundation for our understanding of classical electrodynamics, a theory which describes the electric and magnetic fields originating from charges and currents [82][73]. In their differential form they can be presented as:

$$\nabla \times \vec{E} = \frac{-\partial \vec{B}}{\partial t} \tag{2.13}$$

$$\nabla \times \vec{H} = \vec{J} + \frac{\partial \vec{D}}{\partial t} \tag{2.14}$$

$$\nabla . \vec{D} = \rho \tag{2.15}$$

$$\nabla . \vec{B} = 0 \tag{2.16}$$

By considering the relations:

$$\vec{D} = \varepsilon \vec{E}\ ,\ \ \vec{B} = \mu \vec{H}\ , c = \frac{1}{\sqrt{\varepsilon_0 \mu_0}} \tag{2.17}$$

the equations (2.15) and (2.14) can be transformed into:

$$\nabla . \vec{E} = \frac{\rho}{\mu_0} \tag{2.18}$$

$$\nabla \times \vec{B} = \mu_0 \vec{J} + \frac{\partial \vec{E}}{c^2 \partial t} \tag{2.19}$$

Maxwell's equations present a relationship between the electric-current densities $\vec{J}$, the electric-charge densities ρ, and the vector fields, including the electric displacement field $\vec{D}$, the electric field $\vec{E}$, the magnetic-flux density $\vec{B}$, and the magnetic-field strength $\vec{H}$.

The first equation (2.13) is known as Faraday's law, followed by Ampère's law (2.14) and Gauss's law (2.18) for electric fields, whereas the fourth equation does not have any special name. These equations were consolidated in 1865 by Maxwell [82][83] to define electromagnetism in a compact mathematical form. Maxwell aimed to clarify several experiments performed by Faraday, which had been published decades earlier. Maxwell's equations can be expressed in their integral form through the utilization of the Gauss's and Stokes's theorems:

$$\oint \vec{E} . \frac{d\vec{A}}{d\vec{S}} = \frac{q_{enc}}{\varepsilon_0} \tag{2.20}$$

$$\oint \vec{B} . \frac{d\vec{A}}{d\vec{S}} = 0 \tag{2.21}$$

$$\oint \vec{E} . d\vec{s} = -\frac{d\phi}{dt} \tag{2.22}$$

$$\oint \vec{B} . d\vec{s} = \mu_0 \left(\varepsilon_0 \frac{d\phi_E}{dt} + I_{enc} \right) \tag{2.23}$$

where $-\frac{d\phi}{dt}$ is a time derivative of the magnetic flux $\phi = \sum_{i=1}^{N} \int BdS$ through the area S enclosed by a loop and q_{enc} is the total charge contained in that closed surface, I_{enc} is the electric current flowing through the loop. The equations (2.16) and (2.21) imply that there are no singular

magnetic sources, namely monopoles, which means that all magnets have north and south poles that cannot be isolated.

To solve a problem described by Maxwell's equations it is usually convenient to introduce the scalar φ and the vector $\vec{A}$ potentials, so that:

$$\vec{E} = \frac{-\partial \vec{A}}{\partial t} - \nabla \varphi \,, \tag{2.24}$$

and

$$\vec{B} = \nabla \times \vec{A} \tag{2.25}$$

Assuming a static case $\frac{\partial \vec{D}}{\partial t} = 0$ in the absence of currents $\vec{J} = 0$ equation (2.19) reads as:

$$\nabla \times \vec{B} = 0 \tag{2.26}$$

The relation (2.6) gives:

$$\nabla \times \vec{H} = -\nabla \times \vec{M} \,, \tag{2.27}$$

whereas $\vec{H} = \frac{1}{\mu}\vec{B}$ (2.25) yield a Poisson equation for $\vec{A}$ A by assuming the gauge $\nabla.\vec{A} = 0$:

$$\nabla^2 \vec{A} = -\mu \left[\nabla \times \vec{M} \right], \tag{2.28}$$

$$\nabla^2 \vec{A} = -\mu_0 \vec{J}_M \tag{2.29}$$

where $\vec{J}_M = -\nabla \times \vec{M}$ is the effective magnetic current density and where a homogenous media is assumed.

2.6.1 Scalar Potential

It is more convenient to deal with Poisson's equation for a scalar field. By considering a homogenous media $\vec{H} = \frac{1}{\mu}\vec{B}$ and (2.25) the scalar magnetic potential $\varphi_{\vec{M}}$ is introduced as:

$$\vec{H} = -\nabla \varphi_{\vec{M}} \tag{2.30}$$

A combination of (2.6) and $\left(\vec{B} = \mu_0 \left(\vec{H} + \vec{M} \right) \right)$ yields:

$$\nabla.\vec{B} = \mu_0 \nabla.\left(\vec{H} + \vec{M} \right) = 0 \tag{2.31}$$

and by applying (the equation with "adopt the numbering"):

$$\nabla^2 \varphi_{\vec{M}} = -\rho_{\vec{M}} \,, \tag{2.32}$$

with the effective magnetic-charge density,

$$\rho_{\vec{M}} = -\nabla.\vec{M} \,, \tag{2.33}$$

where we consider the homogeneity of the material in terms of a constant μ. **Poisson's equation** (2.32), which represents the fundamentals of so-called magnetostatics, **is the central**

expression in the present thesis, the solutions of which **describe the magnetic fields produced by the investigated magnets**.

2.7 Electromechanical Energy Conversion

The **working principle of linear electric generators**, introduced in 1.6 and 1.7, is mathematically described by **equations (2.13) and (2.22)** that can be summarized as the Faraday's law:

$$U = -\frac{d\phi}{dt} \tag{2.35}$$

where U is the induced voltage, and ϕ is the magnetic flux, defined as the integral of normal component of the magnetic-flux density B and they are S (the coil cross-section multiplied by the number of turns). The negative sign describes the so-called Lenz's law, which states that the induced voltage produces an electric current generating a magnetic field in the opposite direction to the field inducing the voltage. According to the Faraday's law above, the induced voltage is finite when at least one of the quantities B and S exhibits a time dependence. Since a permanent magnet is static source of the field, the required time dependence is achieved in the case of a relative motion between the magnet and the coil assuming a certain non-homogeneity of the magnetic-flux density. Therefore, i**n principle a non-uniformly magnetized magnet** is required. However, **a similar effect can be achieved** by confining a uniform magnetization within an oddly-shaped area, namely **by applying a specially-shaped magnet**. Since the **flux density *B* and the coil cross-section *S* appear interchangeably** in the definition of the magnetic flux, there is **no intrinsic reason for a different performance** of the oscillating-magnet and the oscillating-coil linear generators by assuming that the magnets in both cases produce similar fields.

Chapter 3

Aims and Hypothesis

3.1 Problem Description

The growing application of portable electronics and demands for a transition to renewable energy sources call for innovations in the field of power management to enhance the autonomy of devices like mobile phones. In this manner, an electromagnetic harvester, which converts mechanical energy of the carrier into electricity for charging a battery, is a very promising option. However, the essential part of such generator is a permanent magnet. Sufficiently strong contemporary magnets, based on the Nd-Fe-B alloy, are made of materials containing the so-called critical rare-earth elements (REEs), particularly neodymium (Nd) and dysprosium (Dy). As it is explained in the section 2.5 their availability and price depend on several factors; hence it is of strategic importance to reduce the consumption. One of the main aims of modern materials science is to reduce the consumption of REEs in magnets. Most of the corresponding research is devoted to optimizing the microstructure, particularly through the so-called grain-boundary engineering or recycling. But there must be other solutions to the problem, most simply by using less material to achieve the same results.

The focus of thesis is design of either an oscillating or static permanent magnet in a linear generator, which represents the most suitable set-up that can be embedded, for example, in a mobile phone. The magnet is not just the most critical part due to the REE content, but also the heaviest and it is not trivial to achieve the Halbach or radial orientations, required to effective energy conversion. The key problem is how to overcome the weaknesses of the concept by an innovative design.

3.2 Dissertation Goals

- To demonstrate theoretically, in the case of a magnetic-induction-based harvester as a test example, that a customized design of magnet can contribute to a reduced material consumption without diminished performance.
- To find the geometry of a uniformly magnetized permanent magnet that provides a comparatively non-homogenous magnetic field as a conventional, uniformly shaped magnet with a non-trivial magnetization pattern.
- To optimize the proposed geometry of the permanent magnet for the linear-generator application in terms of a sufficiently-high induced voltage normalized to the volume ($\sim$4 V/cm^3) with the lowest possible consumption of the materials.
- To optimize the magnets for two variants of the linear generator, where the required time dependence of the magnetic flux can be achieved either with an oscillating magnet in a static coil, or with a static magnet surrounding an oscillating coil.

3.3 Hypothesis

3.3.1 Hypothesis 1

Permanent magnets are integral to many of today's devices and essential for adopting green technologies. They are, for example, crucial parts of electric generators presenting the magnetic field source. According to Faraday's law of magnetic induction, the resulting voltage is proportional to the time derivative of the magnetic flux. In addition to a strong permanent magnet and a sufficiently large cross-section of the pick-up coil, the acceptable performance of a practical device requires a certain degree of inhomogeneity in the magnetic field. Conventional solutions are based on Halbach arrays or similar non-uniformly magnetized magnet configurations. A non-uniform magnetization confined in a proper-shaped area (for example, with a rectangular or circular cross-section) can in principle result in the same surrounding magnetic field as a uniform magnetization confined in an oddly-shaped area. The hypothesis is that comparable results can be achieved using a uniformly magnetized, specially-designed single magnet, thereby simplifying production and reducing material costs.

3.3.2 Hypothesis 2

This solution embodies notches in the magnet design to reduce the weight and to achieve the desired inhomogeneity of the resulting magnetic fields. The hypothesis is that the resulting design is simple enough, so that the respective samples can be produced by means of contemporary techniques like additive manufacturing and by magnetizing the samples in a uniaxial direction.

3.3.3 Hypothesis 3

The theoretically predicted performance of the two considered variants, the oscillating magnet or the oscillating coil, might be comparable in terms of the criterion, defined as the average induced voltage divided by the magnet volume, since both types of magnets are described by similar geometry elements, it is expected that they produce fields of similar strengths and since the magnetic-flux time dependence is either due to the changing field or the changing area. In spite of a reduced consumption of raw material, the required performance can be retained by optimizing the magnet’s design.

3.3.4 Hypothesis 4

According to the respective laws of electromagnetism, introduced in Chapter 2, the outcome of magnetic induction in the case of a varying area (oscillating coil) is equivalent to the case of a varying field (oscillating magnet). Therefore, the performance based on the computational analysis might indicate that both self-generating electromagnetic harvesters exhibit similar optimum yield voltages. However, in practice, one of the two solutions might be better for other technical reasons.

Chapter 4

FEM and Methodology

4.1 A Brief History of the Finite-Element Method

Partial differential equations (PDEs) and some other computational problems can be solved numerically in the frame of the finite-element method (FEM) [84][85][86]. It is one of the most popular and adaptable approaches to solving complex problems in various scientific fields, including engineering, physics, and applied mathematics [87][88].

4.1.1 Origins (1940s-1950s): Engineers and mathematicians like Courant, Friedrichs, and Von-Neumann formulated the finite-difference method for solving PDEs by discretizing the continuous domain into a finite number of points and by taking derivatives as an approximate difference [89].

4.1.2 Early Formulations (1950s-1960s): Researchers like Horvath and Clough introduced the matrix-stiffness method, a forerunner of the FEM, by discretizing the domain into smaller elements and assembling stiffness matrices representing the properties of particular elements [86][90].

4.1.3 Applications Expansion (1970s-1980s): Through improvements in formulation and applications, such as in structural analysis, heat transfer, fluid dynamics, and electrodynamics, the finite-element method was widely accepted and used to address a variety of engineering issues [91].

4.1.4 Advances in Computational Techniques (1990s-2000s): The FEM gained popularity due to the emergence of parallel-computing and multigrid methods. It was used in new fields like biomedical or environmental engineering [92].

4.1.5 Recent Developments (2010s-Present): Methods such as the iso-geometric analysis and reduced-order modeling represent further contributions to the theory of FEM in recent years. Hybrid techniques that combine finite elements with other numerical methods have also been developed [93][90] [94].

4.2 Relation to Analytical Solutions

The FEM is a powerful numerical technique for approximate solutions to complex problems in many branches of science and engineering. For several reasons, it is crucial to comprehend the FEM. First, this method makes an accurate and effective analysis of structures, fluids, and other physical phenomena [95]. Engineers and scientists can use it to simulate and predict a system's behavior under various circumstances, resulting in better designs and optimizations. Second, the FEM offers a flexible and widely applicable methodology that can be used in various disciplines, including physics, computer graphics, materials science, mechanical, aerospace, and biomedical engineering. The third benefit of the FEM is that it fosters analytical and problem-solving abilities. It necessitates an understanding of mathematical ideas fundamental to many branches of science and engineering, such as calculus, linear algebra, and numerical methods.

The FEM also makes it easier for various scientific and industrial fields to collaborate, fostering interdisciplinary research and creative solutions. The FEM is essential for engineers, scientists, and researchers for the analysis of complex problems, to optimize designs, to cultivate interdisciplinary collaborations, and to develop critical thinking abilities. It is important for modern engineering and science practices [90]

4.3 Types of Discrete Numerical Methods for Solving PDEs

To approximatively solve partial differential equations (PDEs), numerical approaches such as the:

- Finite-Element Methods (FEM)
- Finite-Difference Methods (FDM)
- Finite-Volume Methods (FVM)

are used in a variety of scientific and engineering disciplines. They all have in common the ability to deal with a discretized space in different forms.

4.3.1 Finite-Element Method applies the problem domain divided into smaller finite elements, often triangles or quadrilaterals in 2D and tetrahedra or hexahedra in 3D. A linear function of the coordinates is assigned to each element. The set of these functions represents the basis, which is used to expand the approximate solution to the problem. The expansion coefficients are determined by solving an algebraic equation system derived from the variational principle. The FEM is well suited to solving problems associated with complicated geometries and irregular boundaries, and it is frequently utilized in structural analysis, heat transport, fluid mechanics, and electromagnetics.

4.3.2 Finite-Difference Method applies finite differences to approximate the derivatives of a continuous function mapped onto a discrete grid of points. Then, a system of algebraic equations is built and solved to yield the solution. The FDM is usually easier to implement than the FEM, but is limited to regular geometries.

4.3.3 Finite-Volume Method is based on discretizing the domain volume into finite parts-control volumes. The corresponding PDE is solved exactly for each control volume, whereas various approximate schemes are used to merge different contributions. The problems involving flow and transport phenomena, such as fluid dynamics, combustion, and porous-media flow, are well suited to the FVM.

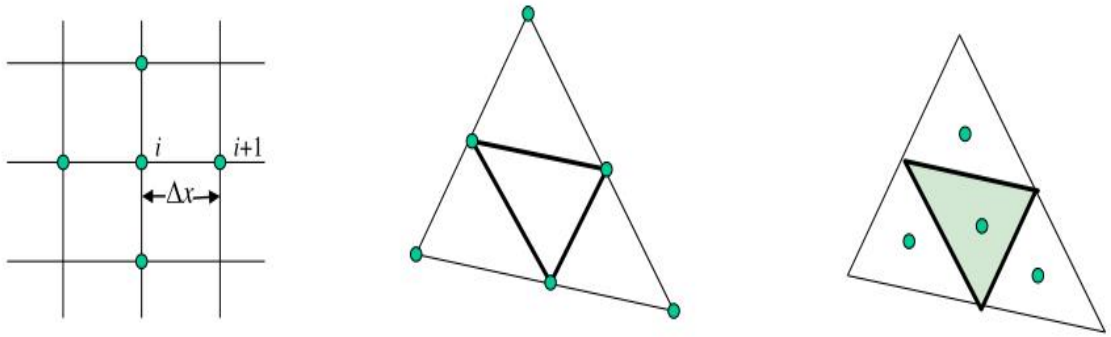

(a) Finite-Difference Method (b) Finite-Element Method (c) Finite-Volume Method

Figure 4.1: The finite-difference and finite-element methods[https://image1.slideserve.com/slide7-l.jpg] [94]

4.4 Problem

The most effective technique to design and evaluate the performance of electromagnetic devices and components is a computer-aided numerical analysis of electromagnetic fields, since analytical methods have limitations, whereas experiments are time-consuming and expensive [96]. The corresponding computations entail finding values of one or more unknown functions, such as magnetic-field strength, magnetic-flux density, magnetic scalar potential, and magnetic vector potential. The problem is defined in terms of Maxwell's equations, which are differential equations with boundary conditions that mathematically describe electromagnetic processes. For relatively fundamental issues, analytical approaches such as conformable representation, variable separation, and Green's function methods can solve problems exactly. On the other hand, complex issues, including heterogeneous materials, loads, and non-trivial boundary conditions, require the application of either analytically solvable, simplified models or numerical methods. The latter are often superior to analytical methods. Numerical methods usually approximate solutions that accurately represent the real problem [97].

4.5 Basic Concept of the FEM

The FEM is a common method for solving electromagnetic problems expressed in terms of differential equations with known boundary conditions [92][90][98]. The continuous field is expressed as a linear combination of contributions from finite elements covering the given domain [99]. The solution for each element is represented by using straightforward interpolation functions. Due to the fact that the FEM formulates all the elements before introducing the boundary condition, it is not necessary to test out the solutions for each element that satisfies the boundary conditions [17]. Because of this, the method can be simplified by using the same interpolation function for all the elements in the domain. The formulation of the variational principle implicitly satisfies the boundary conditions of the second kind (Neumann condition) and the third kind (Dirichlet condition) [88][100], making the FEM even more applicable.

4.5.1 Basic Steps of the FEM

The key is to create and solve a system of algebraic equations [101][102] following the fundamental steps of the FEM:

4.5.1.1 Construction of the functional: which needs to be minimized by applying (usually) the Ritz's variational technique and Galerkin's method in order to solve the PDE.

4.5.1.2 Discretization or subdivision of the solution domain: It is common practice to divide a solution domain into smaller elements based on its geometrical and physical properties. One-dimensional domains may employ linear segments, whereas two-dimensional domains may employ triangular or quadrilateral components. Tetrahedra, triangular prisms, and rectangular bricks are examples of fundamental components that can be employed in three-dimensional domains [103].

4.5.1.3 Selection of the interpolation function: The values of certain fields within a particular element are roughly estimated using interpolation algorithms. The required level of precision and the time commitment determine the choice of the interpolation function, usually in terms of the polynomial order. In general, the precision and formulation complexity grow with the polynomial order. It is typically enough to utilize the first- or the second-order polynomials [104].

4.5.1.4 Solution of the system of equations: The proper boundary conditions (Dirichlet, Neumann or combined) are set, and the algebraic system of equations is solved using techniques like Gaussian elimination or the Newton-Raphson method. A clear and understandable presentation of the results using graphs, plots, or images with color-coded areas is essential once the solution has been found. This makes the evaluation and validation of the results easy for developers [105].

4.6 PDEs Describing the Magnetostatics Problem

The main computational problem here is to calculate the magnetic field around a magnet with a cylindrical symmetry by solving Poisson's equation for the case of the scalar potential. (2.32) [106] [107]. Due to the geometry of the considered magnets, it is convenient to apply the cylindrical coordinates in two dimensions. Since the derivatives with respect to the azimuthal angle vanish, the relevant operators read as:

$$\nabla = \left(\frac{\partial}{\partial x}, \frac{\partial}{\partial y}\right) \tag{4.1}$$

and:

$$\nabla^2 = \frac{1}{x}\frac{\partial}{\partial x} x \frac{\partial}{\partial x} + \frac{\partial^2}{\partial y^2} \tag{4.2}$$

where x is the radial, and y the direction along the magnet's principal axis.

4.7 Triangular Finite Elements

In order to solve Poisson's equation (2.32) in terms of the finite-element method, it is necessary to cover the investigated domain with a discrete mesh of nodes [108]. The mesh is constructed so that three neighboring nodes form a triangle. Each node *i* is associated with a so-called test function $f_i(x, y)$ [100][109], which is equal to one at the node *i* and zero at all other nodes. Within each triangle, which includes the node *i,* it linearly drops from one to zero, forming a pyramid, shown in Figures 4.2 and 4.3. Each facet, defined by the nodes *i*, *j* and *k,* is described by the shape function:

$$f_{ijk}(x, y) = a_{ijk} + b_{ijk}x + c_{ijk}y \tag{4.3}$$

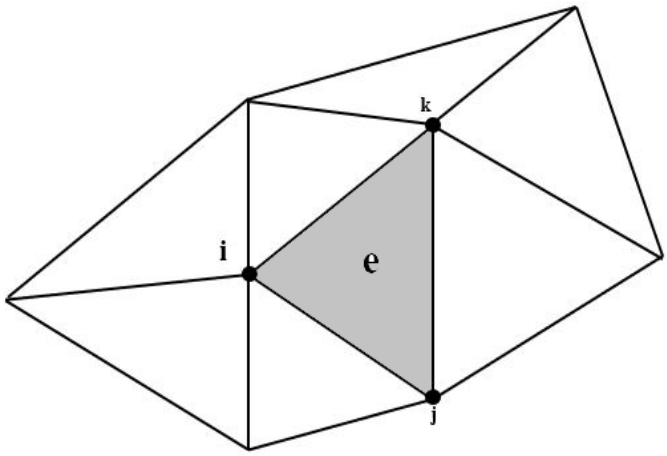

Figure 4.2: Representation of the triangular element „*e*"

where a_{ijk}, b_{ijk} and c_{ijk} are constant coefficients defined by the condition $f_{ijk}(x_i, y_i) = 1$ at the node *i* and zero at the nodes *j* and *k*.

The coefficients a_{ijk}, b_{ijk} and c_{ijk} of the shape function $f_{ijk}(x, y)$ are determined by solving the system of linear equations [27]:

$$\begin{pmatrix} 1 & x_i & y_i \\ 1 & x_j & y_j \\ 1 & x_k & y_k \end{pmatrix} . \begin{pmatrix} a_{ijk} \\ b_{ijk} \\ c_{ijk} \end{pmatrix} = \begin{pmatrix} 1 \\ 0 \\ 0 \end{pmatrix} \tag{4.4}$$

yielding:

$$a_{ijk} = \frac{x_j . y_k - x_k . y_j}{D} \tag{4.5}$$

$$b_{ijk} = \frac{y_k - y_j}{D} \tag{4.6}$$

$$c_{ijk} = \frac{x_k - x_j}{D} \tag{4.7}$$

with:

$$D = x_j y_k - x_k y_j + x_i y_k - x_k y_i + x_i y_j - x_j y_i \tag{4.8}$$

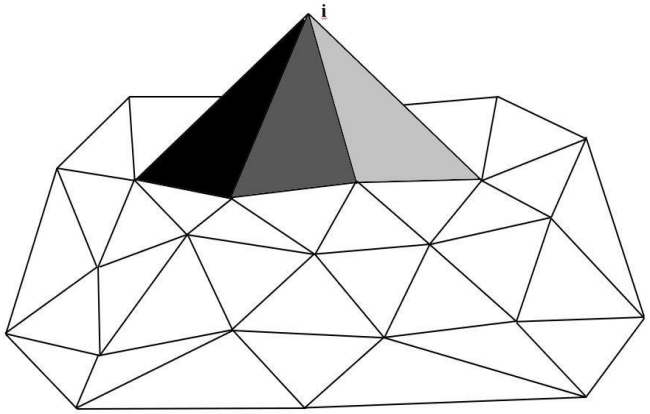

Figure 4.3: Test function f_i in the shape of a pyramid.

The area S_e of the element „*e*" is the determinant:

$$S_e = \frac{1}{2}\begin{vmatrix} 1 & x_i & y_i \\ 1 & x_j & y_j \\ 1 & x_k & y_k \end{vmatrix} \tag{4.9}$$

The test function $f_i(x,y)$ is constructed from the shape functions $f_{ijk}(x,y)$ for each triangle, which includes the node i. Any scalar field $u(x,y)$ defined in the considered domain (x,y) is a linear combination:

$$u(x,y) = \sum_{i=1}^{n(e)} f_i(x,y)A_i \ , \tag{4.10}$$

where A_i are the expansion coefficients and n are the number of nodes in the domain:

4.8 FEM and Poisson's Equation

The Laplace, a second-order operator, of any linear shape function $f_{ijk}(x,y)$ is by default equal to zero. Hence, it is not possible to determine the coefficients A_i simply just by inserting (4.10) into (2.32) and setting a system of linear equations. The workaround is to consider the relations:

$$\int \nabla^2 u(x,y)v(x,y)d\vec{S} = -\int \nabla u(x,y).\nabla v(x,y)d\vec{S}, \tag{4.11}$$

where $v(x,y)$ is an arbitrary scalar field in the domain, vanishing at the boundary. The validity of the above equation can be proved simply by integrating the divergence:

$$\nabla(v\nabla u) = \nabla u.\nabla v + v\nabla^2 u \tag{4.12}$$

and taking into account Stokes' theorem, which yields the left-hand zero due to the condition $v(x,y)=0$ at the domain boundary. It is straightforward to proceed. The Poisson's equation:

$$\sum_i \nabla^2 f_i(x,y)A_i = f \tag{4.13}$$

multiplied by any $f_j(x,y)$ and integrated over domain

$$\int \sum_i \nabla^2 f_i(x,y)\, f_j(x,y) A_i d\vec{S} = \int f \quad f_j(x,y) d\vec{S} \tag{4.14}$$

is transformed into:

$$\begin{pmatrix} M_{11} & \cdots & M_{1n} \\ \vdots & \ddots & \vdots \\ M_{n1} & \cdots & M_{nn} \end{pmatrix} \begin{pmatrix} A_1 \\ \vdots \\ A_n \end{pmatrix} = \begin{pmatrix} f_1^{'} \\ \vdots \\ f_n^{'} \end{pmatrix}, \tag{4.15}$$

where,

$$M_{ij} = -\int \nabla f_i(x,y).\nabla f_j(x,y) d\vec{S} \tag{4.16}$$

$$f_i^{'} = \int \nabla . f_i \quad f_i(x,y) d\vec{S} \tag{4.17}$$

The essential task is to diagonalize the equation (4.15) yielding the coefficients A_i. This task, along with the triangulation of the domain, was accomplished by applying the FEM software [110][107].

4.9 Application to the Simulation of a Self-Generation Electromagnetic Harvester

According to eq. (2.35) the induced voltage U_i is a time derivative of the magnetic flux and it is calculated as a sum of the surface S integrals for each of the N coil turns:

$$\phi = \sum_{i=1}^{N} \int_A B dS \tag{4.18}$$

Here, *B* represents the magnet-flux-density component in the direction along the coil's principal axis.

The magnet-modelling procedure is sketched in Figure 4.4. We utilize the magnetic properties of a modern sintered magnet (NdFeB-N50M) with the remanent magnetization value 1.435 T of the magnetic-flux density and the coercive value 988 kA/m of the magnetic field. In fact, the coercivity of the magnet is in this case not important as long as it is assumed that the generator operates in an absence of external magnetic fields. Furthermore, the specifications of the applied magnetics material are not essential for the investigations in the present thesis since the point is to compare the performance of the proposed solution with the performance obtained by applying standard magnets made of the same material. In this manner, a rather high value of the considered remanent magnetization (~1.4 T) does not affect the results of the simulations on different patterns and shapes of magnetization with a fixed magnitude.

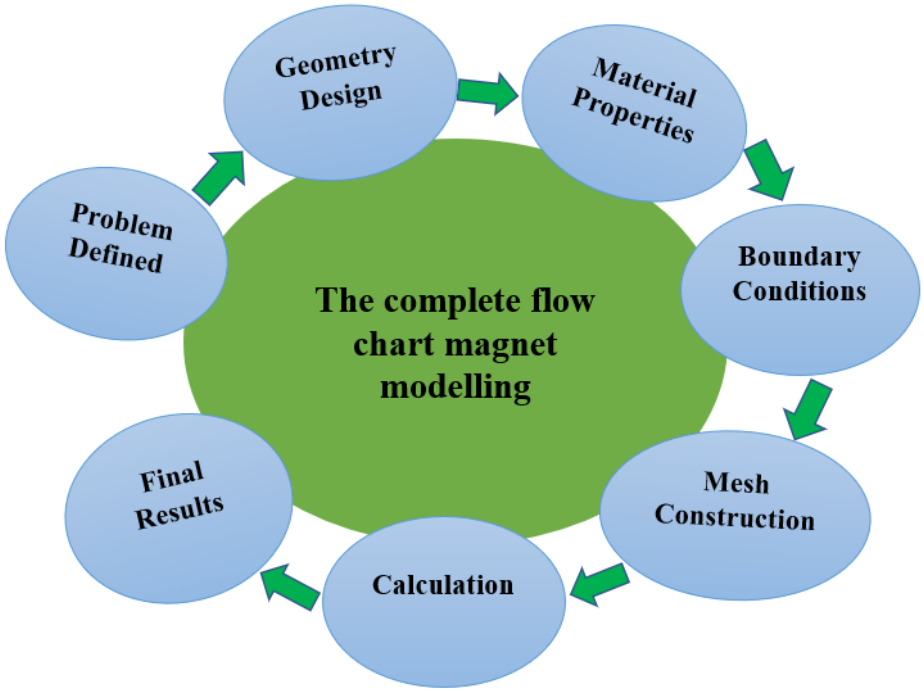

Figure 4.4: Complete flow chart of the magnet-modeling procedure.

The novelty in the presented magnet design are the notches in the sides of cylindrically-shaped magnets which contribute to the magnetic-field inhomogeneity and to a decreasing mass, and so less material being required. Their dimensions need to be optimized in order to gain the best results. Both primary magnet-coil-setup types- the OM and the SM- are sketched in Figure 4.5. The time dependence of the calculated magnetic flux was simulated using the finite-difference approximation of the time derivative in Eq. (4.18) by considering a set of magnet displacements u relative to the coil. A harmonic behavior $u = u_0 \sin(\omega t)$ was taken into account, where u_0 denotes the maximum displacement, and ω the angular frequency, set to $\omega = 1 s^{-1}$ for simplicity.

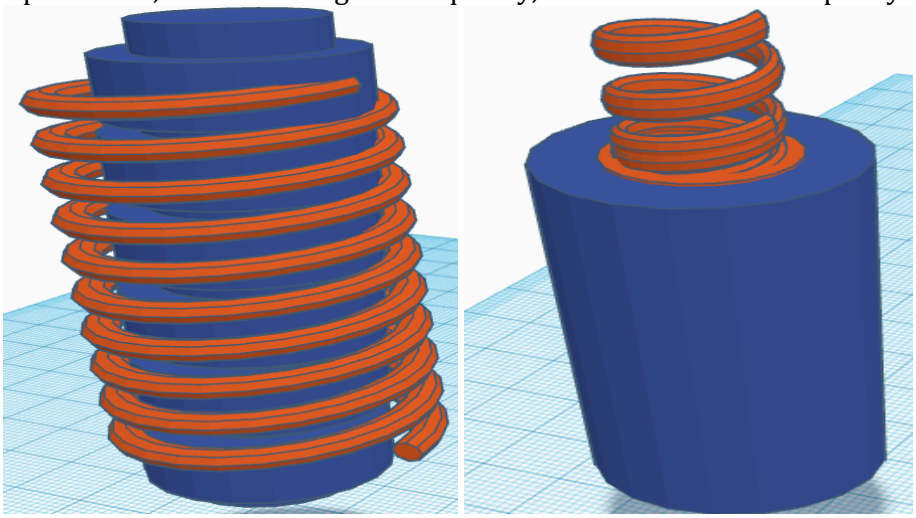

Figure 4.5: Two basic variants of the induction-based harvester: (left) a magnet oscillating within a static coil along its principle axis, (right) a coil oscillating within the hole of a static magnet. The notches engraved either in the outer (oscillating magnet) or in the inner (static magnet) side contribute to the non-homogeneity of the resulting magnetic field, to less weight, and consequently to a smaller amount of material being required. Note, the notches in the case of the static-magnet design (right) are not visible since they are inside the hole.

4.9.1 The oscillating magnet (OM) Modeling-Mesh Construction

The triangular-mesh density was determined on the basis of convergence testing. The mesh of the considered magnets (OM1, OM2, OM3 and OM4), magnetized uniaxially along the principal axis, which corresponds to the vibration direction, are presented in Figures 4.6, 4.7, 4.8 and 4.9. The notches within the simplest geometries OM1 and OM2 resemble single and double rectan-gles, respectively, whereas more complicated considered notches are of trapezoidal (OM3) or triangular (OM4) shape. The triangulation of regions with more pronounced field gradients (closer to the notches) necessitate a finer mesh.

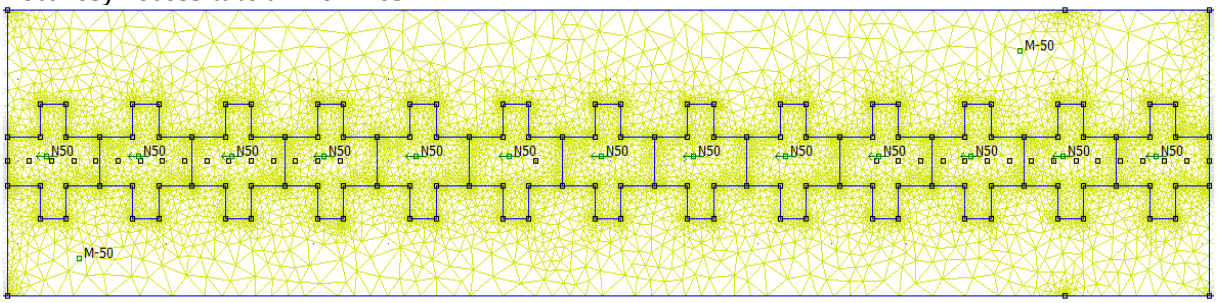

Figure 4.6: Mesh for the OM1 magnet.

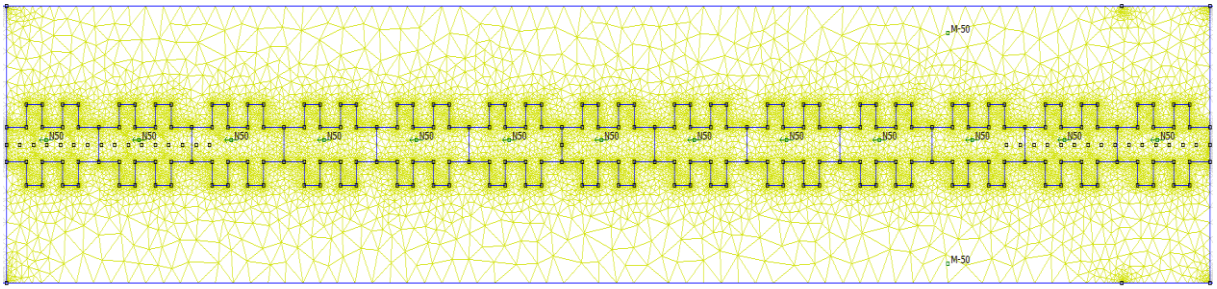

Figure 4.7: Mesh for the OM2 magnet.

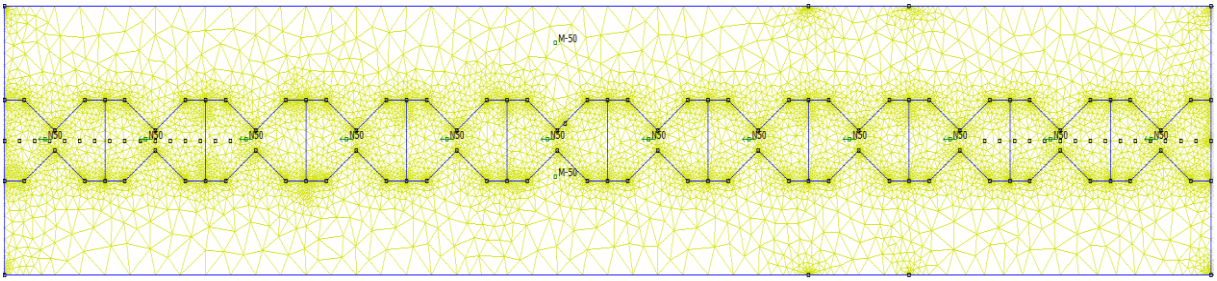

Figure 4.8: Mesh for the OM3 magnet.

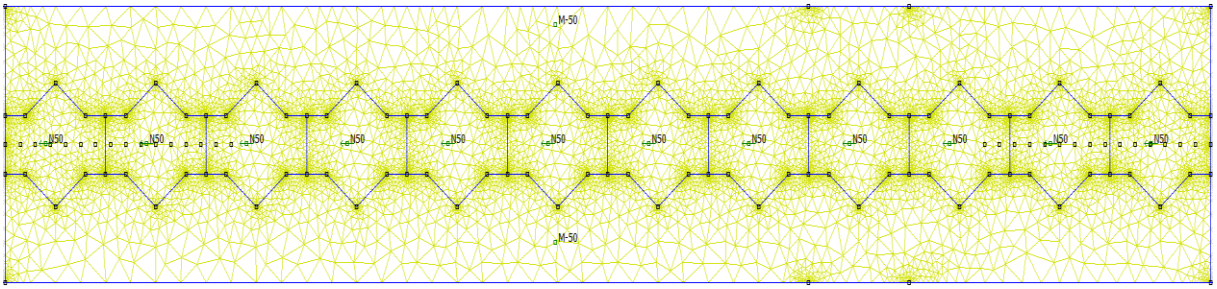

Figure 4.9: Mesh for the OM4 magnet in the equilibrium position.

4.9.2 Static-Magnet (SM) Modeling-Mesh Construction

Figures 4.10 to 4.13 display the meshes for the SM1, SM2, SM3, and SM4 magnets. The notches in the SM1 and SM2 geometry are rectangular, whereas they resemble trapezes and triangles in the SM3 and SM4, respectively.

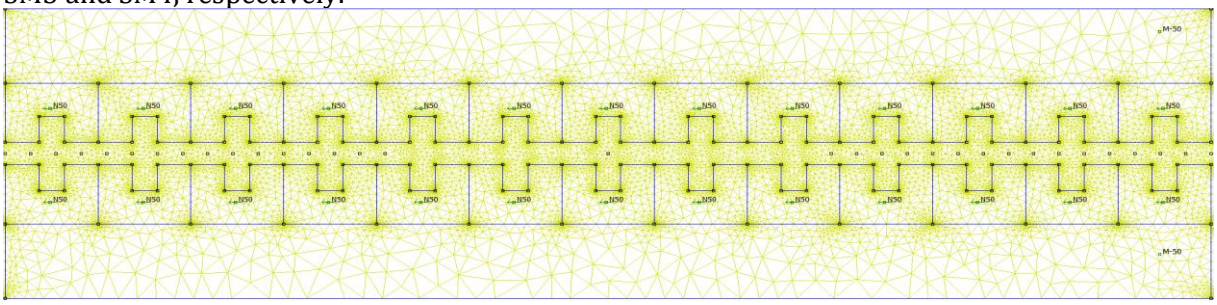

Figure 4.10: Mesh for the SM1 magnet.

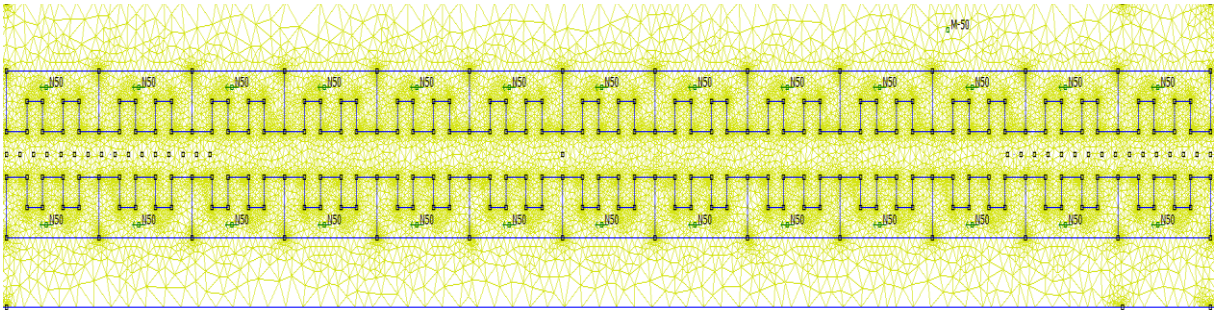

Figure 4.11: Mesh for the SM2 magnet.

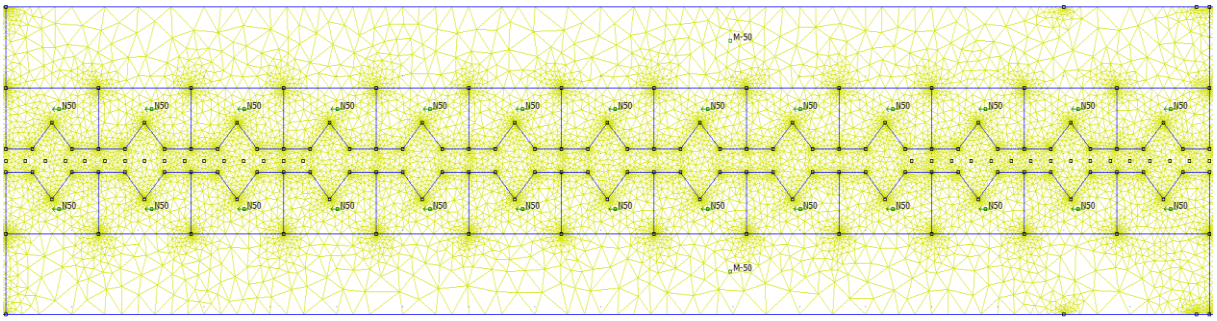

Figure 4.12: Mesh for the SM3.

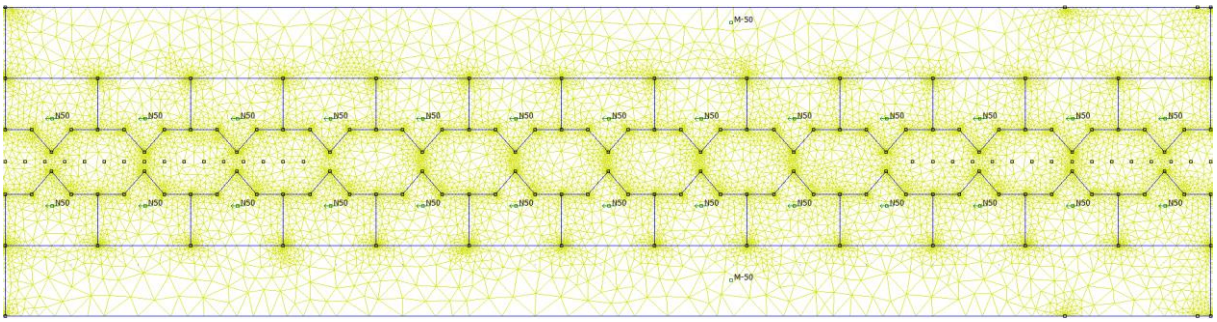

Figure 4.13: Mesh for the SM4 magnet.

Chapter 5

Results and Discussion

This chapter presents the published and some non-published results. According to the main objective of the thesis, to propose the most efficient magnet design, the key performance indicator is the (average) induced voltage per volume of the used material, determined on the basis of finite-element simulations. The comparison is carried out relative to the performance achieved with standard reference cylindrical-shaped magnets of the same outer dimensions made of the same material exhibiting Halbach or radial magnetization patterns. In order to prove the hypothesis that a proper design can result in a reduced material consumption without losing the performance the absolute values are not so important. Still, according to the literature **the normalized voltage of 4 V/cm³ is set as a reasonable threshold value**.

5.1 Oscillating Magnet (OM)

The performance of four oscillating permanent magnets, denoted as OM1, OM2, OM3, and OM4, depicted in Figures 4.6-4.9, is analyzed. The magnets are considered to be magnetized uniaxially along the principal axis, which corresponds to the vibration direction, have the properties specified in Chapter 4 although the resulting patterns do not depend on the remanence and the coercivity values. The magnetic-flux-density lines, calculated for the magnets in equilibrium with the coil, are illustrated in Figures 5.1, 5.2, 5.3, and 5.4. By following the flux-density lines and by assuming that the notches in the OM1 design are the least and the OM4 design are the most complex , in terms of geometrical description, it is obvious that the resulting non-homogeneity of the field grows with the complexity of design. However, the non-homogeneity of the fields (by considering a perfectly homogenous field described by parallel straight lines) in the OM4 as well as in the OM3 design is most pronounced between the neighboring notches, where the magnetic-flux-density component along the principal axis (which only contributes to the flux) is small (since the flux-density lines are dominantly in the transversal direction), , whereas the flux-density patterns around the magnets (in the figures, above and below the magnets) are more comparable. Nevertheless, **the results in Figures 5.1-5.4 clearly demonstrate** the magnet-shape influence on the resulting magnetic fields which is **the basic assumption** for the investigations conducted **in the present thesis**.

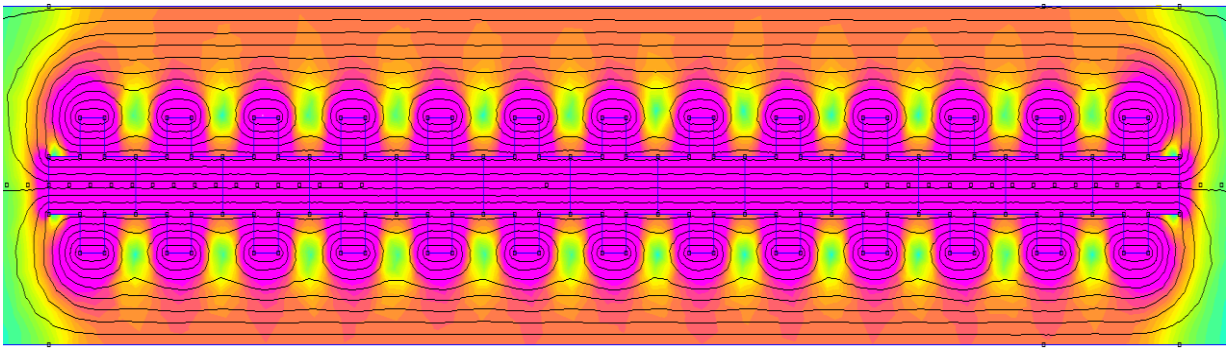

Figure 5.1: Calculated flux-density lines around the OM1 magnet in the equilibrium position.

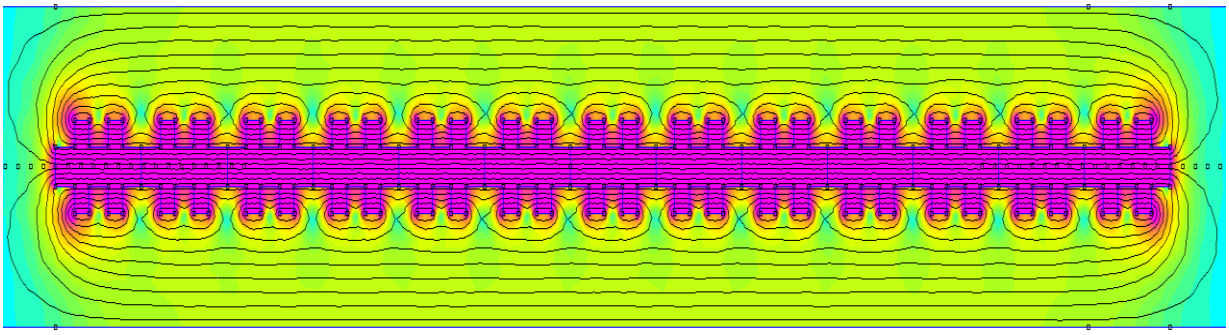

Figure 5.2: Calculated flux-density lines around the OM2 magnet in the equilibrium position.

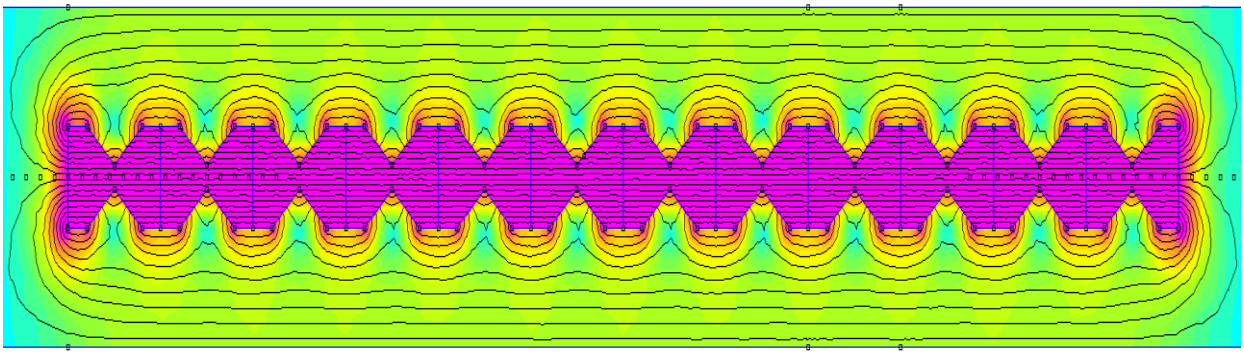

Figure 5.3: Calculated flux-density lines for the OM3 magnet in the equilibrium position.

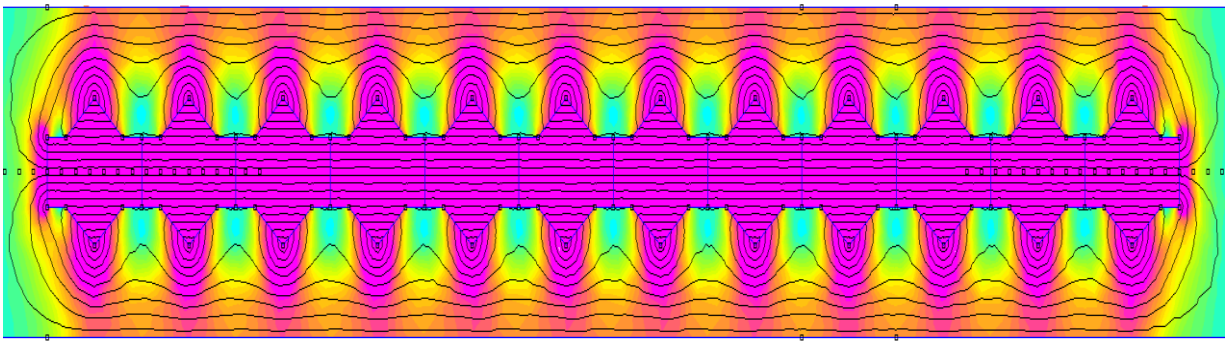

Figure 5.4: Calculated flux-density lines for the OM4 magnet in the equilibrium position.

5.1.1 Time-dependent Magnetic Flux and Induced Voltage for Oscillating Magnet

In order to quantitatively asses the influence of the oscillating-magnet-notch shapes and dimensions, , it is necessary to calculated the magnetic flux $\phi(t)$ as a function of time, presented in Figures 5.5–5.8. The time dependence was taken into account by calculating the along-the-axis component of the magnetic-flux density *B* for a set of the magnet displacements $u = u_0 \sin(\omega t)$, where u_0 is the amplitude and the angular frequency omega is set to $\omega = 1\mathrm{s}^{-1}$ for the sake of simplicity. The same simultaneously display the resulting induced voltage, calculated numerically as the negative time derivative of $\phi(t)$. Visually, the calculated time-dependent flux nearly perfectly replicates sinusoidal curves (magenta) with the amplitudes of about 20 Tm^2, proving the prediction from the previous section that different levels of the field non-homogeneity between neighboring notches do not play an important role, because they do not significantly contribute to the magnetic flux. Note, the flux at the equilibrium coil position with $u = 0$ is set to zero since only the time derivative matters for the further discussion. More characteristic quantity is the induced

voltage. The respective green curves in Figures 5.1-5.4 are not perfect minus cosine graphs. In all four cases the biggest discrepancy is around zero voltages, which correspond to the largest absolute flux values related to the maximum displacements of the oscillating magnet. This situation can be regarded as the end-point effect, where a part of the coil is a nearly-zero field as it follows from inspecting Figures 5.1-5.4, which qualitatively describes the deviation from the harmonic behavior. In all four cases the induced voltage amplitude is about 22 V (note, this quantity represents the output voltage and not the normalized voltage, which defines the set-up efficiency), further proving that the strongest non-homogeneity induced by different shapes of the notches, as shown in Figures 5.1-5.4, does not have an essential impact on the varying flux and consequently on the induced voltage. The numerically-calculated average absolute values of the induced voltage are 15.83 V, 15.5V, 15.11V, and 15.65V for the magnets OM1, OM2, OM3, and OM4, which are closed to $22/\sqrt{2}$ V =15.56 V as it follows analytically for an ideal harmonic function with the amplitude 22 V, reflected a certain inharmonicity in the calculated flux, discussed above.

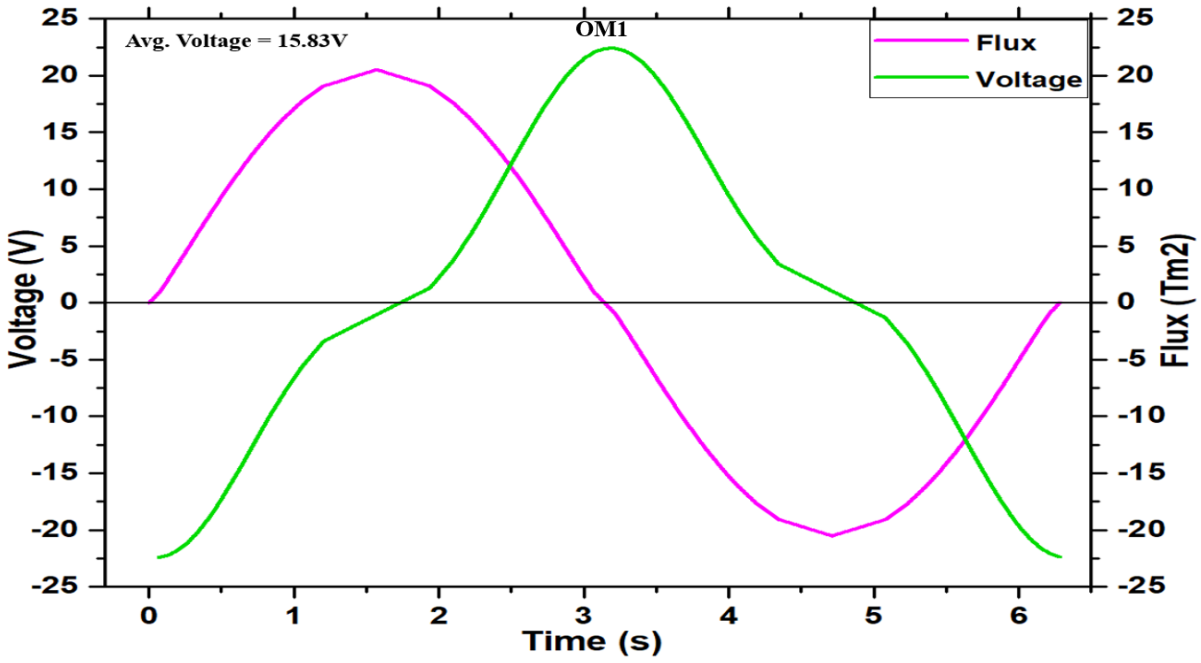

Figure 5.5: Calculated time-dependent magnetic flux relative to the equilibrium position and the induced voltage for the OM1.

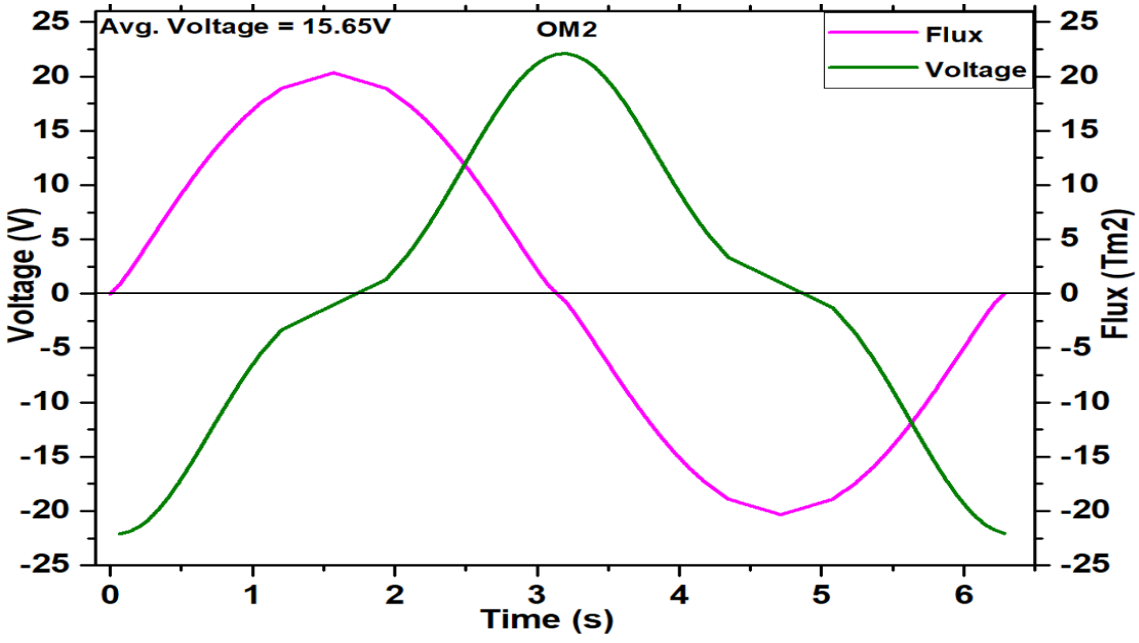

Figure 5.6: Calculated time-dependent magnetic flux relative to the equilibrium position and the induced voltage for the OM2.

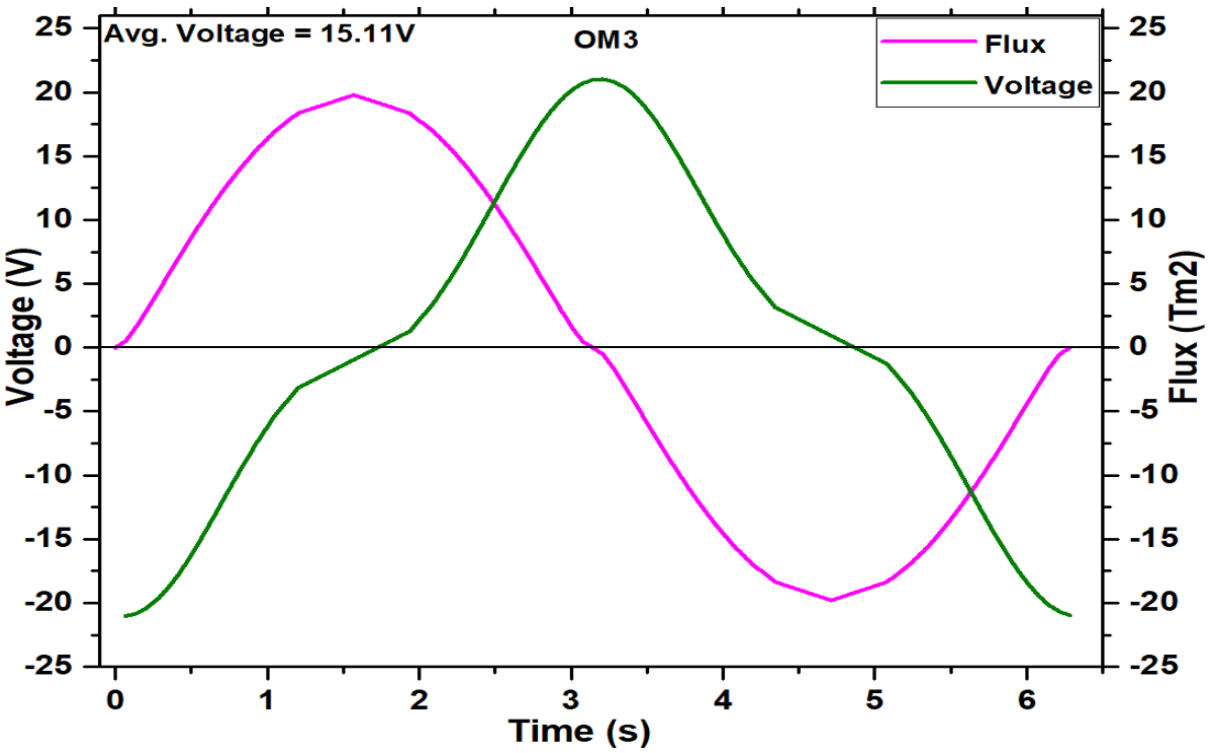

Figure 5.7: Calculated time-dependent magnetic flux relative to the equilibrium position and the induced voltage for the OM3.

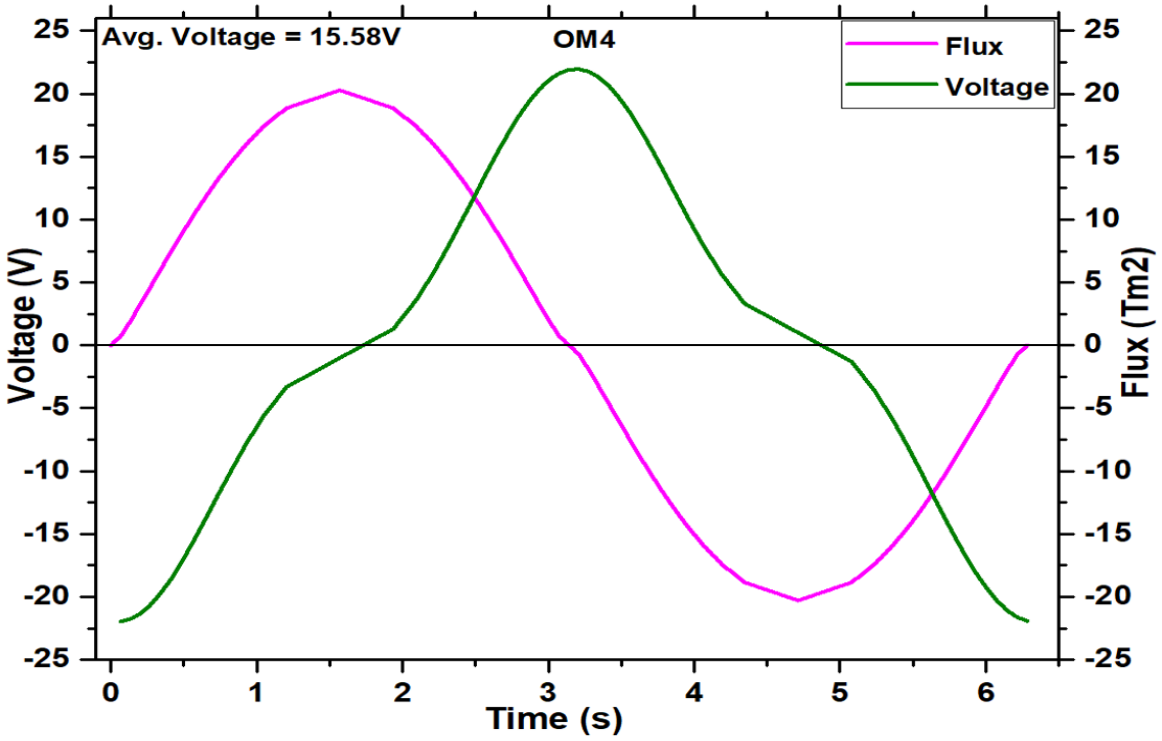

Figure 5.8: Calculated time-dependent magnetic flux relative to the equilibrium position and the induced voltage for the OM4.

5.1.2 Oscillating-Magnet1 Optimization (OM1O)

In order to determine the magnet design, which yields the highest average absolute voltage per volume (sometimes referred as the voltage normalized to volume or shortly normalized voltage) the considered geometries were optimized. The simplest method is to perform the optimization step by step for each of the parameters separately. In a particular step the normalized voltage is calculated as a function of a single parameter, whereas the other parameters are kept fixed either to values determined in the previous steps or to some arbitrary value. The value of the parameter considered at a certain step, for which the normalized voltage exhibits its peak is regarded as the optimized parameter. Since the four considered OM geometries yield very similar average absolute voltages of about 15.5 V, it makes sense to optimize the one defined with the smallest number of parameters, namely the OM1, which can be regarded as made of segments, presented in Figure 5.9, defined by the parameters:

- L1 (height of the notch)
- L2 (width of the notch)
- D0 (outer diameter)

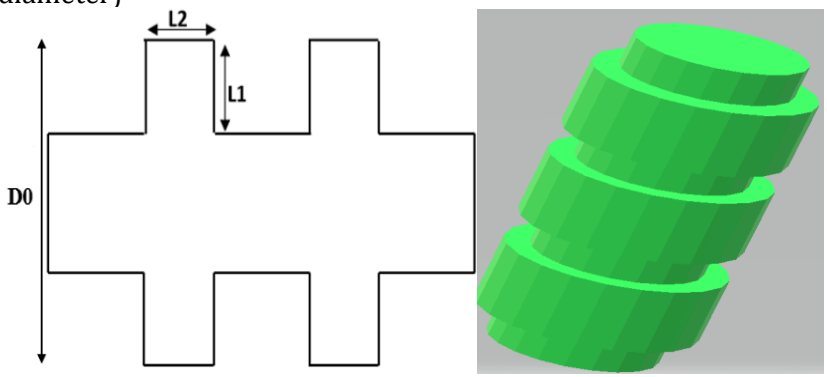

Figure 5.9: Oscillating magnet and the optimization parameters.

Figure 5.10 depicts the normalized voltage as a function of the notch height (L1) for four different notch widths (L2). Obviously, there is no significant influence of the L2 parameter, whereas the L1 dependence exhibits a pronounced peak at L1=3. the optimum combination is obtained for L2=2 and L1=3 in arbitrary units relative to the outer diameter D0 and the magnet length. Finally, the outer diameter D0 is optimized.

As it follows from Figure 5.11, the respective graph, presenting the normalized voltage vs. D0 in cm does not exhibit any peak, which means that the normalized voltage simply decreases with an increasing magnet volume. Therefore, it makes sense to compare the normalized voltage as a function of D0 with the normalized voltage produced by a cylindrical-shaped magnet with the Halbach-like magnetization pattern of the same length and D0. The normalized voltage of the Halbach-like magnet is below 1 V/cm^3 for a wide range of the D0 parameters, whereas the optimized OM magnet exhibits a pronounced D0 dependence, however, with the values well above. Assuming reasonable values of D0 between 1 and 2 cm for linear generators in portable devices, the normalized voltage of about 7 V/cm^3 can be easily achieved, which is well-above the target value of 4 V/cm^3.

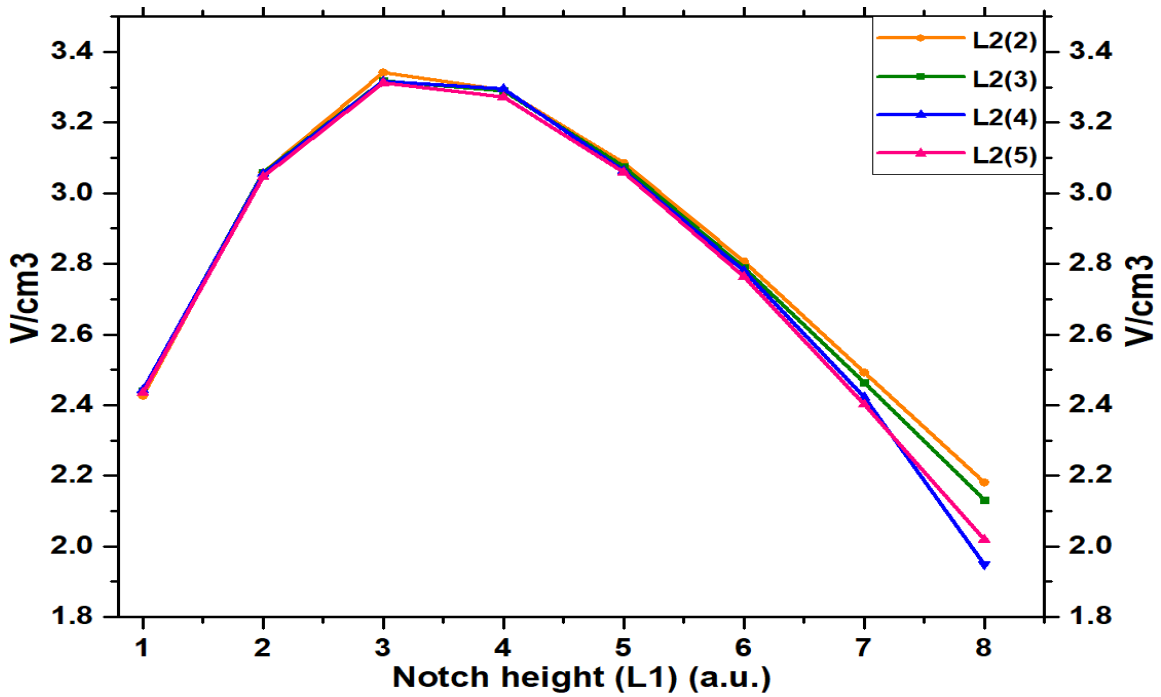

Figure 5.10: Normalized voltage for different values of the notch width L2 as a function of the notch height L1.

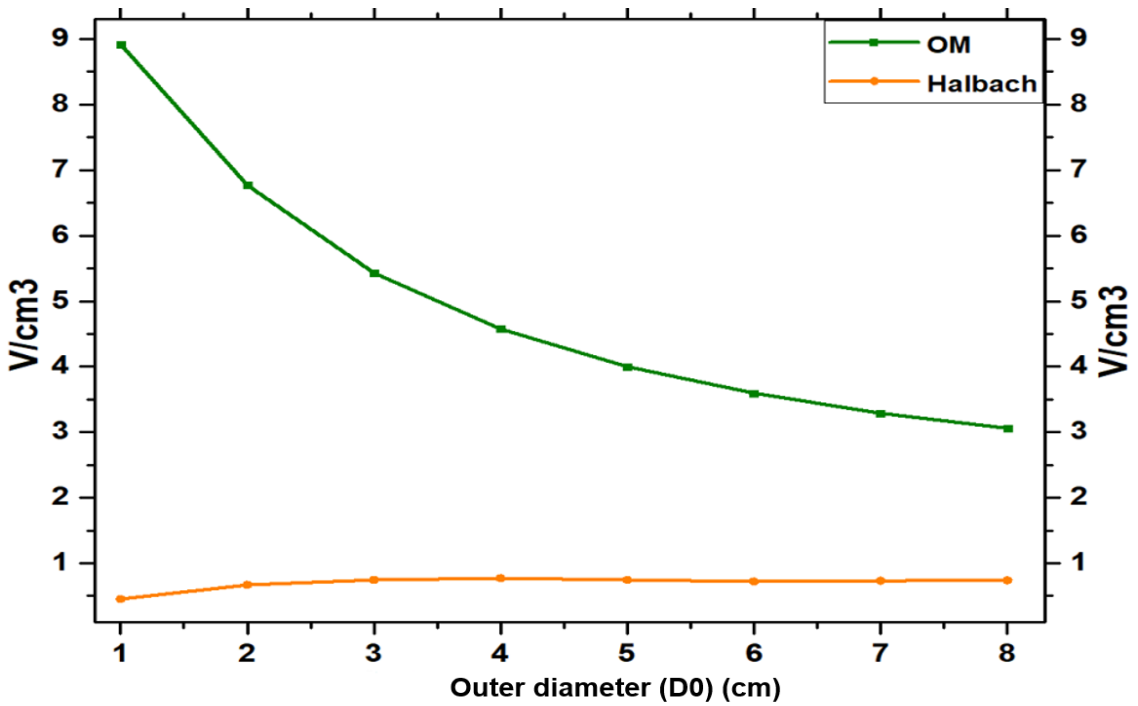

Figure 5.11: A comparison between the normalized voltages produced by the optimized OM and the classic Halbach magnet as functions of the diameter D0.

5.2 Static Magnet (SM)

Similarly, as in the case the oscillating magnets, the performance of four oscillating permanent magnets, denoted as SM1, SM2, SM3, and SM4, depicted in Figures 4.10-4.13, is analyzed. In this case, the notches are engraved in the outer surface, surrounding the hole, where the vibrating coil is located in a linear-generator set-up. The magnets are considered to be magnetized uniaxially along the principal axis, which corresponds to the vibration direction, have the properties

specified in Chapter 4 although the resulting patterns do not depend on the remanence and the coercivity values. The magnetic-flux-density lines, calculated for the magnets SM1, SM2, SM3 and SM4 in equilibrium with the coil, are illustrated in Figures 5.12-5.15.

By following the flux-density lines it is clear that the differences in design have a bigger influence on the resulting fields than in the case of the oscillating magnets. However, it seems that the transversal components (those which are perpendicular to the principal axis) are dominant, which might not be beneficial for the resulting fluxes, their time derivatives and induced voltages. By all means, it is ever more obvious that the magnet shape strongly influences the resulting fields by keeping their magnetization uniform.

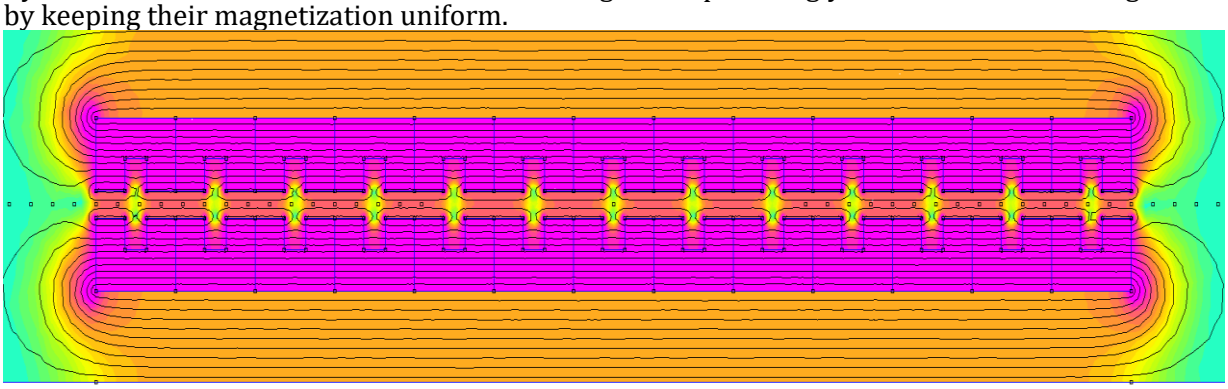

Figure 5.12: Calculated flux-density lines around SM1 for the equilibrium position.

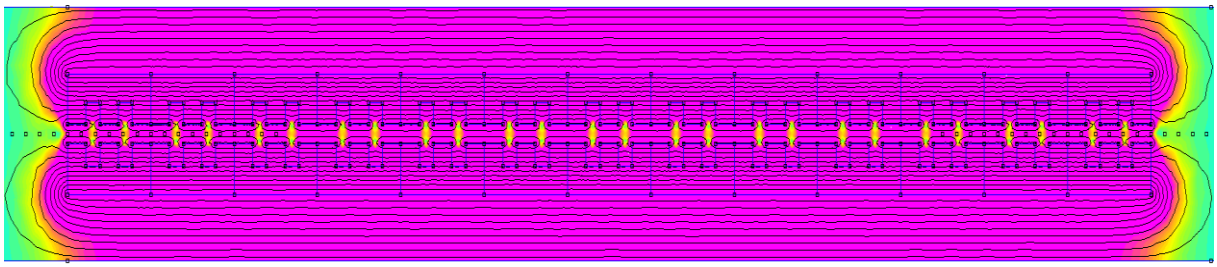

Figure 5.13: Calculated flux-density lines around SM2 for the equilibrium position.

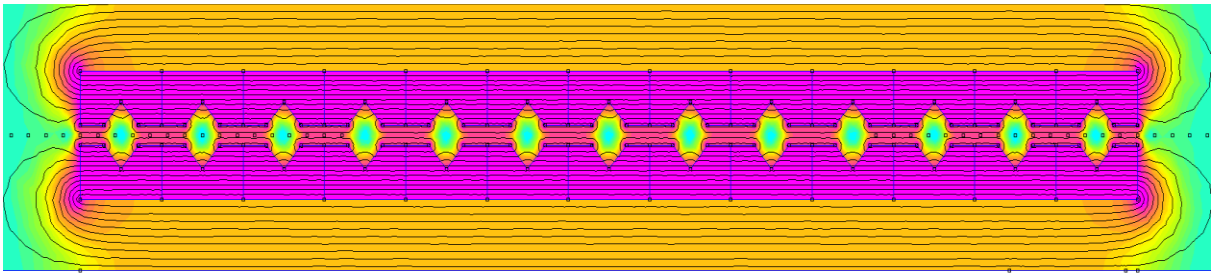

Figure 5.14: Calculated flux-density lines around SM3 for the equilibrium position.

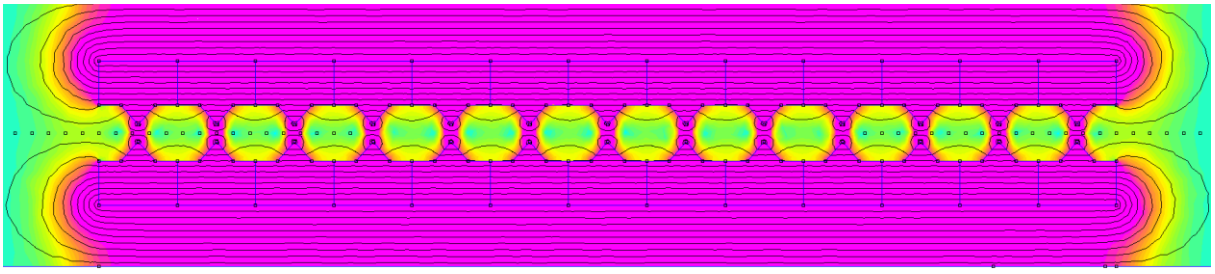

Figure 5.15: Calculated flux-density lines around SM4 for equilibrium position.

5.2.1 Time-dependent Magnetic Flux and Induced Voltage for Static Magnet

As in the case of the oscillating magnets, the qualitative assessment of the influence of static-magnet shape follows from the calculated time-dependent magnetic flux $\phi(t)$ and induced voltage, presented in Figures 5.16-5.19. The time dependence was taken into account by calculating the along-the-axis component of the magnetic-flux density B for a set of the magnet displacements $u = u_0 \sin(\omega t)$, where u_0 is the amplitude and the angular frequency omega is set to $\omega = 1s^{-1}$ for the sake of simplicity. Again, the calculated time-dependent flux visually nearly perfectly replicates sinusoidal curves (magenta). However, the amplitudes are lower than in the OM case, and the shape dependence is more pronounced, reflecting in the amplitudes of about 15 Tm² for the SM1 and SM2, and of about 12 Tm² and 5 Tm² for the SM3 and SM4, respectively as it is hinted from inspecting the flux-density-lines plots in Figures 5.12-5.15. Note again, the flux at the equilibrium coil position with $u = 0$ is set to zero since only the time derivative matters for the further discussion. The curves representing the induced voltage in Figures 5.16-5.19 are not perfect minus co-sinusoidal graphs, which might have a negative influence on the generator efficiency if the rectifier circuit contain active components like capacitors and coils. In all four cases the biggest discrepancy is around zero voltages, which correspond to the largest absolute flux values related to the maximum displacements of the oscillating magnet. This situation can be regarded as the end-point effect, where a part of the coil is a nearly-zero field as it follows from inspecting Figures 5.12-5.15, which qualitatively describes the deviation from the harmonic behavior. Lower flux amplitudes obviously induce lower induced-voltage amplitude of about 17 V (SM1 and SM2), 15 V (SM3), and 9 V (SM4). The numerically-calculated average absolute values are 12.81 V, 11.84 V, 10.66 V, and 8.11 V for OM1, OM2, OM3, and OM4, which means that the analytically-predicted values for an ideal harmonic function (sine or cosine) are exceeded in the case of SM1 (12 V) and SM4 (6.36 V), nearly matched for SM3 (10.6 V), or slightly above for SM2 (12 V). The analytically-predicted values are the induced voltage amplitudes divided by $\sqrt{2}$. That means that the inharmonicity is much more pronounced than in the case of the oscillating magnets, which is expected due to a higher level of non-homogeneity of the produced fields inside the static magnets in Figures 5.12-5.15.

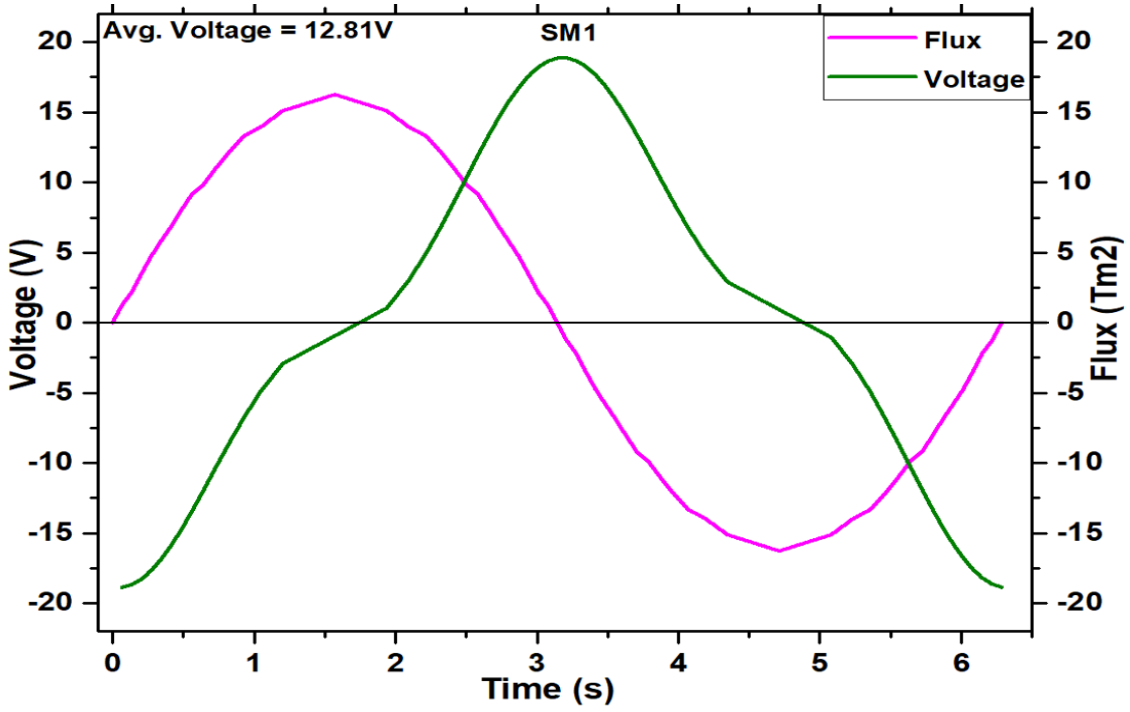

Figure 5.16: Calculated time-dependent magnetic flux relative to the equilibrium position and the induced voltage for the SM1.

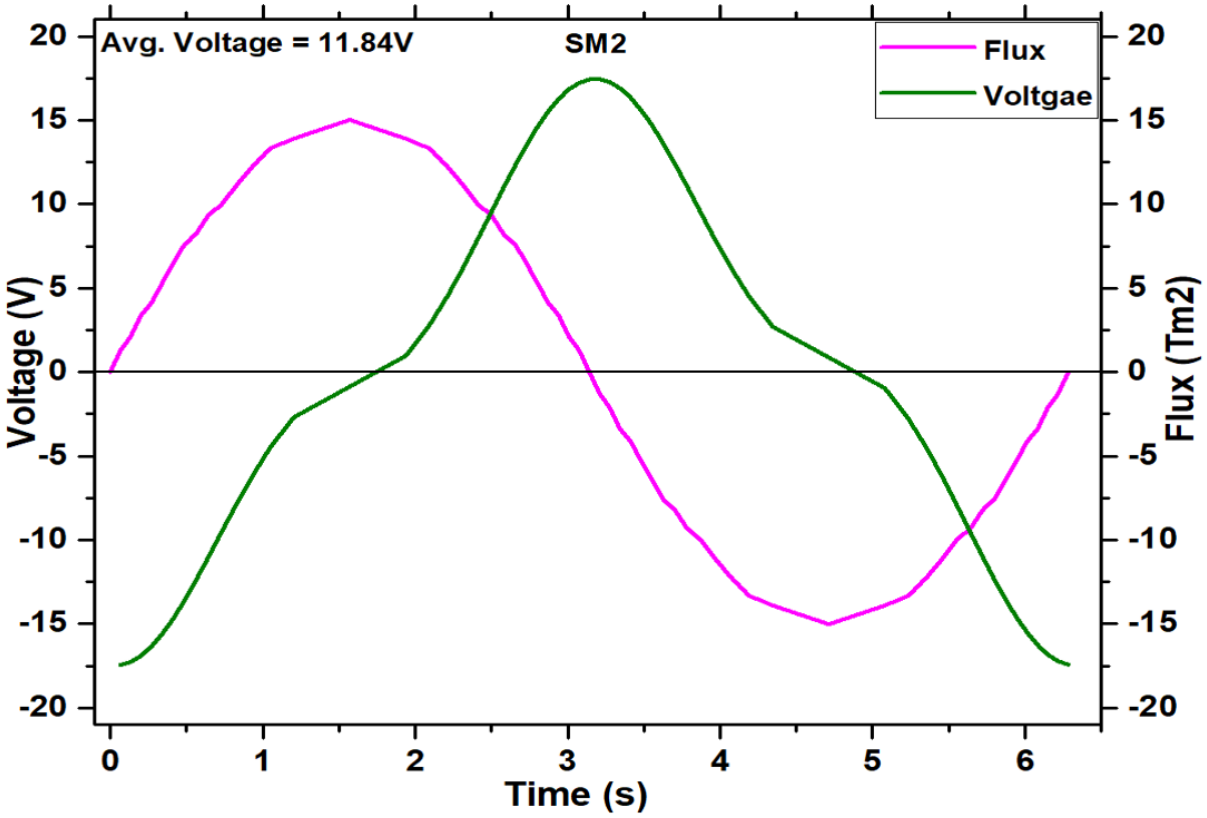

Figure 5.17: The calculated time-dependent magnetic flux relative to the equilibrium position and the induced voltage for the SM2.

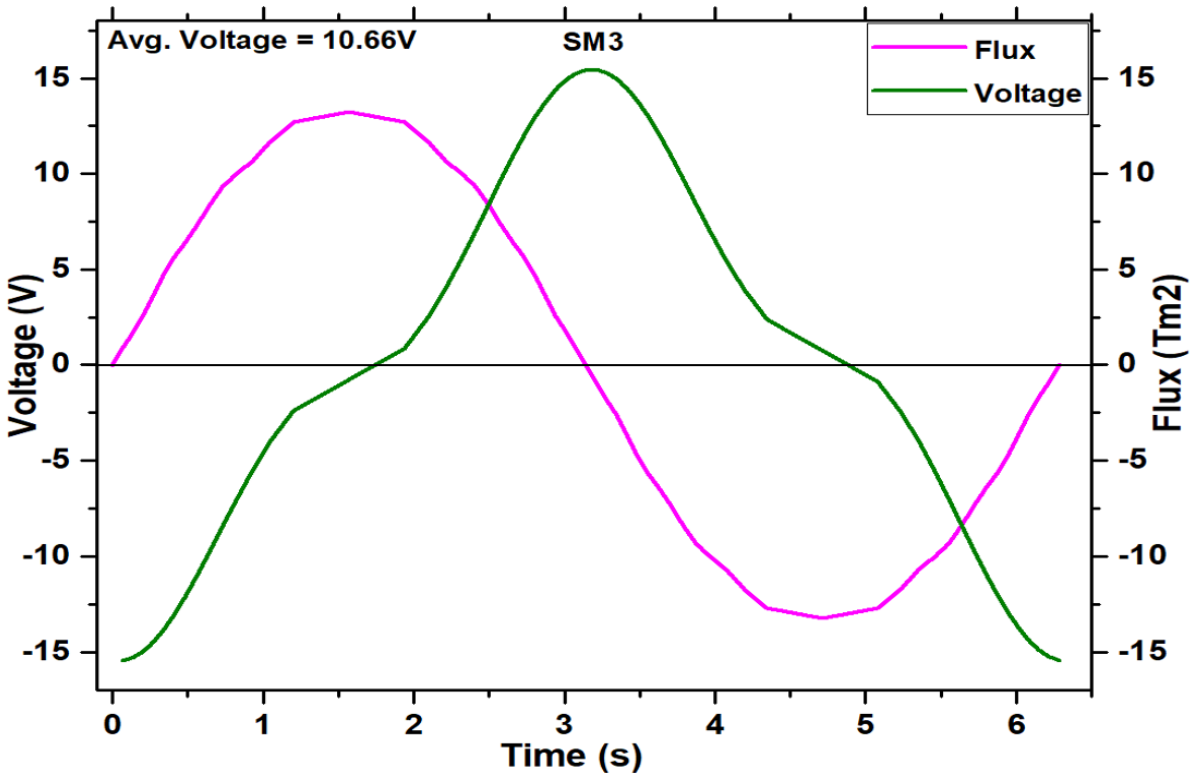

Figure 5.18: Calculated time-dependent magnetic flux relative to the equilibrium position and the induced voltage for the SM3.

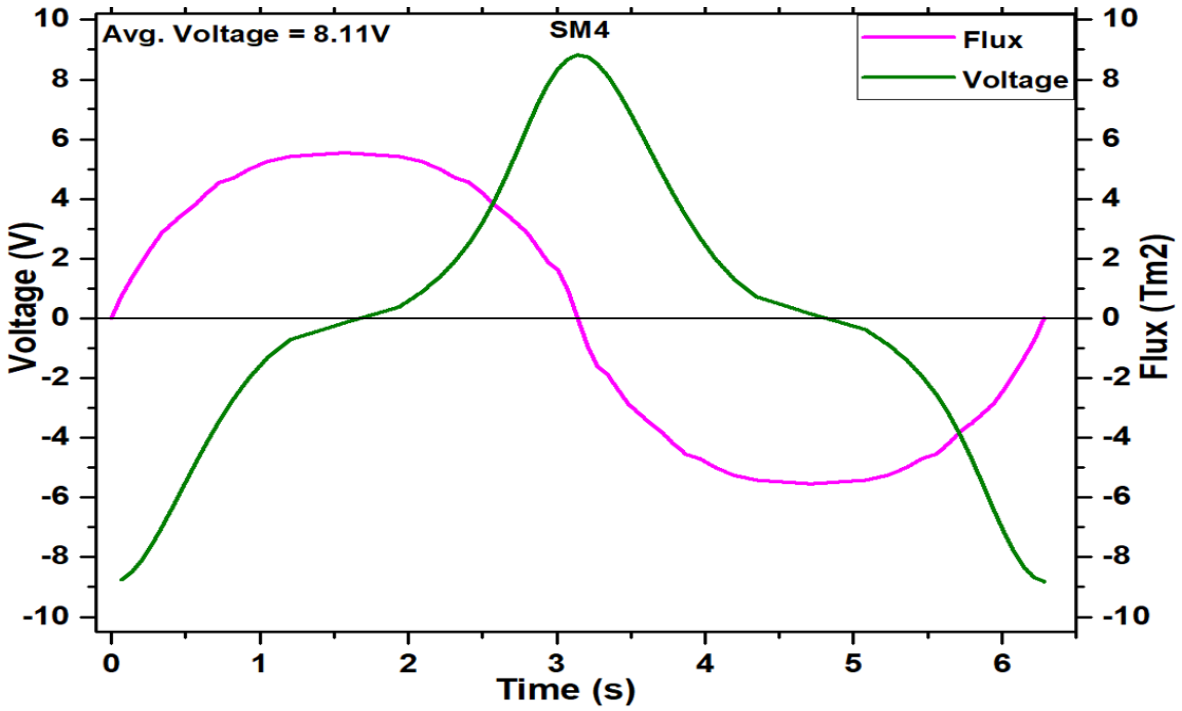

Figure 5.19: Calculated time-dependent magnetic flux relative to the equilibrium position and the induced voltage for the SM4.

5.2.2 Static Magnet1 Optimization (SM1O)

In order to determine the magnet design, which yields the highest average absolute voltage per volume (sometimes referred as the voltage normalized to volume or shortly normalized voltage) the considered geometries were optimized. The simplest method is to perform the optimization step by step for each of the parameters separately. In a particular step the normalized voltage is calculated as a function of a single parameter, whereas the other parameters are kept fixed either to values determined in the previous steps or to some arbitrary value. The value of the parameter considered at a certain step, for which the normalized voltage exhibits its peak is regarded as the optimized parameter. Since the SM1 geometry yields the highest average absolute voltage of 12.81 V and since this geometry is defined by the smallest number of parameters, it makes sense to perform the SM1 optimization. The respective magnet can be regarded as made of segments, presented in Figure 5.20, defined by the parameters:

- L1 (height of the notch)
- L2 (width of the notch)
- The inner diameter of the tube (D0)

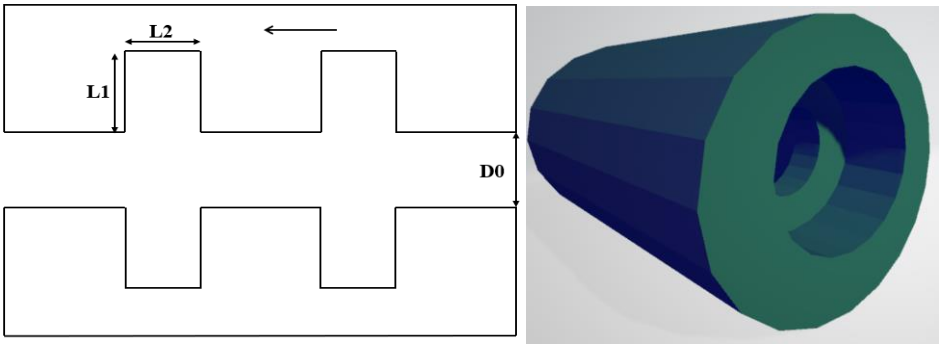

Figure 5.20: The parameters that need to be optimized in the case of a static magnet.

First, the normalized voltage is plotted for four different notch heights (L1) as a function of the notch width (L2) while keeping the diameter (D0) fixed, as shown in Figure 5.21. Contrary to the case of the oscillating magnets, the respective curves exhibit two peaks, reflecting the complexity

in the flux-density-lines plots in Figure 5.12, particularly in the regions between neighboring notches. However, it is obvious that the optimal combination of L1 and L2 is 4 and 6, respectively. After the L1 and L2 optimization the highest normalized voltage is about 3.1 V/cm^3 which is below the target value of at least 4 V/cm^3.

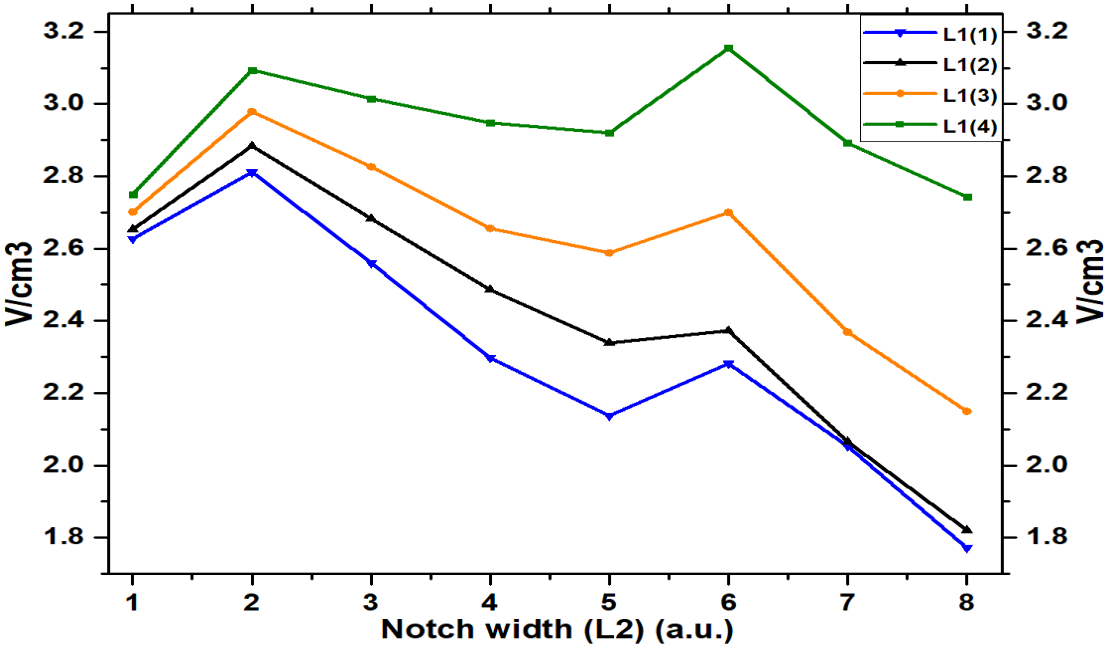

Figure 5.21: Voltage per volume as a function of the notch width L2 for different values of the notch height L1 and a fixed value of D0 in the case of the SM magnets.

However, there is still one parameter to be optimized. In the second phase, the impact of the inner diameter D0 is investigated. Note that the D0 in the SM case is presented in arbitrary units since it is defined relative to the outer dimensions of the magnet. The L2 width is kept constant at six, whereas the results are presented for various L1 values exhibited in Figure 5.22. These curves exhibit only one peak at D0=5 for all L1 values expect for the L1=4, for which the peak is shifted to D0=4, and which represents the optimized parameter associated with the normalized voltage of 5.2 V/cm^3, above the target value of 4 V/cm^3.

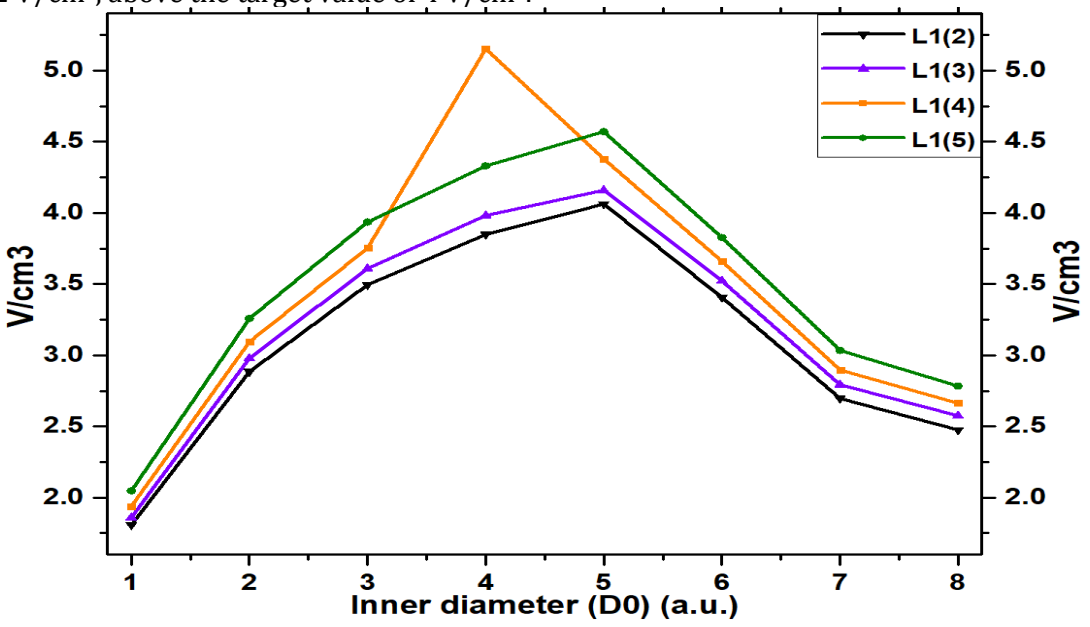

Figure 5.22: Calculated normalized voltage for L2 fixed to 6 for different values of L1 as functions of the inner diameter D0 in the case of the SM magnet.

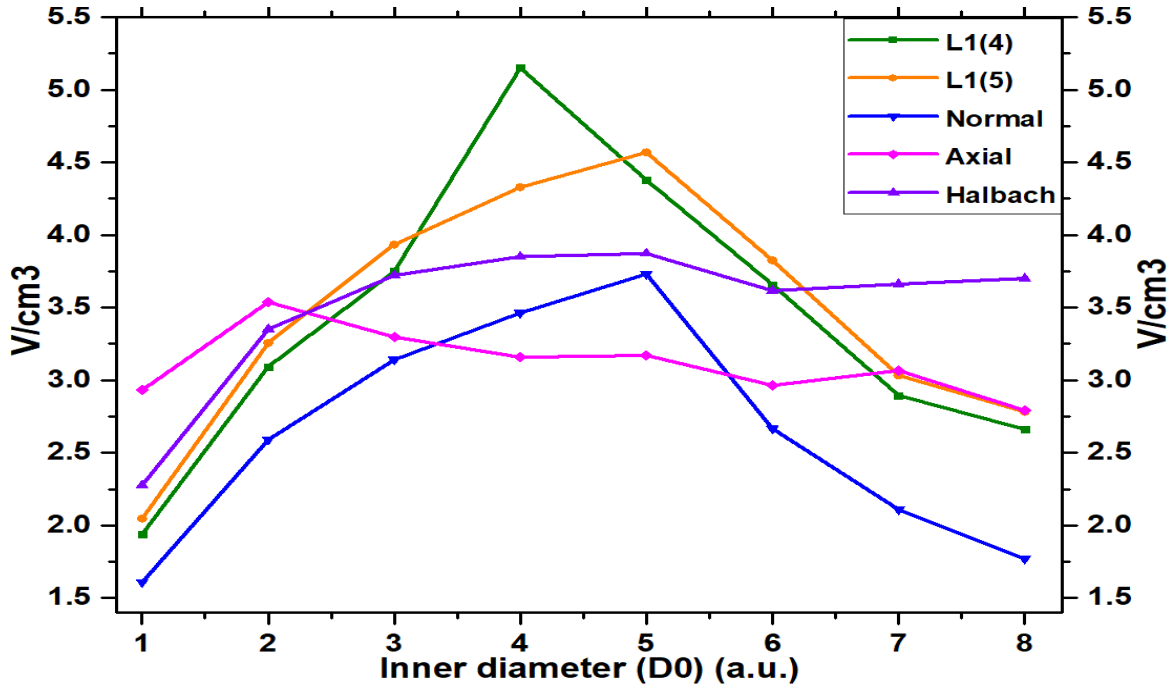

Figure 5.23: Comparison between our SM proposal and conventionally magnetized solid magnets with a tube-like shape.

Figure 5.23 presents a comparison between the calculated normalized voltages as functions of the inner diameter D0 that result from applying the optimized magnet geometry and different conventional solid (without notches) magnets with the same outer dimensions, magnetized uniaxially (Normal), axially (Axial) as a sequence of segments magnetized periodically in the left or right direction, and along the Halbach pattern (Halbach). Although solid magnets, particularly those magnetized along the Halbach pattern, can produce a higher absolute voltage, the advantage of notches is evident due to the reduced amount of material used, and even a non-optimal solution (where L1 equals 5) still yields a higher normalized voltage. Here L2 was kept to the optimum value of 6.

5.2.3 Discussion

The **presence of optimized notches reduces** the magnet volumes by **about 30% compared** to the cylindrical-shaped magnets of the same lengths and diameters, which act as the magnetic-field source in **the state-of-the-art linear generators** described in the available literature. The decreased volume is directly related to the reduced material consumption as it is one of the main motivations for the present thesis. The two considered concepts of the linear generator with either an oscillating or a static magnet are equivalent according to the Maxwell's equations, as stated in the hypothesis. However, static-magnet design is more complex due to the notches engraved in the inner wall surrounding the hole for the coil, which is reflected in a more pronounced non-homogeneity of the resulting field (in agreement with the hypothesis that the field pattern can be controlled by confining a uniform magnetization in an oddly-shaped area). The respective non-homogeneities favor the transversal flux-density-lines components; hence they do not contribute neither to the magnetic flux, nor to the induced voltage. The performance of the oscillating magnet is therefore better in terms of the calculated normalized voltage. Another advantage of the oscillating-magnet design is that the production by means of, for example, 3D printing, is probably simpler since the notches are present in the outer surface, whereas making notches in the inner surface, in the case of the static magnet, might be tricky. Although the static-magnet design is original and in the literature, there are no reports about comparable simulations, it probably represents a dead-end in development unless a certain application requires a sturdy housing, which might be represented by the magnet itself.

On the other hand, the oscillating-magnet-based solution without notches is common and already considered by means of FEM simulations [20], [111]–[113]. **In addition to the material savings**, the **single-step magnetization** along the uniaxial direction is **much simpler** than, for

example, complex Halbach arrangements, which require stacking of 12 [20], [112], 24 [112], 28 [112], 32 [111], [112], or even 82 [113] standard magnets.

The Table 5.2 presents a comparison between the normalized output voltage produced by the optimized OM1 magnet with the published, state-of-the-art results of FEM simulations for Halbach-type arrangements of standard Nd-Fe-B magnets. The **key-performance indicator** is the output voltage, normalized to the magnet volume. According to the literature the target value is 4 V/cm^3. A superior performance of the optimized OM1 magnet is obvious and the advantage of the proposed solution with engraved notches is even more important since it consists of a single, uniformly magnetized magnet. A Halbach (or axial) type of the magnet would be preferential only in the cases when a custom production is not possible or there is any other good reason for using standard, cylindrical-shaped magnets.

Table 5.2: A comparison between the maximum normalized voltage *U/V* for the optimized OM1 magnet with the published results obtained by means of the FEM calculations. The considered magnets are assembled from *N* pieces.

	[48]	[123]	[124]	[125]	OM1
U/V[V/cm^3*]*	2.5	3.9	4.2	5.1	6.6
N	12	32	32	82	1

As it follows from Figure 5.11, the normalized voltage exhibited by the optimized OM1 magnet can be even much higher by decreasing the diameter but this would imply technical problems related to the miniaturization of the respective coils, hence sticking to the diameters of about 1 cm makes sense.

Chapter 6

Conclusions

The thesis is devoted to the design of permanent magnets for application in linear, magnetic-induction-based generators as sustainable-energy sources for charging portable electronic devices. Several benefits of custom magnet design are demonstrated by means of the finite-element-method simulations. The magnetic field patterns, characterized by magnetic-flux-density lines, can substantially influenced by shaping a uniformly-magnetized magnet. It means that an oddly-shaped magnet, magnetized in a single step along one direction, can in principle yield the same magnetic field as a complex arrangement of many magnets, magnetized in different directions, which might be very beneficial in contemporary technologies, like additive manufacturing. At the same time, properly-designed magnets can contain less material as it is the main central goal of the thesis. The novelty in the magnet design are notches of various shapes and dimensions, engraved either in the outer or in inner surface of the magnet. As the measure for the magnet performance in the linear generator, the output induced voltage normalized to the magnet volume is considered. The target value is set to 4 V/cm^3, and it is achieved after optimizing the geometry parameters. It is demonstrated that a magnet of a special design, which volume is about 70% of a standard, cylindrical-shaped magnet, performs equally or even better. Two different concepts are tested. Although there is no principle differences in magnetic induction between an oscillating magnet- static coil and an oscillating coil- static magnet, the magnetic fields in the latter case exhibits the type of undesired non-homogeneities, which are not desired (with pronounced transversal components, which do not contribute to the flux), reflected in a lower output normalized voltage, not proving the Hypothesis 4.

The optimization curve for the oscillating magnet does not exhibit the peak with the highest normalized voltage as a function of outer diameter, which means that by decreasing the magnet size, the performance (in units of V/cm^3) would grow, contrary to the case of the standard Halbach arrangement with a nearly no dependence, which is used for a comparison. In this case the limit is the minimum accessible coil dimension.

Overall, the thesis goals are achieved, proposing alternative ways towards green-energy transition and reduced raw-material consumption.

6.1 Future Scope

The proposed magnets, designed and optimized in the frame of the thesis, will be produced by means of additive manufacturing and incorporated in a testing harvester. Its performance will be investigated by charging various portable devices. The real application will reveal potential problems, and the results will quantitatively assess the magnet's performance; the information will serve for further design improvements.

References

[1] W. Yang *et al.*, 'Harvesting energy from the natural vibration of human walking', *ACS Nano*, vol. 7, no. 12, pp. 11317–11324, 2013, doi: 10.1021/nn405175z.

[2] M. Wiatros-Motyka, 'Global Electricity Review: Global Trends', *Ember*, no. April, 2023, [Online]. Available: https://ember-climate.org/app/uploads/2021/03/Global-Electricity-Review-2021.pdf

[3] I. Baginsky, E. Kostsov, and A. Sokolov, 'Single-capacitor electret impact microgenerator', *Micromachines*, vol. 7, no. 1, pp. 1–11, 2016, doi: 10.3390/mi7010005.

[4] F. A. Baoquan Kou, S. B. Liyi Li, and T. C. Chengming Zhang, 'Analysis and optimization of thrust characteristics of tubular linear electromagnetic launcher for space-use', *2008 14th Symp. Electromagn. Launch Technol. EML, Proc.*, no. 2, pp. 48–53, 2008, doi: 10.1109/ELT.2008.16.

[5] A. Boduroglu, Y. Demir, R. Lyra, and M. Aydin, 'Influence of auxiliary teeth on performance of a permanent magnet linear motor', *Proc. - 2018 23rd Int. Conf. Electr. Mach. ICEM 2018*, pp. 779–784, 2018, doi: 10.1109/ICELMACH.2018.8507040.

[6] Y. Bp, S. Review, and W. Energy, '1951–201 1', 1951.

[7] BP, 'The Oil industry in 1951: Statistical Review', p. 7, 1951, [Online]. Available: https://www.bp.com/content/dam/bp/business-sites/en/global/corporate/pdfs/energy-economics/statistical-review/bp-statistical-review-1951.pdf

[8] BP, 'Statistical Review of World Energy globally consistent data on world energy markets and authoritative publications in the field of energy', *BP Energy Outlook*, vol. 70, p. 72, 2021.

[9] Z. L. Wang and J. Song, 'Piezoelectric nanogenerators based on zinc oxide nanowire arrays', *Science (80-.).*, vol. 312, no. 5771, pp. 242–246, 2006, doi: 10.1126/science.1124005.

[10] L. Cappelli, F. Marignetti, E. De Santis, Y. Coia, and R. Di Stefano, 'Design of a moving-coil linear generator for marine energy conversion', *Appl. Mech. Mater.*, vol. 416–417, pp. 311–316, 2013, doi: 10.4028/www.scientific.net/AMM.416-417.311.

[11] J. Bolt and J. Luiten Van Zanden, 'The Maddison Project: Maddison style estimates of the evolution of the world economy. A new 2020 update.', *Maddison Proj. Database, version 2020*, p. 44, 2020, [Online]. Available: https://www.rug.nl/ggdc/historicaldevelopment/maddison/publications/wp15.pdf

[12] V. De Aquino Neumann and R. P. Homrich, 'Comparison between radial and axial permanent magnet generators for low speed application', *Conf. Rec. - IEEE Instrum. Meas. Technol. Conf.*, pp. 251–256, 2014, doi: 10.1109/I2MTC.2014.6860746.

[13] M. Eid and H. Lee, 'Cogging Force Minimization of Linear', *Main*, pp. 116–120.

[14] A. E. ELGebaly and M. K. El-Nemr, 'Optimized design of PM halbach array linear generator for sea wave energy converters operate at maximum power transfer', *Adv. Sci. Technol. Eng. Syst.*, vol. 4, no. 4, pp. 440–448, 2019, doi: 10.25046/aj040453.

[15] A. E. Elgebaly and M. K. El-Nemr, 'Design and performance evaluation of halbach array linear generator for wave energy converters', *2015 IEEE 8th GCC Conf. Exhib. GCCCE 2015*, pp. 1–4, 2015, doi: 10.1109/IEEEGCC.2015.7060035.

[16] A. E. ElGebaly and M. K. El-Nemr, 'Bach Array Linear Generator for Wave Energy Converters', *J. Eng. Res.*, vol. 1, no. 2015, pp. 202–211, 2015, doi: 10.21608/erjeng.2015.126847.

[17] J. Elmes, V. Gaydarzhiev, A. Mensah, K. Rustom, J. Shen, and I. Batarseh, 'Maximum energy harvesting control for oscillating energy harvesting systems', *PESC Rec. - IEEE Annu. Power Electron. Spec. Conf.*, pp. 2792–2798, 2007, doi: 10.1109/PESC.2007.4342461.

[18] H. (Xi'an J. U. Shi, Z. (Zhejiang U. Liu, and X. (Xi'an J. U. Mei, 'Overview of Human Walking Induced Energy', *Energies*, 2019.

[19] Z. L. W. Xudong Wang, Jinhui Song, Jin Liu, 'Direct-Current Nanogenerator', *Science (80-.).*, vol. 316, no. April, pp. 102–105, 2007.

[20] S. Park, B. Kim, S. Kim, K. Lee, and J. Kim, '1461. Electric generator embedded in cellular phone for self-recharge', *J. Vibroengineering*, vol. 16, no. 8, pp. 3797–3806, 2014.

[21] T. Starner, 'Human Powered wearable', *Ibm Syst. J.*, vol. 35, no. 3, 1996.

[22] V. I. Goncharov, Y. V. Yezhov, V. G. Chirkin, S. V. Shirinskii, and D. A. Petrichenko, 'Linear reciprocating generator - sizing equations and mathematical model', *Glob. J. Pure Appl. Math.*, vol. 12, no. 4, pp. 3445–3462, 2016.

[23] I. Fazal, K. S. Rama Rao, and M. N. Karsiti, 'Modeling and simulation of a moving-coil linear generator', *Appl. Mech. Mater.*, vol. 110–116, pp. 2458–2463, 2012, doi: 10.4028/www.scientific.net/AMM.110-116.2458.

[24] B. J. Hansen, Y. Liu, R. Yang, and Z. L. Wang, 'Hybrid nanogenerator for concurrently harvesting biomechanical and biochemical energy', *ACS Nano*, vol. 4, no. 7, pp. 3647–3652, 2010, doi: 10.1021/nn100845b.

[25] N. Z. Governments, 'Product Profile : Battery Chargers', no. April, 2013.

[26] R. Jafari, P. Asef, M. Ardebili, and M. M. Derakhshani, 'Linear Permanent Magnet Vernier Generators for Wave Energy Applications: Analysis, Challenges, and Opportunities', *Sustain.*, vol. 14, no. 17, pp. 1–35, 2022, doi: 10.3390/su141710912.

[27] J. Jin *et al.*, 'Applied Superconductivity and Electromagnetic Devices - Principles and Current Exploration Highlights', *IEEE Trans. Appl. Supercond.*, vol. 31, no. 8, pp. 1–29, 2021, doi: 10.1109/TASC.2021.3108740.

[28] T. D. Kefalas and A. G. Kladas, 'Thermal investigation of permanent-magnet synchronous motor for aerospace applications', *IEEE Trans. Ind. Electron.*, vol. 61, no. 8, pp. 4404–4411, 2014, doi: 10.1109/TIE.2013.2278521.

[29] A. Pirisi, G. Gruosso, and R. E. Zich, 'Novel modeling design of three phase tubular permanent magnet linear generator for marine applications', *POWERENG 2009 - 2nd Int. Conf. Power Eng. Energy Electr. Drives Proc.*, pp. 78–83, 2009, doi: 10.1109/POWERENG.2009.4915209.

[30] N. M. Kimoulakis, A. G. Kladas, and J. A. Tegopoulos, 'Cogging force minimization in a coupled permanent magnet linear generator for sea wave energy extraction applications', *IEEE Trans. Magn.*, vol. 45, no. 3, pp. 1246–1249, 2009, doi: 10.1109/TMAG.2009.2012581.

[31] J. Jun, Y. Shin, S. J. Cho, Y. W. Cho, S. H. Lee, and J. H. Kim, 'Optimal linear generator with Halbach array for harvesting of vibration energy during human walking', *Adv. Mech. Eng.*, vol. 8, no. 5, pp. 1–8, 2016, doi: 10.1177/1687814016649880.

[32] H. W. Lee, C. B. Park, B. S. Lee, and H. J. Park, 'Exit end effect reduction of a linear induction motor for the deep-underground GTX', *19th Int. Conf. Electr. Mach. ICEM 2010*, pp. 10–13, 2010, doi: 10.1109/ICELMACH.2010.5607723.

[33] C. R. Saha, T. O'Donnell, N. Wang, and P. McCloskey, 'Electromagnetic generator for harvesting energy from human motion', *Sensors Actuators, A Phys.*, vol. 147, no. 1, pp. 248–253, 2008, doi: 10.1016/j.sna.2008.03.008.

[34] K. B. Lee, C. H. Park, and J. H. Kim, 'Optimal design of one-folded leaf spring with high fatigue life applied to horizontally vibrating linear actuator in smart phone', *Adv. Mech. Eng.*, vol. 2014, 2014, doi: 10.1155/2014/545126.

[35] C. Ranjan, 'Modelling Theory and Applications of the Electromagnetic Vibrational Generator', *Sustain. Energy Harvest. Technol. - Past, Present Futur.*, 2011, doi: 10.5772/27236.

[36] S. J. Cho and J. H. Kim, 'Linear electromagnetic electric generator for harvesting vibration energy at frequencies more than 50 Hz', *Adv. Mech. Eng.*, vol. 9, no. 10, pp. 1–9, 2017, doi: 10.1177/1687814017719001.

[37] G. Lei, J. Zhu, Y. Guo, C. Liu, and B. Ma, 'A review of design optimization methods for electrical machines', *Energies*, vol. 10, no. 12, 2017, doi: 10.3390/en10121962.

[38] G. Lei, J. Zhu, Y. Guo, C. Liu, and B. Ma, 'A review of design optimization methods for electrical machines', *Energies*, vol. 10, no. 12, pp. 1–31, 2017, doi: 10.3390/en10121962.

[39] J. Liu, F. Lin, Z. Yang, and T. Q. Zheng, 'Field oriented control of linear induction motor considering attraction force & end-effects', *Conf. Proc. - IPEMC 2006 CES/IEEE 5th Int. Power Electron. Motion Control Conf.*, vol. 1, pp. 184–188, 2007, doi: 10.1109/IPEMC.2006.297070.

[40] Y. Xu, D. Zhao, Y. Wang, and M. Ai, 'Electromagnetic Characteristics of Permanent Magnet Linear Generator (PMLG) Applied to Free-Piston Engine (FPE)', *IEEE Access*, vol. 7, pp. 48013–48023, 2019, doi: 10.1109/ACCESS.2019.2909278.

[41] D. Li, B. Bai, Q. Yu, and D. Chen, 'Cogging force minimization in a permanent magnet linear generator for sea wave energy extraction applications', *2009 Int. Conf. Energy Environ. Technol. ICEET 2009*, vol. 1, pp. 552–554, 2009, doi: 10.1109/ICEET.2009.140.

[42] L. Li, W. Li, D. Li, J. Li, and Y. Fan, 'Research on strategies and methods suppressing permanent magnet demagnetization in permanent magnet synchronous motors based on a multi-physical field and rotor multi-topology structure', *Energies*, vol. 11, no. 1, 2018, doi: 10.3390/en11010040.

[43] Y. Qin, X. Wang, and Z. L. Wang, 'Microfibre-nanowire hybrid structure for energy scavenging', *Nature*, vol. 451, no. 7180, pp. 809–813, 2008, doi: 10.1038/nature06601.

[44] J. M. Kim, M. M. Koo, J. H. Jeong, K. Hong, I. H. Cho, and J. Y. Choi, 'Design and analysis of tubular permanent magnet linear generator for small-scale wave energy converter', *AIP Adv.*, vol. 7, no. 5, pp. 1–6, 2017, doi: 10.1063/1.4974496.

[45] D. L. Trumper, M. E. Williams, and T. H. Nguyen, 'Magnet arrays for synchronous machines', *Conf. Rec. - IAS Annu. Meet. (IEEE Ind. Appl. Soc.*, vol. 1, pp. 9–18, 1993, doi: 10.1109/ias.1993.298897.

[46] H. Li and C. Xia, 'Halbach array magnet and its application to PM spherical motor', *Proc. 11th Int. Conf. Electr. Mach. Syst. ICEMS 2008*, pp. 3064–3069, 2008.

[47] C. Oprea, L. Szabo, and C. Martis, 'Multi-Phase Linear Generator for Electric Vehicle Applications', *Adv. Eng. Forum*, vol. 8–9, pp. 461–468, 2013, doi: 10.4028/www.scientific.net/aef.8-9.461.

[48] '1. https://electronics.stackexchange.com/questions/12851/why-is-three-phase-offset-by-120- degrees', p. 12851.

[49] M. Sáez and M. Loreto, 'Energy harvesting from human passive power', p. 263, 2009, [Online]. Available: http://www.tesisenred.net/handle/10803/48637

[50] A. H. Selçuk and H. Kürüm, 'Investigation of end effects in linear induction motors by using the finite-element method', *IEEE Trans. Magn.*, vol. 44, no. 7, pp. 1791–1795, 2008, doi:

10.1109/TMAG.2008.918277.

[51] A. S. Sergaliyev and L. A. Khajiyeva, 'Advances in Mechanism Design II', vol. 44, pp. 231–237, 2017, doi: 10.1007/978-3-319-44087-3.

[52] A. Raed and A. Mohammed, 'FEM Based Prototype of Moving-Coil Coreless Linear-Generator (MCCLG) for Wave Energy Extraction', *E3S Web Conf.*, vol. 64, 2018, doi: 10.1051/e3sconf/20186407005.

[53] J. Shendure *et al.*, 'Molecular biology: Accurate multiplex polony sequencing of an evolved bacterial genome', *Science (80-.).*, vol. 309, no. 5741, pp. 1728–1732, 2005, doi: 10.1126/science.1117389.

[54] H. Moradi CheshmehBeigi, 'Slotless tubular PM generator with dual quasi-Halbach magnetized PM Array: Analytical and numerical magnetic field analysis', *Int. J. Numer. Model. Electron. Networks, Devices Fields*, vol. 33, no. 2, pp. 1–14, 2020, doi: 10.1002/jnm.2569.

[55] K. Sitapati and R. Krishnan, 'Performance comparisons of radial and axial field, permanent-magnet, brushless machines', *IEEE Trans. Ind. Appl.*, vol. 37, no. 5, pp. 1219–1226, 2001, doi: 10.1109/28.952495.

[56] T. Yang, L. Zhou, and L. Li, 'Influence of design parameters on end effect in long primary double-sided linear induction motor', *IEEE Trans. Plasma Sci.*, vol. 39, no. 1 PART 1, pp. 192–197, 2011, doi: 10.1109/TPS.2010.2049383.

[57] M. A. Stelzer and R. P. Joshi, 'Evaluation of wave energy generation from buoy heave response based on linear generator concepts', *J. Renew. Sustain. Energy*, vol. 4, no. 6, 2012, doi: 10.1063/1.4771693.

[58] J. Subramanian, 'Design, Modeling and Optimization of Reciprocating Tubular Permanent Magnet Linear Generators for Free Piston Engine Applications', 2020, [Online]. Available: https://researchrepository.wvu.edu/etd/7869

[59] M. Trapanese, G. Cipriani, D. Curto, V. DI DIo, and V. Franzitta, 'Optimization of cogging force in a linear permanent magnet generator for the conversion of sea waves energy', *Proc. - 2015 IEEE Int. Electr. Mach. Drives Conf. IEMDC 2015*, pp. 769–773, 2016, doi: 10.1109/IEMDC.2015.7409146.

[60] B. Ekergård and M. Leijon, 'Longitudinal end effects in a linear wave power generator', *Energies*, vol. 13, no. 2, 2020, doi: 10.3390/en13020327.

[61] P. R. Upadhyay and K. R. Rajagopal, 'Comparison of performance of the axial-field and radial-field permanent magnet brushless direct current motors using computer aided design and finite element methods', *J. Appl. Phys.*, vol. 97, no. 10, 2005, doi: 10.1063/1.1853239.

[62] Y. W. Zhu, D. H. Koo, and Y. H. Cho, 'Detent force minimization of permanent magnet linear synchronous motor by means of two different methods', *IEEE Trans. Magn.*, vol. 44, no. 11 PART 2, pp. 4345–4348, 2008, doi: 10.1109/TMAG.2008.2001320.

[63] V. T. Nguyen, 'Analytical computation of the magnetic field of a conical permanent magnet with arbitrarily uniform magnetization', *AIP Adv.*, vol. 10, no. 4, 2020, doi: 10.1063/5.0004211.

[64] Y. Zou, L. Bo, and Z. Li, 'Recent progress in human body energy harvesting for smart bioelectronic system', *Fundam. Res.*, vol. 1, no. 3, pp. 364–382, 2021, doi: 10.1016/j.fmre.2021.05.002.

[65] S. A. Vargas, G. R. T. Esteves, P. M. Maçaira, B. Q. Bastos, F. L. Cyrino Oliveira, and R. C. Souza, 'Wind power generation: A review and a research agenda', *J. Clean. Prod.*, vol. 218, pp. 850–870, 2019, doi: 10.1016/j.jclepro.2019.02.015.

[66] K. Binnemans, P. T. Jones, K. Van Acker, B. Blanpain, B. Mishra, and D. Apelian, 'Rare-earth economics: The balance problem', *Jom*, vol. 65, no. 7, pp. 846–848, 2013, doi:

10.1007/s11837-013-0639-7.

[67] A. Chaudhuri, R. Datta, M. P. Kumar, J. P. Davim, and S. Pramanik, 'Energy Conversion Strategies for Wind Energy System: Electrical, Mechanical and Material Aspects', *Materials (Basel).*, vol. 15, no. 3, pp. 1–34, 2022, doi: 10.3390/ma15031232.

[68] Ф. Котлер, 'No TitleМаркетинг по Котлеру', p. 282, 2008.

[69] C. Five, 'MAGNETISM AND', no. ii.

[70] J. M. D. Coey, 'Magnetism and magnetic materials', *Magn. Magn. Mater.*, vol. 9780521816, pp. 1–617, 2010, doi: 10.1017/CBO9780511845000.

[71] 'Fig5,6.pdf'.

[72] 'fig24.pdf'.

[73] L. Vinet and A. Zhedanov, 'Atomistic Spin dynamics code', *J. Phys. A Math. Theor.*, vol. 44, no. 8, pp. 951–952, 2011.

[74] D. J. Sellmyer, A. Ahmed, G. Muench, and G. Hadjipanayis, 'Magnetic hardening in rapidly quenched Fe-Pr and Fe-Nd alloys', *J. Appl. Phys.*, vol. 55, no. 6, pp. 2088–2090, 1984, doi: 10.1063/1.333573.

[75] O. Gutfleisch, M. A. Willard, E. Brück, C. H. Chen, S. G. Sankar, and J. P. Liu, 'Magnetic materials and devices for the 21st century: Stronger, lighter, and more energy efficient', *Adv. Mater.*, vol. 23, no. 7, pp. 821–842, 2011, doi: 10.1002/adma.201002180.

[76] R. L. Stamps *et al.*, 'The 2014 Magnetism Roadmap', *J. Phys. D. Appl. Phys.*, vol. 47, no. 33, 2014, doi: 10.1088/0022-3727/47/33/333001.

[77] I. R. Harris and G. W. Jewell, 'Rare-earth magnets: Properties, processing and applications', *Funct. Mater. Sustain. Energy Appl.*, pp. 600–639, 2012, doi: 10.1533/9780857096371.4.600.

[78] M. Sagawa, S. Fujimura, H. Yamamoto, Y. Matsuura, and K. Hiraga, 'Permanent Magnet Materials Based on the Rare Earth-Iron-Boron Tetragonal Compounds.', *IEEE Trans. Magn.*, vol. MAG-20, no. 5, pp. 1584–1589, 1984.

[79] J. F. Herbst, 'R2Fe14B materials: Intrinsic properties and technological aspects', *Rev. Mod. Phys.*, vol. 63, no. 4, pp. 819–898, 1991, doi: 10.1103/RevModPhys.63.819.

[80] G. C. Hadjipanayis, R. C. Hazelton, and K. R. Lawless, 'Cobalt-free permanent magnet materials based on iron-rare-earth alloys (invited)', *J. Appl. Phys.*, vol. 55, no. 6, pp. 2073–2077, 1984, doi: 10.1063/1.333570.

[81] N. C. Koon and B. N. Das, 'Crystallization of FeB alloys with rare earths to produce hard magnetic materials (invited)', *J. Appl. Phys.*, vol. 55, no. 6, pp. 2063–2066, 1984, doi: 10.1063/1.333568.

[82] J. D. Jackson, 'Classical_Electrodynamics_Jackson_1a_Edicion.pdf'. p. 625, 1962.

[83] N. E. Helwig, S. Hong, and E. T. Hsiao-wecksler, 'No 主観的健康感を中心とした在宅高齢者における 健康関連指標に関する共分散構造分析Title'.

[84] R. Paul and S. J. Paddison, 'Variational methods for the solution of the Ornstein-Zernicke equation in inhomogeneous systems', *Phys. Rev. E - Stat. Physics, Plasmas, Fluids, Relat. Interdiscip. Top.*, vol. 67, no. 1, p. 11, 2003, doi: 10.1103/PhysRevE.67.016108.

[85] R. P. Boas, 'George Polya 1887 - 1985', *Natl. Acad. Sci.*, 1990.

[86] J. G. Davis and H. L. Bohon, 'First NASA Advanced Composites Technology Conference', *NASA Conf. Publ. 3104 - Part 1*, p. 421, 1990, [Online]. Available: https://apps.dtic.mil/sti/pdfs/ADA310200.pdf

[87] 'Finite Elements in Fluids, Volume 1: Viscous Flow and Hydrodynamics, and Volume 2: Mathematical Foundations, Aerodynamics and Lubrication.' 1975.

[88] O. . Zienkiewicz, R. . Taylor, and J. . Zhu, 'Finite Element Method for Solid and Structural

Mechanics', no. 1, pp. 6–8, 2005.

[89] R. W. Clough, 'Original formulation of the finite element method', *Finite Elem. Anal. Des.*, vol. 7, no. 2, pp. 89–101, 1990, doi: 10.1016/0168-874X(90)90001-U.

[90] D. V. Griffiths and I. M. Smith, *Numerical Methods for Engineers*. McGraw-Hill Science/Engineering/Math, 2006. doi: 10.1201/9781420010244.

[91] F. Rieg, R. Hackenschmidt, and B. Alber-Laukant, 'Finite Element Analysis for Engineers', *Finite Elem. Anal. Eng.*, pp. i–xiii, 2014, doi: 10.3139/9781569904886.fm.

[92] R. Fitzpatrick, '好书Fitzpatrick.R.@.Classical.Electromagnetism - The University of Texas at Austin.pdf'.

[93] J. A. M. Mchugh, 'and Turning Points with a Large Parameter and Turning Points', vol. 7, no. 4, pp. 277–324, 1971.

[94] 'Finite Elements for Electrical', *Electr. Eng.*, 2006.

[95] C. Keil, 'Aircraft Engineering and Aerospace Technology: 75th Anniversary', *Aircr. Eng. Aerosp. Technol.*, vol. 76, no. 2, pp. 76–79, 2004, doi: 10.1108/aeat.2004.12776baf.001.

[96] J. Morozionkov and J. A. Virbalis, 'Investigation of electric reactor magnetic field using finite element method', *Elektron. ir Elektrotechnika*, no. 5, pp. 9–12, 2008.

[97] O. Craiu, N. Dan, and E. A. Badea, 'Numerical Analysis of Permanent Magnet DC Motor Performances', *IEEE Trans. Magn.*, vol. 31, no. 6, pp. 3500–3502, 1995, doi: 10.1109/20.489549.

[98] D. M. Grimes and C. A. Grimes, 'Classical Electrodynamics', *Phot. Creat. — Annihil.*, pp. 1–42, 2012, doi: 10.1142/9789814383370_0001.

[99] Amalia Yunia Rahmawati, '済無No Title No Title No Title', no. July, pp. 1–23, 2020.

[100] E. Otilia, D. Enescu, M.-F. Stan, and M. Ionel, 'Finite Element Analysis of Stationary Magnetic Field', *Finite Elem. Anal. - New Trends Dev.*, 2012, doi: 10.5772/50846.

[101] J. H. A. S. K. H. Kamel, 'Matrix Methods of Structural Analysis: A Précis of recent developments', *AGARDograph 72*, pp. 1–164, 1964, [Online]. Available: https://www.cambridge.org/core/product/identifier/S0368393100079700/type/journal_article

[102] A. Konrad, C. A. Brebbia, P. P. (Peter P. Silvester, Wessex Institute of Technology., and International Compumag Society., *Software for electrical engineering analysis and design*. 1999.

[103] Q. Wang, 'Practical Design of Magnetostatic Structure Using Numerical Simulation', *Pract. Des. Magnetostatic Struct. Using Numer. Simul.*, 2013, doi: 10.1002/9781118398159.

[104] '28. Aparate-electrice-g-hortopan-567931a5ddcc1.pdf'.

[105] '36. abbdf72c13c25052189610ff178.pdf'.

[106] D. Milter, 'Mathematical functions', *Journal of Applied Mechanics, Transactions ASME*, vol. 32, no. 1. p. 239, 1964. doi: 10.1115/1.3625776.

[107] I. To and M. Methods, 'UNIT- 1 Matrix Method'.

[108] J. Jiang *et al.*, 'We are IntechOpen , the world ' s leading publisher of Open Access books Built by scientists , for scientists TOP 1 %', *Intech*, vol. 34, no. 8, pp. 57–67, 2010, [Online]. Available: https://doi.org/10.1007/s12559-021-09926-6%0Ahttps://www.intechopen.com/books/advanced-biometric-technologies/liveness-detection-in-biometrics%0Ahttp://dx.doi.org/10.1016/j.compmedimag.2010.07.003

[109] M. G. Pantelyat, M. G. Shulzhenko, and I. Doležel, 'Numerical field simulation in electrical engineering devices: Magneto-thermo-mechanical coupling', *15th Int. Symp. Theor. Electr. Eng. ISTET 2009*, no. July 2009, pp. 236–240, 2009.

[110] D. Meeker, 'Finite Element Method Magnetics: Version 4.2 User Manual', pp. 1–161, 2020, [Online]. Available: https://www.femm.info/wiki/Documentation/

[111] J. Jun, Y. Shin, S. J. Cho, Y. W. Cho, S. H. Lee, and J. H. Kim, 'Optimal linear generator with Halbach array for harvesting of vibration energy during human walking', *Adv. Mech. Eng.*, vol. 8, no. 5, pp. 1–8, 2016, doi: 10.1177/1687814016649880.

[112] J. Jun, Y. Shin, and J. H. Kim, '1914. Linear electric generator with Halbach array to self-charge a smartphone', *J. Vibroengineering*, vol. 18, no. 1, pp. 587–594, 2016.

[113] C. Ma, W. Zhao, and L. Qu, 'Design optimization of a linear generator with dual Halbach array for human motion energy harvesting', *Proc. - 2015 IEEE Int. Electr. Mach. Drives Conf. IEMDC 2015*, pp. 703–708, 2016, doi: 10.1109/IEMDC.2015.7409136.

Bibliography

Publication Related to the Thesis

Journal Articles

VISHWAKARMA, Anubhav, KOMELJ, Matej. Optimum design of a permanent-magnet-based self-charging device for a smartphone. *Materials and technologies*. [Print ed.]. Nov.-Dec. 2023, vol. 57, well. 6, p. 627-630. ISSN 1580-2949. DOI: 10.17222/mit.2023.968 .

VISHWAKARMA, Anubhav, KOMELJ, Matej. A permanent magnet-based design for a smartphone self-charger. Materials today: proceedings. 2022, vol. 65, part 8, p. 3642-3645. ISSN 2214-7853. DOI: 10.1016/j.matpr.2022.06.190.

Scientific Conference Paper Publication Related to the Thesis

VISHWAKARMA, Anubhav, KOMELJ, Matej. Design of a smartphone self-charger based on a permanent magnet. 56th International Conference on Microelectronics, Devices, and Materials & the Workshop on Personal Sensor for Remote Health Care Monitoring: proceedings: September 22 - September 24, 2021, Ljubljana, Slovenia, Pg. 52-56, illustr. ISBN 978-961-95495-0-6.

VISHWAKARMA, Anubhav, KOMELJ, Matej. Design of a permanent magnet-based self-charging device for a smartphone. 57th International Conference on Microelectronics, Devices, and Materials & The Workshop on Energy Harvesting: proceedings: September 14 - September 16, 2022, Maribor, Slovenia, Pg. 62. ISBN 978-961-95495-1-3.

Vishwakarma Anubhav, Komelj Matej "Design of a Smart Phone Self-Charging Device Based on Permanent Magnets." Advanced Production and Industrial Engineering, p, 507–513, DOI: 10.3233/ATDE220787.

Vishwakarma Anubhav, Komelj Matej "Design of a smartphone self-charging device based on permanent magnets." AIP Conference Proceedings 2768,020007, (2023), https://doi.org/10.1063/5.0149736.

Scientific Conference Contribution Abstract Related to the Thesis

VISHWAKARMA, Anubhav, KOMELJ, Matej. Design of a smartphone self-charging device based on permanent magnets. 14th Jožef Stefan International Postgraduate School Students' Conference: book of abstracts: 1st - 3rd June 2022, Kamnik, Slovenia = 1st - 3rd June 2022, Kamnik, Slovenia.

VISHWAKARMA, Anubhav, KOMELJ, Matej. Design of a smartphone self-charging device based on permanent magnets. The 1st International Conference on Computational Science and its Applications (ICCSA 2022) April 28th – April 29th, 2022, Jaipur, Rajasthan, India.

VISHWAKARMA, Anubhav, KOMELJ, Matej. Design of a smartphone self-charging device based on permanent magnets. 23rd International Conference on Advances in Materials & Processing Technologies, 10-14 October 2022, Portorož, Slovenia. Ljubljana: Institute for Metal Materials and Technologies, 2022. P. 16.

VISHWAKARMA, Anubhav, KOMELJ, Matej. Design of permanent magnets by solving the inverse magnetostatics problem. 13th Jožef Stefan International Postgraduate School Students' Conference and 15th Young Researchers' Day (KMBO Conference), 27-28 May 2021, Ljubljana, Slovenia.

VISHWAKARMA, Anubhav, KOMELJ, Matej. Design and modeling of arbitrary-shape permanent magnet field calculation. 12th Jožef Stefan International Postgraduate School Students'

Conference and 14th Young Researchers' Day (KMBO Conference) Day, 13th -15th May 2020 Ljubljana, Slovenia.

Vishwakarma Anubhav, Komelj Matej "Permanent-magnet design for a smartphone self-charger" Indo-European Conference on Advanced Manufacturing and Materials Processing (IECAdvaMAP-2023), Feb 6-8, 2023, Alappuzha, Kerala state, India – pin 688004.

VISHWAKARMA, Anubhav, KOMELJ, Matej. Geometry-based reduction of rare-earth-containing raw materials for permanent magnets. *The 27th International Workshop on Rare Earth and Future Permanent Magnets and their Applications: Birmingham, 3rd-7th September 2023*. Birmingham: University of Birmingham, 2023. Pp. 115. https://uobevents.eventsair.com/repm2023/

Lecture at a Foreign University Related to the Thesis

VISHWAKARMA, Anubhav. Green deal and circular economy challenges of rare-earth-based permanent magnets (PMs) with technical aspects and Workshop Green deal and circular economy challenges of rare-earth-based permanent magnets (PMs) with technical aspects, 12.12.2022.

Vishwakarma, Anubhav. Indo- Slovenia Joint Workshop on Material Science and Technology & Electronics and Computer Engineering jointly organized by Indian Institute of Technology Indore, India on Feb 20, 2023.

Vishwakarma Anubhav, workshop on the Innovation Day Ljubljana-Clean energy & manufacturing, 6th December 2023, grand Hotel Union 1000 Ljubljana, Slovenia.

VISHWAKARMA, Anubhav. Machine learning in physics: invited talk, VDSP-ESI Winter School 2022, University of Vienna, February 10-14 Feb. 2020.

Biography

The author of this thesis is a Bharat (Indian) national born on 5th September 1994 in Maharajganj, Uttar Pradesh. He completed his BTech. (Bachelor of Technology) in Mechanical Engineering from APJ Abdul Kalam Technical University, Lucknow, U.P., India in 2016. He continued his master study and he completed his M.Tech. (Master of Technology) in Energy Technology and Management at Madan Mohan Malviya Technical University (MMMUT) Gorakhpur, U.P., India, in 2018. His MTech. thesis is related to the Theoretical study of Computational Fluid Dynamics in Convergent-Divergent nozzles. After this he worked as a research intern in a theoretical computing laboratory at the Indian Institute of Technology (IIT), Indore M.P., India and his internship topic was the design of metallic glass using FEM software.

At present, he is a 4th-year student at Jožef Stefan International Postgraduate School. He recently finished his Ph.D. degree at the K-7 Department of Nanostructured Materials. His research was framed in a Young Researcher fellowship in the Slovenia training program for the Design-based optimization of a custom permanent magnet focused on reduced raw-material consumption. He has worked, and the dissertation aims to demonstrate how a smart design of a custom magnet for a particular application can yield an efficient solution by using considerably less critical material without affecting the final product's performance. The focus is on a magnet, which represents the source of the field in a magnetic harvester for portable devices like smartphones. A harvester is meant to be used for charging a smartphone's battery in an emergency; hence, it needs to be produced in a simple and low-cost way. The proposed design can be realized by utilizing modern techniques, such as additive manufacturing, making non-uniformly-shaped magnets possible without additional cutting or grinding, which could lead to non-desired material waste. He has published three papers in International peer-reviewed journals; another joint publication is a conference paper.